VOLUME 31 | SUPPLEMENT 2 | MARCH 2018

MODERN PATHOLOGY

USCAP 2018

ABSTRACTS

DERMATOPATHOLOGY

(524-585)

107TH ANNUAL MEETING

GEARED TO LEARN

MARCH 17-23, 2018

Vancouver Convention Centre
Vancouver, BC, Canada

Published by
SPRINGER NATURE
www.ModernPathology.org

USCAP Creating a Better Pathologist
AN OFFICIAL JOURNAL OF THE UNITED STATES AND CANADIAN ACADEMY OF PATHOLOGY

EDUCATION COMMITTEE

Jason L. Hornick, Chair
Rhonda Yantiss, Chair, Abstract Review Board and Assignment Committee
Laura W. Lamps, Chair, CME Subcommittee
Steven D. Billings, Chair, Interactive Microscopy
Shree G. Sharma, Chair, Informatics Subcommittee
Raja R. Seethala, Short Course Coordinator
Ilan Weinreb, Chair, Subcommittee for Unique Live Course Offerings
David B. Kaminsky, Executive Vice President (Ex-Officio)
Aleodor (Doru) Andea
Zubair Baloch
Olca Basturk
Gregory R. Bean, Pathologist-in-Training
Daniel J. Brat
Amy Chadburn
Ashley M. Cimino-Mathews
James R. Cook
Carol F. Farver
Meera R. Hameed
Michelle S. Hirsch
Anna Marie Mulligan
Rish Pai
Vinita Parkash
Anil Parwani
Deepa Patil
Lakshmi Priya Kunju
John D. Reith
Raja R. Seethala
Kwun Wah Wen, Pathologist-in-Training

ABSTRACT REVIEW BOARD

Narasimhan Agaram
Christina Arnold
Dan Berney
Ritu Bhalla
Parul Bhargava
Justin Bishop
Jennifer Black
Thomas Brenn
Fadi Brimo
Natalia Buza
Yingbei Chen
Benjamin Chen
Rebecca Chernock
Andres Chiesa-Vottero
James Conner
Claudiu Cotta
Tim D'Alfonso
Leona Doyle
Daniel Dye
Andrew Evans
Alton Farris
Dennis Firchau
Ann Folkins
Karen Fritchie
Karuna Garg
James Gill
Anthony Gill
Ryan Gill
Tamara Giorgadze
Raul Gonzalez
Anuradha Gopalan
Jennifer Gordetsky
Ilyssa Gordon
Alejandro Gru
Mamta Gupta
Omar Habeeb
Marc Halushka
Krisztina Hanley
Douglas Hartman
Yael Heher
Walter Henricks
John Higgins
Jason Hornick
Mojgan Hosseini
David Hwang
Michael Idowu
Peter Illei
Kristin Jensen
Vickie Jo
Kirk Jones
Chia-Sui Kao
Ashraf Khan
Michael Kluk
Kristine Konopka
Gregor Krings
Asangi Kumarapeli
Frank Kuo
Alvaro Laga
Robin LeGallo
Melinda Lerwill
Rebecca Levy
Zaibo Li
Yen-Chun Liu
Tamara Lotan
Joe Maleszewski
Adrian Marino-Enriquez
Jonathan Marotti
Jerri McLemore
David Meredith
Dylan Miller
Roberto Miranda
Elizabeth Morgan
Juan-Miguel Mosquera
Atis Muehlenbachs
Raouf Nakhleh
Ericka Olgaard
Horatiu Olteanu
Kay Park
Rajiv Patel
Yan Peng
David Pisapia
Jenny Pogoriler
Alexi Polydorides
Sonam Prakash
Manju Prasad
Bobbi Pritt
Peter Pytel
Charles Quick
Joseph Rabban
Raga Ramachandran
Preetha Ramalingam
Priya Rao
Vijaya Reddy
Robyn Reed
Michelle Reid
Natasha Rekhtman
Michael Rivera
Mike Roh
Marianna Ruzinova
Peter Sadow
Safia Salaria
Steven Salvatore
Souzan Sanati
Sandro Santagata
Anjali Saqi
Frank Schneider
Michael Seidman
Shree Sharma
Jeanne Shen
Steven Shen
Jiaqi Shi
Wun-Ju Shieh
Konstantin Shilo
Steven Smith
Lauren Smith
Aliyah Sohani
Heather Stevenson-Lerner
Khin Thway
Evi Vakiani
Sonal Varma
Marina Vivero
Yihong Wang
Christopher Weber
Olga Weinberg
Astrid Weins
Maria Westerhoff
Sean Williamson
Laura Wood
Wei Xin
Mina Xu
Rhonda Yantiss
Akihiko Yoshida
Xuefeng Zhang
Debra Zynger

To cite abstracts in this publication, please use the following format: **Author A, Author B, Author C, et al. Abstract title (abs#).** ***Modern Pathology*** **2018; 31 (suppl 2): page#**

524 Immunohistochemical Analysis of Diagnosed Melanoma Cases in Nigeria

Fatimah Y Abdulqadir[1], *Modupeola O Samaila*[2], *Yawale Iliyasu*[1], *Saad Ahmed*[3]. [1]Ahmadu Bello University, Zaria, Kaduna, [2]Ahmadu Bello University, [3]Ahmadu Bello University Teaching Hospital, Zaria

Background: Melanoma disease burden is confounded by its propensity for mimicry of many cancers histologically. Afflicted cancer patients in our setting present with advanced diseases. Thus, accurate diagnosis is mandatory for the treatment and management of these deadly diseases. This study was aimed at confirming the histological diagnosis of melanoma over a ten year period in a tertiary institution in Nigeria, using immunohistochemical (IHC) markers and to establish the immunohistochemical profile of melanoma cases in our setting.

Design: All morphologically diagnosed cases of melanoma from 1st January 2005 to 31st December 2014 formed the study material. All the relevant tissue blocks and slides stained with Haematoxylin and Eosin (H&E) were retrieved from the departmental records. IHC staining using HMB45, Melan A, S100 and Vimentin was done on all relevant stored paraffin embedded tissue blocks for a confirmatory diagnosis of melanoma.

Results: Eighty eight cases of melanoma were diagnosed during the study period. 72 cases met the study criteria. There were 26 males and 46 females with a male: female ratio of 1.0:1.8. The ages ranged from 16 to 85 years with a mean age of 54 years. The highest incidence was in the 6th decade of life. The foot was the commonest site with 38 (52.9%) cases, while 7 (9.8%) cases were seen in the rest of the lower limbs. There were 6 (8.2%) cases in the lymph nodes and 5 (6.8%) in the groin. Clark's level was applicable to 61 (84.7%) cases. There were 4 (6.6%) cases in level III, 20 (32.8%) cases in level IV and 37 (60.7%) cases in level V. No case was seen in levels I and II. Histologically, 46 (63.0%) cases were distributed in sheets predominantly and 18 (25.0%) cases were in nests, while pseudopapillary had 4 (5.6%) cases, trabecular had 3 (4.2%) cases and pseudoglandular had only 1 (1.4%) case. Immunohistochemical staining showed S100 and Vimentin had 98.6% positivity rates each, while HMB45 had 94.4% positivity rate and Melan A had 87.5% positivity rate. 62 (86.1%) cases were positive for all 4 markers, 5 (6.9%) cases were positive for a combination of vimentin, S100 and HMB45. Only 2 (2.8%) cases were positive for a combination of vimentin and S100. A single case (1.4%) was positive for Vimentin only.

Conclusions:

The study showed S100 and Vimentin with highest positivity rates. It is recommended that S100 and HMB45 or Vimentin should be part of the confirmatory diagnostic parameters of melanoma in resource constraint setting.

525 Characterizing the Demographics, Histopathology and Immunohistochemical Expression of CK5/6 and p40/p63 in Triple Negative Breast Carcinoma Metastatic to Skin

Muhammad Ahmad[1], *Indu Agarwal*[2], *Megan E Sullivan*[3], *Thomas Cibull*[4], *Antoinette Thomas*[5]. [1]NorthShore University Health System, Chicago, IL, [2]NorthShore University Health System, Evanston, IL, [3]NorthShore University Healthsystem, Evanston, IL, [4]NorthShore University, Evanston, IL, [5]Evanston, IL

Background: Differentiating primary cutaneous adnexal neoplasms (CAN) from metastatic carcinoma can prove challenging. CK5/6 and p40/p63 have been shown to be helpful in differentiating typical low grade ductal carcinoma without mucinous or significant apocrine differentiation from CAN. CAN usually demonstrate diffuse strong CK5/6 and p40/p63 expression, while breast carcinoma is typically negative for these markers. Triple negative breast cancer (TNBC), specifically with basal phenotype, has been shown to demonstrate expression of high molecular weight cytokeratin. Therefore, we analyzed the expression of CK5/6 and p40/p63 in cutaneous metastases of TNBC to see if these markers have the same utility in differentiating CAN from metastatic TNBC.

Design: Six cases of metastatic TNBC to skin were identified from archival files (2006-2017). The patients' sex, age and site of metastasis were recorded. The H&E slides were evaluated for histologic features. One block from each case was stained with CK5/6, p40 and p63.

Results: All six patients were female. Their ages ranged from 35 to 90 years (mean age: 58.8 years). The cutaneous metastasis of each patient was local, located on the chest wall, breast and upper flank. Histological examination revealed that all were grade 3 invasive ductal carcinoma; one demonstrated apocrine differentiation. CK5/6 reactivity was strong and diffuse in one case (17%), focal in two cases (33.3%), and absent in three cases (50%). p40 and p63 were focally positive in the case with strong diffuse CK5/6 expression (17%) and were negative in other five cases (83%).

- Skin metastasis of TNBC is typically local.
- Metastatic TNBC is typically histologically high grade.
- CK5/6, p40 and p63 expression can be seen in metastatic TNBC to the skin, but is usually focal. However, rarely, CK5/6 can demonstrate strong diffuse expression, correlating to basal phenotype.
- p40 and p63 were more specific than CK5/6, with metastatic TNBC demonstrating no to focal expression of p40 and p63.
- CK5/6, p40 and p63 remains a useful panel in differentiating metastatic breast carcinoma from CAN, even with TNBC.

526 cBioportal as a Tool to Monitor and Analyze Next Generation Sequencing Based Melanoma Mutation Profiling Data for Quality Control and Quality Assurance

Amro Almradi[1], *Maohua Xie*[2], *NHU T NGO*[3], *Geoffrey Smith*[4], *Charles Hill*[5], *Linsheng Zhang*[6]. [1]Emory University Hospital, [2]Emory University, [3]Emory School of Medicine, Atlanta, GA, [4]Emory University School of Medicine, Atlanta, GA, [5]Emory Univ/Medicine [6]Emory University Hospital

Background: cBioportal is a platform that facilitates data exploration and analysis using a variety of visualization and analytical tools in a web browser. It allows local installation, uploading custom data and provides a database to interrogate variants across samples and genes. We created a local cBioportal database for our next generation sequencing based solid tumor mutation profiling. The monitoring and analysis of variants detected in melanoma are presented here.

Design: Totally 168 melanoma samples from 07/27/15 to 07/24/17 were tested in Emory Molecular Diagnostic Laboratory for next generation sequencing (NGS) based mutation profiling with Illumina TruSight® Tumor 26 gene panel. The cases were de-identified and the presumably significant variants reported by pathologists were uploaded to a local cBioportal platform. The anatomic site and tumor percentage were included. We compared the variant profiles in our local database with TCGA database of variants from cutaneous melanoma provisional cohort (471 samples). The results were used for monthly quality review and molecular tumor board presentation.

Results: BRAF, NRAS and TP53 are the three most commonly mutated genes found in our melanoma cases. MUC16 is the most commonly mutated gene in TCGA dataset; however, it is not tested in our targeted panel (Fig. 1, MUC16 not included). The prevalence of *NRAS* and *TP53* variants are comparable between our data and TCGA dataset; BRAF mutations are more common in TCGA cohort. The types of genetic alterations detected in our cases are also similar to TCGA cohort (Fig. 2). All the variants we reported, were detected in TCGA dataset. The main source of differences can be attributed to the different number of genes targeted, because TCGA data was collected from whole exome sequencing.

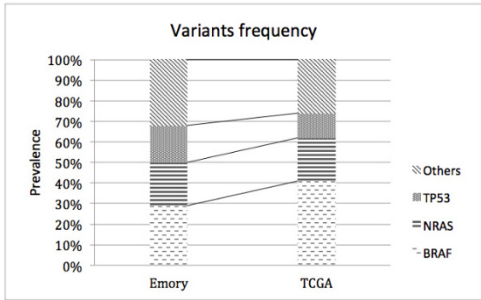

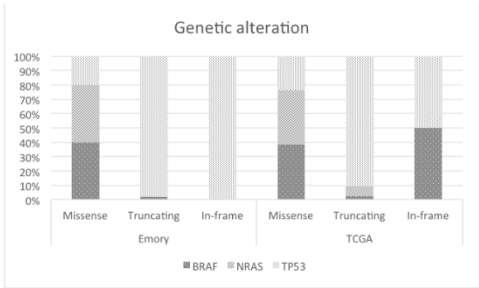

Conclusions: In our study, we noticed that our melanoma cases match well with those from TCGA provisional cohort. cBioportal is a useful platform for quality control and quality assurance. The web browser interface also makes it a convenient tool for our monthly molecular tumor board to present the cumulative data to the clinical oncology team.

527 Expression of PDL-1 in Kaposi Sarcoma with Comparison between Immunocompetent and Immunocompromised Patients

Afaf Alsolami[1], *Hatim Khoja*[2], *Fouad Aldayel*, *Tariq Al-Zaid*. [1]King Faisal Specialist Hospital and Research Center, Riyadh, [2]King Faisal Specialist Hospital, Riyadh

Background: Kaposi sarcoma (KS) is an HHV-8 infection related vasoproliferative disorder that may arise in different clinical backgrounds including immunocompetent and immunocompromised patients (classic and endemic vs. AIDS-related and iatrogenic). KS lesions in immunocompromised patients may regress after restoration of the immune system by antiretroviral therapy or withdrawal of the immunosuppressive agents. In this study we sought to evaluate a possible interaction between Programmed Death-1 (PD-1) receptor on T-cells and its potential ligands on KS cells that may play a role in which tumor cells evade immunity in immunocompetent patients.

Design: PDL-1 expression was assessed by immunohistochemistry using *VENTANA PD-L1 (SP263)* Rabbit Monoclonal Primary Antibody on a series of 42 KS lesions from 31 patients of different clinical backgrounds, summarized in table. Early patch stage lesions were not included in the study. Three pathologists blinded to the clinical background performed the evaluation of PDL-1 expression. A 1% cutoff value was used for positive staining in tumor cells. PDL-1 expression was scored by multiplying staining intensity by percentage of positive tumors cells (H-score). The mean of H-scores in positive samples was calculated for each patients group.

Results: PDL-1 was more frequently expressed with higher mean H-score in iatrogenic KS due to autoimmune diseases (6/7; 85%/ mean score=24) and immunocompetent patients (11/14; 78%/ mean score=21) in contrast to transplanted patients (3/9; 33%/ mean score=6). PDL-1 expression in AIDS related KS was present in (7/12; 58%/ mean score=10). None of the lesions in any patients group showed strong and diffuse staining. PDL-1 expression in all patients groups was present in (27/42; 64%) with overall mean H-score for positive samples=15.

	No. Patients	No. Samples	Positive samples	Mean H-score for positive samples
Immunocompromised				
1. AIDS	7	12	7/12 (58%)	10
2a. Iatrogenic: post-transplant	6	9	3/9 (33%)	6
2b. Iatrogenic: Autoimmune	5	7	6/7 (85%)	24
Immunocompetent	13	14	11/14 (78%)	21
TOTAL	31	42	27/42 (64%)	15

Conclusions: PDL-1 expression in KS is seen in 64% of cases, which tends to be focal and weak to moderate at most. PDL-1 is expressed more frequently in iatrogenic KS due to autoimmune diseases (85%) and immunocompetent patients (78%) in contrast to transplanted patients (33%). PDL-1 expression in AIDS related KS is seen in 58% of cases. The variable expressions of PDL-1 among different patient groups may represent a minor adaptive mechanism of tumors cells to evade the immune response. To the best of our knowledge, this is the first study evaluating PDL-1 expression in KS of different clinical backgrounds. Additional studies may be needed to explore the role of PDL-1 in Kaposi sarcoma.

528 Melanoma with Loss of Bap1 Expression in Patients with No Family History of BAP1-Associated Cancer Susceptibility Syndrome

Phyu Aung[1], *Priyadharsini Nagarajan*[1], *Michael Tetzlaff*[1], *Jonathan Curry*[1], *Guilin Tang*[1], *Zied Abdullaev*[1], *Svetlana D Pack*[1], *Doina Ivan*[1], *Victor Prieto*[1], *Carlos Torres-Cabala*[1]. [1]The University of Texas MD Anderson Cancer Center, Houston, TX

Background: Presence of multiple BAP1-negative melanocytic neoplasms is a hallmark of familial cancer susceptibility syndrome caused by germline mutations in *BAP1*. The syndrome is characterized by increased incidence of renal cell carcinoma, mesothelioma, cholangiocarcinoma, cutaneous and uveal melanoma and other neoplasms, including basal cell carcinoma. Melanocytic tumors lacking BAP1 expression may also present as sporadic lesions in patients lacking a germline mutation.

Design: Here, we report histomorphologic and clinical characteristics of cutaneous melanomas with loss of BAP1 expression in 4 patients with no known history of BAP1-associated cancer susceptibility syndrome (Figure 1).

Results: The tumors were nodular melanomas characterized by predominantly intradermal proliferation of large epithelioid (spitzoid) melanocytes with nuclear pseudoinclusions as well as scattered multinucleated cells, arising in association with a standard intradermal nevus. Of all 4 patients, only 1 had multiple recurrences with in-transit and regional lymph node metastases.

FOR TABLE DATA, SEE PAGE 215, FIG. 452

Conclusions: To the best of our knowledge, this is the first series of cutaneous melanomas with loss of BAP1 expression arising in a sporadic setting.

529 Keratoacanthomas Associated with Anti-PD-L1/ TGF-beta Trap Fusion Protein Treatment

Mairead Baker[1], *Hong Jiang*[2], *Julius Strauss*[3], *James Gulley*[4], *Isaac Brownell*[1]. [1]NIAMS, NIH, [2]National Institutes of Health, Bethesda, MD, [3]NCI, NIH, [4]NCI, NIH

Background: Keratoacanthomas (KAs) are fast-growing, benign, ephemeral tumors that occur on sun-exposed skin and resemble well differentiated cutaneous squamous cell carcinoma (SCC). Transforming growth factor-beta (TGF-beta) inhibits cell cycle progression, and reduced TGF-beta signaling has been implicated in KA formation. Patients with Ferguson-Smith disease develop KA-like multiple self-healing squamous epitheliomas due to loss-of-function germline mutations in the TGF-beta receptor gene. Here we report four cases of treatment-emergent KAs developing in cancer patients receiving a novel bifunctional protein that fuses a human monoclonal antibody against programmed death ligand 1 (PD-L1) to the soluble extracellular domain of TGF-beta receptor II. This drug functionally traps and neutralizes TGF-beta.

Design: The clinical courses of four cases of treatment-related KAs were reviewed. Lesions were biopsied and confirmed by histopathological examination.

Results: Four patients (mean ages: 60.5; arrange: 50-73), including 3 females and 1 males, with diagnosed solid malignancies received infusions of the novel bifunctional protein every two weeks as part of a Phase I clinical trial. Three patients developed multiple KA-like lesions on sun-exposed areas within 2-3 moth treatment, and one patient had one solitary, crateriform nodule on his chin within one month treatment. Representative lesions from each patient were biopsied and confirmed to be KAs or well differentiated SCC, KA-type by histopathological examination. Lesions on two patients were documented to partially spontaneously regress by serial clinical evaluations over the course of weeks while continuing treatment.

Conclusions: Together with the genetic defect in patients with Ferguson-Smith disease, these cases confirm the pathophysiological importance of reduced TGF-beta signaling in KA formation. Further investigations are needed to identify the predisposing molecular and genetic changes required for KA formation as well as to define the natural history of these treatment-associated skin tumors.

530 A Magnifying Glass on Spiradenoma and Cylindroma Histogenesis- Systematic Transcriptome Analysis

Achim H Bell[1], *Victor Prieto*[1], *Diana Bell*[1]. [1]The University of Texas MD Anderson Cancer Center, Houston, TX

Background: Spiradenoma and cylindroma are related tumors, with morphological overlap and hybrid tumors encountered. These are described as sweat gland tumors and considered to be of eccrine lineage. The associations with trichoepitheliomas/ Brooke-Spiegler, combinations with hair follicle tumors, and anatomical considerations are proposing a folliculosebaceous-apocrine lineage. A subset of dermal cylindromas shows the *MYB-NFIB* gene fusion/ MYB protein overexpression, similar to adenoid cystic carcinoma. Quantifying the differential expression of genes in various human organs/tissues/ cell types is vital to understand physiology/disease. Several studies analyzed expression of protein-coding genes across tissues.

Design: 22 cutaneous neoplasms formed the material of this study. 14 of these along with 7 normal skin were microdisected from FFPE. RNA pools were subjected to expression profiling using whole-transcriptome shotgun sequencing; differentially expressed candidates were analyzed by IHC.

Results: The tumors were classified as 11 spiradenomas, 4 cylindromas, 3 hybrids (spiradenomas/cylindromas), 1 chondroid syringoma, 2 adnexal carcinomas, 1 BCC. Age at diagnosis 25-92 yo, female predominance (n=14), more frequent in head and neck (n=13: scalp-7, ear-4, face-2). Differential gene expression profiles from 7 spiradenomas, 2 cylindromas, 3 hybrids, 2 adnexal carcinomas versus 7 normal skins were generated and compared to each other. 4004 genes and noncoding transcripts were detected as differentially expressed at 0.01 FDR. These genes and transcripts were annotated and analyzed using the IPA program. Highest expressed genes were predominantly developmental-related genes

(ODAM,DMRTA2,HOXB13,TLX1,SOX14, BARX1,HOTAIR,HOXC11) along with lincRNAs. For RNA-Seq results validation, IHC assessed protein expression of 4 genes highly upregulated and considered important for spiradenomas/ cylindromas. These candidates were ODAM, HOXB13, MYB and SOX10 with expressions at 69%, 74%, 79% and 81% respectively.

Conclusions: We assume that spiradenomas and cylindromas are mainly defined by high number of overexpressed developmental/ homeobox genes, which provide the potential for transformation/ plasticity, along with differentiation and proliferation behavior of neoplastic cells. These data form the basis for understanding cell fate determination and cellular homeostasis in the normal adnexal epithelium and the contribution of different adnexal cell types to the etiology/ molecular pathology of dermal adnexal disease.

531 microRNA Molecular Signature of Ultraviolet B (UVB) is Present in Sun-Exposed Melanocytic Nevi

Achim H Bell[1], *Diana Bell*[2], *Nitin Chakravarti*[3], *Nicholas K Henton*[4], *Victor Prieto*[5]. [1]UT MD Anderson Cancer Center, [2]UT-MD Anderson Cancer Center, Houston, TX, [3]The Research Institute at Nationwide Children's Hospital, [4]UT- MD Anderson Cancer Center, [5]UT - MD Anderson Cancer Center, Houston, TX

Background: It still remains largely unknown how melanocytes transform into melanoma cells. However, there is enough evidence documenting the link between intense UVR exposure and melanoma, characterized with an elevated number of C>T (by UVB) or G>C (by UVA) conversions in the DNA of melanomas arising in sun-exposed skin (lentigo maligna-type melanoma).

Mature microRNAs (miRNAs) are small (~22 nucleotides) endogenous RNAs that may regulate gene expression such as by post-transcriptional induction of mRNA decay or by repressing mRNA translation into proteins. It is estimated that miRNAs are able to modulate up to 60% of protein-coding genes in the human genome and are centrally involved in the control of proliferation, differentiation, apoptosis, and other important biological pathways. miRNAs may be aberrantly expressed or mutated in cancer and can function as potential oncomiRs (miRNAs with either oncogenic or tumor-suppressing functions), by targeting the transcripts of the genes involved in carcinogenesis. miRNA expression profiles can also be employed for classification of human cancers according to the development lineage and differentiation state.

Questions: 1) Do superficial (UV-damaged) and deep melanocytes of nevi in sun-exposed skin differ in their miRNA expression? 2) Are some of those differentially expressed miRNAs known potential oncomiRs?

Design: Superficial and deep melanocytes were LCM microdissected from nevi of 15 patients. The suspensions were processed for hybridization to a ribonucleotide protection system with 2280 total probes including 2256 micro RNA probes targeting 2083 human micro RNAs.

Results: A comprehensive analysis of all human miRNAs registered in miRBase 11.0 was performed using the HTG Molecular Diagnostic database. A hierarchical cluster analysis of the miRNAs (FDR<0.1) was performed to visualize the miRNA species upon which the samples can be best classified as superficial or deep melanocytes. This yielded statistical relevant miRNA profiles with FDR<0.1 for 14 samples.

We identified 39 miRNAs that were differentially expressed between the superficial and deep melanocytes. Ingenuity pathway analysis (IPA) suggested the gene transcripts AR, MDM2, Smad2/3, YBX1 as most probable miRNA targets, with ongoing validation at the protein level.

Conclusions: Superficial (UV-damaged) melanocytes can be differentiated from deep melanocytes on the basis of the expression of 39 miRNAs, with AR, MDM2, Smad2/3, YBX1 as candidates for the gene transcript and protein targets.

532 Molecular Testing of Borderline Cutaneous Melanocytic Tumors: SNP Array is More Sensitive and Specific than FISH

Michael Carter[1], *Paul Harms*[2], *May P Chan*[2], *Rajiv Patel*[3], *Lori Lowe*[4], *Douglas Fullen*[2], *Alexandra Hristov*[3], *Min Wang*[4], *Aleodor Andea*[2]. [1]Halifax, NS, [2]University of Michigan, Ann Arbor, MI, [3]Univ. of Michigan, Ann Arbor, MI, [4]University of Michigan

Background: Melanocytic lesions with borderline features are diagnostically challenging. Molecular techniques based on detection of genomic copy number alterations (CNA) using single nucleotide polymorphism (SNP) arrays can be helpful in predicting whether a lesion is likely to behave in an indolent or aggressive manner (i.e. like a nevus or a melanoma). Fluorescence in situ hybridization (FISH) has been used as a quicker, less expensive alternative to SNP array, employing a panel of probes that may be gained (*RREB1*, *MYC*, *CCND1*), or lost (*MYB*, homozygous *CDKN2A* loss) in melanoma. While the sensitivity and specificity of FISH testing are both reported to be in excess of 90%, validation studies are based on well-characterized nevi and melanoma rather than borderline melanocytic tumors.

Design: We used SNP array data from 63 borderline cutaneous melanocytic lesions and 45 definitive melanomas, which served as a control group, to predict the performance of FISH testing. Lesions were considered positive by "virtual FISH" if one or more of the 5 FISH-probed loci demonstrated appropriate CNAs by SNP array. Cases were classified as positive by SNP array if 3 or more CNA (>3 MB each) were present, or if the FISH criteria were met. Additionally, lesions which had only gains or losses of entire chromosomes were designated as negative, regardless of changes at the FISH loci, as this pattern is characteristic of benign proliferative nodules. Conventional FISH was performed in 31 cases.

Results: Of the 63 borderline cases, 44 (70%) were positive by SNP array and 29 (46%) were positive by virtual FISH. A higher proportion of melanomas were positive by SNP array (42/45, 93%) and virtual FISH (36/45, 80%). Compared to SNP array, virtual FISH failed to recognize 19 cases with concerning CNAs (false negatives, Fig. 1A) and incorrectly classified as positive 3 cases with whole chromosome gains and losses (false positives, Fig. 1B). Sensitivity of virtual FISH compared to SNP array was 86% in the melanoma group but only 57% in the borderline group, while specificity was 100% and 84% in these groups, respectively. There was good correlation between conventional and virtual FISH, with agreement in 18/19 conventional FISH positive and 11/12 negative cases.

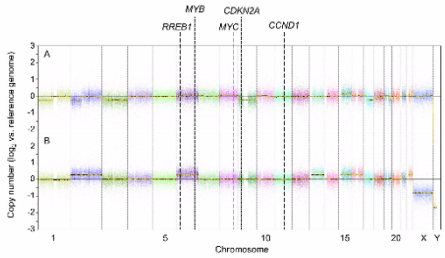

Fig. 1. SNP arrays showing examples of borderline melanocytic lesions with false negative and false positive virtual FISH results. A. False negative case in which 8 copy number aberrations are present, consistent with an aggressive lesion, but negative by FISH (only heterozygous loss of *CDKN2A*). B. False positive case in which only whole chromosome gains (2, 6, 13, 15,16, 22) and loss (X) are present, consistent with a benign proliferative nodule, despite a positive result by FISH (copy number gain of *RREB1*). FISH loci indicated by dashed lines (gains associated with melanoma) and dotted lines (losses associated with melanoma, with only homozygous *CDKN2A* loss considered positive).

Conclusions: While FISH is highly effective in distinguishing between nevi and melanoma in cases where the histological diagnosis is straightforward, it is not nearly as sensitive or specific as SNP array when applied to borderline melanocytic lesions.

533 Institutional Decade Comparison of Subungual and Extradigital Glomus Tumors with Novel Observations

Carla Caruso[1], *Elizabeth Frauenhoffer*[2], *Julie C. Fanburg-Smith*[2]. [1]MS Hershey Medical Center, Hershey, PA, [2]Penn State Health, Milton S. Hershey Medical Center, Hershey, PA

Background: Glomus tumors (GT) arise from modified smooth muscle of the normal neuromyoarterial glomus body that regulates temperature and pressure, usually benign and subungual in females. We previously defined malignant GT as >2 cm, subfacial/visceral, with nuclear atypia, atypical or increased mitoses, and often with a benign peripheral rim and wanted to review our recent institutional experience.

Design: Slides, blocks, clinical, phenotypic and molecular data of cases coded as "GT" from 2007-2017 were pulled and analyzed, excluding glomus jugulare and other tumors.

Results: 27 subungual (5M;21F, mean age 46 years, mean size 0.6 cm) and 28 extradigital (20M: 8F, mean age 56 years, mean size 2.0 cm) GT were identified in local, obese patients, with BMI mean 33 and 31, respectively. Subungual GT patients had cold intolerance, nail dystrophy, and pain worse at night, involving 8 thumb, 7 ring, 4 5th, 4 index, and 1 each of 3rd toe, 3rd and unknown finger, of equal sides. Extradigital GT patients had friable, bleeding, blue masses that caused regional paresthesia, involving 15 forearm, 6 leg, 3 thigh/buttock, and 1 each neck, flank, stomach, and palm. Both types had a feeder vessel with surrounding nerve twigs and scattered mast cells. Extradigital GT exhibited greater internal staghorn vascularity and even cavernous with thrombus, whereas subungual had fewer staghorn. Most GT were located in reticular dermis and abutted subcutis (suprafascial equivalent), composed of epithelioid cells without classic distinctive cytoplasmic borders. One subungual and 10 extradigital had "atypical" features of blue rim with central pink larger cells, at least moderate nuclear atypia, and a multifocal infiltrative pattern; one locally recurred. Extradigital with larger size, deep, spindling, binucleation, increased mitotic activity, or rare necrosis met criteria for uncertain (n=2) or malignant (n=2), without known recurrences or metastases over 6 years follow-up.

Conclusions: Most GT occur at normal glomus body depth and do not exhibit distinctive cytoplasmic borders. Feeder vessel neurovasoconstriction, possibly influenced by mast cell histamine, may cause pain in subungual and paresthesia in extradigital. Extradigital appears to be as common as subungual GT, with a striking male predilection, older age, larger size, and higher propensity for deep, atypical and malignant. The relationships of higher regional BMI to clinical symptoms and our genetic and phenotypic data to outcome are yet to be determined.

534 Novel Observations of Recent Institutional Granular Cell Tumors: Recurrent, Multifocal, Multicentric, or Metastatic?

Carla Caruso[1], *Elizabeth Frauenhoffer*[2], *Julie C. Fanburg-Smith*[2]. [1]MS Hershey Medical Center, Hershey, PA, [2]Penn State Health, Milton S. Hershey Medical Center, Hershey, PA

Background: Granular cell tumors (GrCT) of granular nerve sheath phenotype exhibit distinctive cytoplasmic lysosomal inclusions. We previously described histologic criteria for atypical and malignant GrCT. After an index malignant case, we wanted to review our recent institutional experience with GrCT.

Design: Slides, blocks, phenotype, and reports on cases coded as "GrCT" from our institutional files, 2007-2017, were pulled and analyzed. Cases re-classified as congenital granular cell epulis or other were excluded. Histologic criteria used for atypical and malignant were as we previously described, additionally requiring increased or atypical mitoses and/or necrosis for malignant. Targeted molecular phenotypic data and multivariate analysis are pending.

Results: 44 GrCT occurred in 33 patients: 22 females, 11 males, mean age 36, age range 4-70, years, and mean tumor size 1.7 cm. The largest sizes, 4.6, 6.0, and 15.5 cm, ultimately correlated with histologically malignant. GrCT were equal sided and originally involved aerodigestive mucosa of esophagus (n=5), cecum/colon (n=5), and one each stomach, trachea, endobronchial, *or* skin/soft tissue of arm/finger (n=5), thigh/leg/foot (n=5), chest/breast (n=4), head and neck (n=3), vulva (n=2) and penis (n=1). 8 patients, one each leg, arm, head and neck, penis, trachea, endobronchial, and two esophageal, underwent 1-3 reexcisions at the same site over 1 to 7 years. Lesions without atypia were considered multifocal synchronous and metachronous, with persistent disease, including penis, both esophageal, and endobronchial. Most granular cell tumors were infiltrative in dermis/subcutis equivalent, with recurrent and ultimately atypical or malignant tumors involving deep muscle. Tumors classified as atypical (n=6, recurrent = 2) or ultimately malignant (n=3, recurrent = 2, metastatic = 1) demonstrated looser Zellballen pattern, in addition to other required histologic criteria.

Conclusions: GrCT, most common in skin/soft tissue sites in middle aged females, exhibit loss of cohesive Zellballen pattern as another atypical feature. Multiple GrCT are multifocal rather than multicentric and involve skin/soft tissue-only or visceral-only, synchronous or metachronous, including histologically-benign usually upper aerodigestive tract "persistent" disease. Our designation as "atypical" or "malignant" correlates with size, depth and behavior. Studies to compare genetic/phenotypic analysis with classification and outcome are underway.

535 Genetic Profiling of Microcystic Adnexal Carcinoma

May P Chan[1], *Aaron M Udager*[2], *Komal Kunder*[3], *Rajiv Patel*[4], *Aleodor Andea*[1], *Lori Lowe*[3], *Douglas Fullen*[1], *Alison B Durham*[3], *Timothy M Johnson*[3], *Chia-Jen Liu*[3], *Scott Tomlins*[1], *Paul Harms*[1]. [1]University of Michigan, Ann Arbor, MI, [2]University of Michigan Medical School, Ann Arbor, MI, [3]University of Michigan, [4]Univ. of Michigan, Ann Arbor, MI

Disclosures:
Scott Tomlins: *Employee*, Strata Oncology

Background: Microcystic adnexal carcinoma (MAC) can be difficult to diagnose clinically and histopathologically, especially in partial biopsies. Complete resection is the key to ensuring favorable outcome, however, clear margins are often difficult to obtain owing to its typically infiltrative growth. Genetic profiling of MAC may help facilitate accurate diagnosis and identify potential targetable oncogenic drivers.

Design: Paraffin-embedded formalin-fixed tissues from 10 MACs were studied by targeted, multiplexed PCR-based DNA next-generation sequencing (NGS) of the coding sequence of over 400 cancer-relevant genes.

Results: Somatic mutation burden was variable, with an average of 10 prioritized nonsynonymous mutations per tumor (range: 2-30). Based upon prioritized mutations, the majority of tumors lacked UV signature mutational profiles. Mutations in either *NOTCH2* or *NOTCH4* were present in 3 tumors. *EGFR* mutations were detected in 2 tumors, including 1 mutation previously identified in lung carcinoma. *TP53* mutations were not detected. Multiple copy number alterations were detected in 9 tumors. Recurrent alterations included gains of *MAF* or *MAFB* (40%), gains of *CEBPA* (40%), losses of *TCF3* (40%), and losses of *PAX7* (40%). Arm-level gains were identified in 4 tumors, 2 of which displayed gains of 8q suggesting a role for *MYC*. Considering both amplifications and mutations, mutually exclusive alterations in *EGFR* or *FGFR* family tyrosine kinases were present in 4 tumors. None of the genetic changes were significantly associated with clinical or histopathologic features.

Conclusions: To our knowledge, this is the first NGS study of MACs. Our cases demonstrate heterogeneous genetic changes including both somatic mutations and copy number alterations, with potential drivers involved in dysregulated receptor tyrosine kinase signaling and MAF transcription factor activation. Despite classically arising on sun-damaged skin, MAC differs from more common skin tumors such as squamous cell carcinoma and basal cell carcinoma, in that MAC is less consistently associated with UV signature mutations and lacks *TP53* mutations. Our findings suggest that there may be multiple molecular subtypes of MAC, and their distinct genetic changes may have potential diagnostic and therapeutic implications.

536 Programmed Death Ligand-1 (PD-L1), a Potential Marker to Distinguish Dermatomyositis and Systemic Lupus Erythematosus

Dong Chen[1], *Kara M Braudis*[2]. [1]University of Missouri Columbia, Columbia, MO, [2]University of Missouri Columbia

Background: Dermatomyositis (DM) is an idiopathic inflammatory myopathy with distinct skin rashes. Systemic lupus erythematosus (SLE) is a chronic immune disorder majorly affecting skin and joints. There are 4-16% of the clinical cases presented with overlapping symptoms of SLE with idiopathic polymyositis or DM. Characteristic DM skin rashes can occur before or after lupus or present simultaneously. The gold standard to diagnose DM is muscle biopsy. Skin biopsies cannot always distinguish DM from lupus. The immune-checkpoint protein, Programmed Death Ligand-1 (PD-L1) has been studied for a decade but PD-L1 expressions in biopsied skin of DM and SLE patients are still unclear. Here we investigate PD-L1 as a biomarker to distinguish DM and SLE in skin biopsies.

Design: Twenty patients' specimens (seven DM, seven SLE, four subacute spongiotic dermatitis and two cytotoxicity interface dermatitis) are obtained from the University Healthcare System. The patients with SLE and DM in this study are diagnosed by dermatologist and dermatopathologist based on 2012 Systemic Lupus International Collaborating Clinics (SLICC) and 2016 Lundberg, Miller and Bottai's criteria. The skin biopsy slides are stained with Hematoxylin and Eosin (H&E) and sent to Boyce and Bynum Laboratory for Immunohistochemical study of Programmed Death Ligand-1 protein expression (antibody concentration 1:100). All results are evaluated by one pathologist and one dermatopathologist as followed. The PD-L1 protein expression on lymphocytes is scaled from 0 to 3 in the dermoepidermal junction (DEJ) and dermis respectively and the mean of PD-L1 protein expression in patients with DM and SLE are compared with Student's t-test and $p<0.05$ is regarded as statistical significant.

Results: In skin biopsies, patients with dermatomyositis have brisker PD-L1 protein expression (DEJ mean 2.29, 95% Confidence Interval CI 1.58 to 2.99, $p=0.02$; dermis mean 2.71, 95% CI 2.35 to 3.08, $p<0.01$) than patients with SLE (DEJ mean 0.57, 95% CI -0.01 to 1.15; dermis mean 0.71, 95% CI 0.70 to 0.73). In patients with cytotoxicity interface dermatitis, weak protein expressions of PD-L1 are identified in DEJ and dermis. In subacute spongiotic dermatitis PD-L1 protein is absent in DEJ and weakly expressed in dermis (mean 0.75, 95% CI 0.26 to 1.24). (Figure 1 & 2).

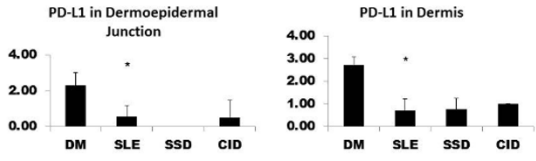

Figure 1. PD-L1 protein expression in patients with Dermatomyositis (DM), Systemic Lupus Erythematosus (SLE), Subacute Spongiotic Dermatitis (SSD) and Cytotoxicity Interface Dermatitis (CID) in the Dermoepidermal junction (DEJ) and Dermis areas respectively. The PD-L1 expression in patients with DM are stronger than the ones with SLE ($p<0.05$).

" * " means statistical significant.

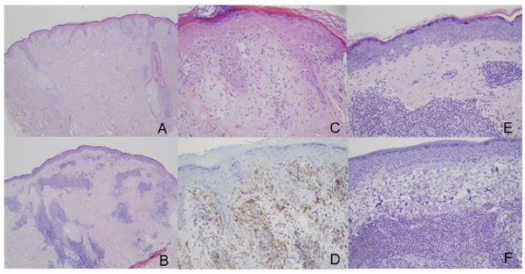

Figure 2. Staining patterns of PD-L1 protein in Dermatomyositis (DM) and Systemic Lupus Erythematosus (SLE). (A) DM (H&E x 50). (B) SLE (H&E x 50). (C) DM (H&E x 200). (D) Strong positivity for PD-L1 immunostain of lymphocytes in patient with DM in Dermoepidermal junction (DEJ) and Dermis area. (E) SLE (H&E x 200). (F) Weak expression of PD-L1 on lymphocytes in patient with SLE in DEJ and Dermis area.

Conclusions: PD-L1 protein expression can aid in the histopathologic differentiation between Dermatomyositis and Systemic Lupus Erythematosus.

537 Expression of Neuroendocrine Key Regulators in Merkel cell carcinoma

Emil Chteinberg[1], *Christopher Sauer*[1], *Dorit Rennspiess*[1], *Véronique Winnepenninckx*[1], *Anna Kordelia Kurz*[2], *Ernst-Jan Speel*[β], *Martin Zenke*[2], *Axel zur Hausen*[4]. [1]Maastricht University Medical Center, [2]University Hospital RWTH Aachen, [3]Maastricht University Medical Centre, Maastricht, Limburg, NLD, [4]Maastricht

Background: Merkel cell carcinoma (MCC) is a highly aggressive non-melanoma skin cancer of the elderly which is associated with the Merkel cell polyomavirus (MCPyV). MCC reveals a trilinear differentiation characterized by neuroendocrine, epithelial and pre/pro B-cell lymphocytic marker expression. However, the cellular origin of MCC remains elusive.

Design: Here we investigated the expression of the neuroendocrine key regulators Re-1 silencing transcription factor (REST), neurogenic differentiation 1 (NeuroD1) and the Achaete-scute homologe 1 (ASCL1) in MCC.

Results: The expression of REST in MCC was analysed by immunohistochemistry (IHC) in 28 formalin fixed and paraffin embedded MCC tissues. Further, MCPyV-positive (MKL-1, MKL-2 and WaGa) and MCPyV–negative (MCC13 and MCC26) MCC cell lines and the B-ALL cell-line REH as positive control were tested for REST, ASCL1 and NeuroD1 expression. Quantitive and normal RT-PCR was used to confirm the results of the cell lines on the transcriptional level. Q-RT-PCR was used to illustrate the expression of neuroendocrine genes: chromogranin A, synaptophysin and miRNA miR-9 and miR-9* in the cell lines.

REST tagged with GFP was inserted into WaGa cells and analyzed for their expression of chromogranin A and synaptophysin. In addition, the regulation of the REST expression by methylation was assessed with the demethylating agent 5-aza-2′-deoxycytidin. Further the methylation status of the CpG islands of the REST promoter was analysed with a methyl specific PCR (MSP).

We found that all MCCs are devoid of REST and ASCL1 and express NeuroD1. Further, the REST expression is restricted to MCPyV-negative MCC cell lines. NeuroD1 was detected in all cells and tissues. The lack of the neuroendocrine master regulator ASCL1 in almost all tested MCCs points to an important role of the absence of the negative regulator REST towards the MCC neuroendocrine phenotype. This is underlined by the expression of the REST-regulated microRNAs miR-9/9* in REST-negative MCC cell lines.

Table 1: Summary of the clinico-pathological data of the MCC patients and MCC tisssues including the results of the immunohistochemical assessment of REST, ASCL1 and NeuroD1.

ID= identity, M= male, F= female, Dx= diagnosis, MCC= Merkel cell carcinoma; Histo: histology; int = intermediate, s. c. = small cell, pos.= positive, neg.= negative, - = no expression, + = weak expression, ++ = moderate expression, +++ = strong expression.

ID	gen-der	age	location	Dx	Histo	MCPyV	REST	Ascl1	NeuroD1
Primary MCCs									
1	m	63	head	MCC	int.	pos.	-	-	++ heter.
2	m	92	ear	MCC	s.c.	neg.	-	-	+++
3	f	85	buttocks	MCC	s.c.	pos.	-	-	+++
4	m	69	lip	MCC	int.	pos.	-	-	++
5	f	93	upper eye lid	MCC	int.	pos.	-	-	+
6	f	60	tongue	MCC	int./ s.c	pos.	-	-	++ heter.
7	m	74	upper leg	MCC	int.	pos.	-	-	+++
8	m	93	head	MCC	int.	neg.	-	++ foc.	+++
9	f	76	buccal	MCC	int.	pos.	-	-	++
10	f	91	arm	MCC	int.	pos.	-	n.a.	n.a.
11	f	83	upper eye lid	MCC	int.	pos.	-	-	+++
12	f	76	head	MCC	int.	pos.	-	n.a.	n.a.
13	m	77	neck	MCC	int.	neg.	-	-	+++
14	m	79	head	MCC	int.	pos.	-	-	++
15	f	71	buccal	MCC	int.	pos.	-	-	++
16	m	68	buttocks	MCC	int.	pos.	-	-	+++
17	f	58	buccal	MCC	int./ s.c	pos.	-	-	+++
18	m	75	upper leg	MCC	int	pos.	-	-	+++
19	f	65	arm	MCC	in	pos.	-	-	++
20	m	63	buccal	MCC	int./ s.c	neg.	-	-	++
Metastatic MCC s									
21	m	71	pancreas	MCC met.	int.	pos.	-	-	++
22	f	75	LN neck	MCC met.	int.	pos.	-	-	++
23	f	66	skin	MCC met.	int.	pos.	-	-	(+)
24	m	74	groin	MCC met.	int.	pos.	-	-	+++heter.
25	f	67	upper arm	MCC met.	int.	pos.	-	-	+++heter.
26	m	65	LN neck	MCC met.	int.	neg.	-	-	++heter.
27	f	43	LN groin	MCC met.	int.	pos.	-	-	++
28	m	69	LN iliaca	MCC met.	int./ s.c.	pos.	-	++het-er.	++

Conclusions: The REST-less state of MCC and of MCPyV-positive MCC cell lines, in combination with REST expression in MCPyV-negative cell lines points to an important role of MCPyV in the regulation of REST expression. This is emphasized by the unmethylated REST promoter CpGs of all tested cell lines. Our data provide the basis for the neuroendocrine gene expression profile in MCC which might be induced by MCPyV and thus will help to elucidate the cellular origin of MCC.

538 Is PI3K p110δ Expressed and Functional in Merkel Cell Carcinoma?

Emil Chteinberg[1], *Dorit Rennspiess*[1], *Véronique Winnepenninckx*[1], *Ernst-Jan Speel*[β], *Anna Kordelia Kurz*[3], *Martin Zenke*[3], *Axel zur Hausen*[4]. [1]Maastricht University Medical Center, [2]Maastricht University Medical Centre, Maastricht, Limburg, NLD, [3]University Hospital RWTH Aachen, [4]Maastricht

Background: Merkel cell carcinoma (MCC) is a highly malignant skin cancer of the elderly. The majority of MCC is causally linked to Merkel cell polyomavirus (MCPyV). The prognosis of stage III/IV MCC is very poor. Recently a complete clinical response induced by the PI3K p110δ specific inhibitor idelalisib in a patient with stage IV MCC - with proven p110δ transcript expression by qRT-PCR -has been reported by Shiver et al. Here we aimed to assess the expression and functionality of p110δ in MCC cell lines.

Design: The expression of p110δ in MCC was tested in 5 MCPyV+ MCC cell lines, 2 MCPyV- MCC cell lines, the multiple myeloma cell line U266 and the B-ALL cell line REH by immunofluorescence microscopy (IFM). Further, MKL-1, MKL-2, MCC13, MCC26, REH and U266 were treated with idelalisib and the specific p110α inhibitor Byl719. The decrease of cell viability was analysed with XTT assay. Further the functional inhibition of p110δ subunit in the treated cell lines was assessed by Western-blotting for the presence of phosphorylated AKT.

Results: Immunofluorescence microscopy revealed a specific cytoplasmic p110δ expression in 71.4% of the tested MCCs. Moreover, the MCPyV-positive MKL-1, MKL-2, WaGa, PeTa as well as the MCPyV-negative MCC cell lines MCC13 and MCC26 were positive for p110δ. Treatment with idelalisib of these cell lines resulted in high IC_{50} values. Only MKL-1 showed a 10-fold higher IC_{50} compared to REH. The cell viability of the other MCC cell lines were much more resistant towards the treatment with idelalisib. Moreover, only MKL-1 showed a significant decrease of phosphorylated Akt. Of interest, the inhibition of the p110α subunit with BYL719 revealed a higher impact compared to idelalisib: a 30-fold on WaGa cells, 15-fold on PeTa cells and 3-fold on the other MCC cell lines.

primary MCCs							
ID	gender	age	location	dx	histo	MCPyV	PI3K p110δ
1	m	63	head	MCC	int.	pos.	+
2	m	92	ear	MCC	s.c.	neg.	++
3	f	85	buttocks	MCC	s.c.	pos.	++
4	m	69	lip	MCC	int.	pos.	++
5	f	93	upper eye lid	MCC	int.	pos.	+heterogen
6	f	60	tongue	MCC	int./s.c	pos.	-
7	m	74	upper leg	MCC	int.	pos.	-
8	m	93	head	MCC	int.	neg.	++
9	f	76	buccal	MCC	int.	pos.	-
12	f	83	upper eye lid	MCC	int.	pos.	++
14	m	74	upper leg	MCC	int.	pos.	++
15	m	77	neck	MCC	int.	neg.	++
16	f	66	arm	MCC	int.	pos.	++
17	m	79	head	MCC	int.	pos.	-
19	m	68	buttocks	MCC	int.	pos.	++
20	f	58	buccal	MCC	int./s.c	pos.	++
24	m	74	Upper leg	MCC	int.	pos.	-
30	m	63	upper lip	MCC	int.	n.a.	++

metastases MCC							
ID	gender	age	location	dx	histo	MCPyV	PI3K p110δ
21	m	71	pancreas	MCC met.	int.	pos.	+
22	f	75	LN neck	MCC met.	int.	pos.	++
25	f	66	skin	MCC met.	int.	pos.	-

Conclusions: Here we report the expression of PI3K p110δ in MCC tissues and cell lines. However, the treatment with idelalisib of MCPyV-positive and -negative cell lines revealed a higher resistance towards the p110δ specific inhibitor idelalisib compared to the leukemia cell line REH. Based on these results it might be insufficient to treat MCCs alone with idelalisib.

539 Immunohistochemical Evaluation of Galectin-3 and Cathepsin K Expression in Cutaneous Fibrohistiocytic and Undifferentiated Lesions

Antonio De Leo[1], *Claudio Ceccarelli*[2], *Doriana Donatella Di Nanni*[3], *Valentina Agostini*[4], *Costantino Ricci*[5], *Barbara Corti*[6]. [1]S.Orsola-Malpighi Hospital, University of Bologna, Bologna, [2]S.Orsola-Malpighi Hospital, University of Bologna, Bologna, [3]S.Orsola-Malpighi Hospital, University of Bologna, Bologna, Italy, [4]S.Orsola-Malpighi Hospital, University of Bologna, Bologna, [5]Sant'Orsola-Malpighi Hospital, University of Bologna, Bologna, Italy [6]S.Orsola-Malpighi Hospitale, University of Bologna, Bologna

Background: The fibrohistiocytic tumors of the skin constitute a heterogeneous group of mesenchymal neoplasms whose diagnosis can be particularly challanging, especially in superficial biopsies. The assessment of an appropriate immunohistochemical panel is crucial to guide pathologists in the diagnosis and classification of these tumors.

Design: The aim of the study was to evaluate the immunohistochemical expression of Galectin-3 and Cathepsin K in a cohort of cutaneous fibrohistiocytic and undifferentiated lesions (25 dermatofibromas, 3 atypical dermatofibromas, 3 dermatofibrosarcoma protuberans, 4 undifferentiated pleomorphic sarcomas). A group of several other lesions (3 Kaposi sarcomas, 3 neurofibromas, 1 cutaneous leiomyoma, 1 piloleiomyoma,) were also taken into account as reference. Each case was semiquantitavely scored by the proportion of positive cells and staining intensity.

Results: Strong and diffuse immunoreactivity for Galectin-3 and Cathepsin K was found in all dermatofibromas (25/25, 100%) and atypical dermatofibromas (3/3, 100%), and in all undifferentiated pleomorphic sarcomas (4/4, 100%). Cases of dermatofibrosarcoma protuberans have shown a patchy and weak background staining, in contrast to the diffuse, strong and crisp staining seen in fibrohistiocytic tumors. None of the other lesions were immunolabeled by the two markers.

Conclusions: Galectin-3 resulted to be a novel and sensitive marker in cutaneous fibrohistiocytic and undifferentiated lesions. Interestingly, the combined expression of Galectin-3 and Cathepsin K was found to be constantly and strongly observed in dermatofibroma, including its variants, and in cutaneous undifferentiated pleomorphic sarcoma. Our findings suggest that Galectin-3 and Cathepsin K can be used as a part of the immunohistochemical panel for the diagnosis of fibrohistiocytic and undifferentiated lesions, and they result to be particularly helpful in superficial biopsies when facing problematic and ambiguous cases.

540 PREVIOUSLY PUBLISHED

541 Epithelioid Fibrous Histiocytoma: Molecular Characterization of ALK Fusion Partners in 23 Cases

Brendan C Dickson[1], *David Swanson*[2], *George S Charames*[1], *Christopher D Fletcher*[3], *Jason L Hornick*[3]. [1]Mount Sinai Hospital, Toronto, ON, [2]Mount Sinai Hospital, Toronto, ON, [3]Brigham and Women's Hospital, Boston, MA

Background: Epithelioid fibrous histiocytoma is a rare and distinctive cutaneous neoplasm. Most cases harbor *ALK* rearrangement and show ALK overexpression, which distinguish this neoplasm from conventional cutaneous fibrous histiocytoma and variants. *SQSTM1* and *VCL* have previously been shown to partner with *ALK* in one case each of epithelioid fibrous histiocytoma. The purpose of this study was to examine a large cohort of epithelioid fibrous histiocytomas by next-generation sequencing to characterize the nature and prevalence of *ALK* fusion partners.

Design: A retrospective archival review was performed to identify cases of epithelioid fibrous histiocytoma received from 2012 – 2016. Each case was re-reviewed to confirm the diagnosis, and immunohistochemistry was performed to confirm the presence and pattern of ALK expression. Targeted next-generation sequencing was applied on RNA extracted from formalin-fixed paraffin-embedded tissue to identify the fusion partners. The results were analyzed using both Manta and JAFFA fusion callers.

Results: Twenty-three cases fulfilled inclusion criteria and contained RNA suitable for analysis. The mean patient age was 39 years (range, 8 – 74 years), there was no sex predilection, and >75% of cases involved the lower extremities. The most common gene fusions were *SQSTM1-ALK* (N=12; 52%) and *VCL-ALK* (N=7; 30%); the other four cases harbored novel fusion partners (*DCTN1*, *ETV6*, *PPFIBP1*, and *SPECC1L*). The pattern of ALK immunoreactivity was usually granular cytoplasmic staining (N=12; 52%) or granular cytoplasmic and nuclear (N=10; 43%); the case containing an *ETV6* fusion partner showed nuclear staining alone. There was no apparent relationship between tumor morphology and the *ALK* fusion partner.

Conclusions: *SQSTM1* and *VCL* are the most common *ALK* fusion partners in epithelioid fibrous histiocytoma; *DCTN1*, *ETV6*, *PPFIBP1*, and *SPECC1L* represent rare fusion partners. The proteins encoded by these genes play diverse roles in scaffolding, cell adhesion, and transcription (among others) without clear commonalities. These findings expand the oncogenic promiscuity of many of these *ALK* fusion genes, which drive neoplasia in tumors of diverse lineages with widely varied clinical behavior. This is the first documented account of *ETV6-ALK* and *SPECC1L-ALK* translocations in neoplasms.

542 Tumor Microenvironment in Mycosis Fungoides: Role of Lymphocyte Exhaustion

Caterina Fumagalli[1], *Maria del Valle Rodríguez Santás*, *Maitane Perez-Olabarria*[2], *M. Pilar García-Muret*[3], *Silvana Novelli*[3], *Justyna Szfranska*[4], *Ana Mozos Rocafort*[5]. [1]Hospital de la Santa Creu i Sant Pau, Barcelona, [2]Hospital Sant Pau, Barcelona, [3]Hospital de la Santa Creu i Sant Pau, [4]Hospital Santa Creu i Sant Pau, Barcelona, [5]Hospital Sant Pau, Barcelona, Spain

Background: Mycosis fungoides (MF) is an indolent cutaneous T-Cell lymphoma. Recent studies show that tumor microenvironment (TM) plays a crucial role and may determine disease progression and tumor escape from immunosurveillance. T cells are exposed to persistent inflammatory signals that lead to "T cell exhaustion", which manifests with progressive loss of effector functions and sustained upregulation of multiple inhibitory receptors, including programmed cell death protein 1 (PD1) and lymphocyte activation gene 3 protein (LAG3).

Our aims are to evaluate the expression of PD1, its ligand PDL1 and LAG3 in a cohort of patients (pts) with MF and to evaluate whether it may have an impact on overall survival (OS).

Design: 65 patients (36males, 29 females, median age: 55yo) with MF were reviewed, with a mean follow-up of 125 months (range: 6-450m). 52 pts were diagnosed as early stage (I&IIa) and 13 pts as advanced stage (>IIb). Large cell transformation was observed in 12 pts. All cases were stained with PD1 (clone NAT105), PDL1 (clone 22C3) and LAG3 (clone 11E3). Statistical analysis was performed.

Results: MF cells expressed PD1 in 92% of cases, in early stages with a low proportion (<20%) of PD1-positive cells, while in advanced stages most cases expressed PD1 in more than 20% of neoplastic cells (p=0.001) (Table 1). PDL1 was expressed in more than 5% of cells in 15 cases, mainly in the cytoplasm of macrophages, but not in neoplastic cells (Table 1). LAG3 was positive in few lymphocytes in only 2 cases. We found no correlation between PD1, PDL1 and LAG3 expression. Cytological atypia, age >60yo and advanced stage had a negative impact on OS (p<0.05). A weak correlation between atypia, PD1-positive cells and PD1 intensity was found (r<0.5).

	PD1 < 20%	PD1 >20%	PDL1 <5%	PDL1>5%
Early stage	37	15	40	12
Advanced stage	3	10	10	3

Conclusions: In our series, most cases expressed PD1 indicating that TM may play a role in MF. We also found PDL1 expression in TM of our cases, suggesting that PD1/PDL1 pathway could be implicated in tumor escape from immunosurveillance, as seen in different solid tumors. However, we couldn't demonstrate a statistical correlation between PD1, PDL1 and LAG3, raising the possibility that others PD1-ligands, such as PDL2, have a role in MF. Moreover, the high expression of PD1 in MF indicates that it could be useful as an additional therapeutic target in MF.

543 Utility of Multi-Step Protocols in the Analysis of Sentinel Lymph Nodes in Cutaneous Melanoma: An Assessment of 195 Cases

Pavandeep Gill[1], *Jenika Howell*[2], *Christopher Naugler*[3], *Marie Abi Daoud*[4]. [1]University of Calgary, Calgary, AB, [2]Calgary Lab Services, Calgary, AB, [3]University of Calgary, [4]University of Calgary and Calgary Lab Services, Calgary, AB

Background: Currently, no universal protocol exists for the assessment of sentinel lymph nodes (SLNs) in cutaneous melanoma. Many institutions employ a multi-step approach with multiple hematoxylin and eosin (H&E) and immunohistochemical stains. However, this can be a costly and time-, and resource-consuming task. Our objective is to assess the utility for multi-step protocols in the analysis of melanoma SLNs by specifically evaluating the SLN protocol at our institution (which consists of 3 H&Es, one S-100 protein, one HMB-45, and one Melan-A slide per melanoma SLN block) and to develop a more streamlined protocol.

Design: Histological slides from SLN resections from 195 patients with diagnosed cutaneous melanoma were submitted to our dermatopathology group. Tissue blocks were processed according to our institutional SLN protocol. The slides were re-reviewed to determine whether or not metastatic melanoma was identified microscopically at each step of the protocol. Using SPSS software, a decision tree was then created to determine which step most accurately reflected the true diagnosis.

Results: We found with Melan-A immunostain, 99.4% of negative SLNs are correctly diagnosed as negative and 100% of positive nodes are correctly diagnosed as positive. With the addition of an H&E level, 100% of SLNs are accurately diagnosed.

Conclusions: We recommend routine melanoma SLN evaluation protocols be limited to two steps: one routine H&E stain and one Melan-A stain. This protocol is both time- and cost-efficient and yields high diagnostic accuracy.

544 Consultation Patterns in Cutaneous Sarcomas, Mesenchymal Tumors of Intermediate Malignancy, and Their Mimics

John Gross[1], *Jennifer Ko*[2], *Steven Billings*[3]. [1]Creighton University, Omaha, NE, [2]Cleveland Clinic, Cleveland, OH, [3]Cleveland Clinic, Cleveland, OH

Background: Cutaneous sarcomas, mesenchymal tumors of intermediate malignancy, and their mimics are a frequent source of diagnostic difficulty necessitating second opinion consultation for accurate classification.

Design: With IRB approval, cutaneous soft tissue pathology consultation archives of senior authors from 2015 to 2017 were reviewed for diagnoses of cutaneous sarcomas, mesenchymal tumors of intermediate malignancy, and mimics, with clinicopathologic annotation. All cases were reviewed by an additional pathologist with a special interest in soft tissue pathology. Submitting pathologist diagnoses and/or differential diagnoses were recorded.

Results: In total, 277 cases met criteria (186 cutaneous sarcomas and mesenchymal tumors of intermediate malignancy, 33 sarcomatoid squamous cell carcinomas, 16 spindle cell/desmoplastic melanomas and 42 cases of nodular fasciitis). Of these, 194 (70%) cases were submitted with either final diagnoses (137, 49%) or differential diagnoses which included (40, 14%) or did not include (17, 6%) final diagnoses. The most frequent misdiagnosis was sarcomatoid squamous cell carcinoma (15/25, 60%), followed by spindle cell/desmoplastic melanoma (4/10, 40%), cutaneous sarcomas and mesenchymal tumors of intermediate malignancy (28/131, 21%) and nodular fasciitis (4/28, 14%). Findings by misdiagnosis are summarized in Table 1 whereas the breakdown by diagnosis of cutaneous sarcomas and mesenchymal tumors of intermediate malignancy is summarized in Table 2.

TABLE 1. Cutaneous Sarcomas and Tumors of Intermediate Malignancy, Their Mimics, And Misdiagnosis (Single Institution Consultation Experience, 2015-2017).

FINAL DIAGNOSIS	Sarcomas and Mesenchymal Tumors of Intermediate Malignancy	Sarcomatoid squamous cell carcinoma	Spindle cell desmoplastic melanoma	Nodular fasciitis
Benign diagnosed sarcoma	----------	----------	----------	4/28 (14%)
Sarcoma diagnosed benign	20/131 (15%)	----------	----------	----------
Mesenchymal diagnosed non-mesenchymal	8/131 (6%)	----------	----------	0/28 (0%)
Non-mesenchymal diagnosed mesenchymal	----------	15/25 (60%)	4/10 (40%)	----------
No submitting pathologist diagnosis	55/186 (30%)	8/33 (24%)	6/16 (38%)	14/42 (33%)
Total	28/131 (21%)	15/25 (60%)	4/10 (40%)	4/28 (14%)

TABLE 2. Cutaneous Sarcomas and Mesenchymal Tumors of Intermediate Malignancy by Number (Single Institution Consultation Experience, 2015-2017).

SARCOMA TYPE	No. (%) of Cases	MESENCHYMAL TUMORS OF INTERMEDIATE MALIGNANCY	No. (%) of Cases
Myxofibrosarcoma	20/186 (11%)	Atypical fibroxanthoma/Pleomorphic dermal sarcoma	57/186 (31%)
Angiosarcoma	16/186 (9%)	Dermatofibrosarcoma protuberans	23/186 (12%)
Undifferentiated pleomorphic sarcoma	11/186 (6%)	Vascular (Hemangioendothelioma, Kaposi sarcoma)	9/186 (5%)
Leiomyosarcoma	10/186 (5%)	PEComa	3/186 (2%)
Other	33/186 (17%)	Other	4/186 (2%)
Total	90/186 (48%)	Total	96/186 (52%)

Conclusions: The recognition and subsequent diagnosis of cutaneous sarcomas and mesenchymal tumors of intermediate malignancy and their mimics is critical for accurate treatment and clinical decision-making. Increased awareness by pathologists of these diagnostic pitfalls should improve tumor classification and patient outcomes.

545 An Integrated Approach to Prognostic Biomarker Discovery in Malignant Melanomas

James A Isom[1], *Alan E Siroy*[2], *Jena Auerbach*[3], *Nemanja Rodic*[4]. [1]University of Florida, Gainesville, FL, [2]University of Florida College of Medicine, Gainesville, FL, [3]Montefiore Medical Center, Scottsdale, AZ, [4]University of Florida

Background: Studies of heritable changes in human neoplasms traditionally focus on identification of single nucleotide changes that may have diagnostic, prognostic, and/or predictive clinical ramifications. Such approaches can cause delay in discovery as methodology relies on cancer gene panels, requiring *a priori* knowledge about putative target genes. Moreover, recurrent mutations in many cancers often mark only a portion of all incident cases, due to underlying heterogeneity and variable chromosomal abnormalities that are hallmarks of all cancers.

Design: Herein, we performed a meta-analysis of the melanoma transcriptome available from the Human Protein Atlas database. Specifically, we analyzed 163 genes associated with unfavorable prognosis in a cohort of 102 cutaneous malignant melanoma cases. To start, we manually procured, annotated, and cataloged previous reports on all identified genes using PubMed Central archive to determine whether they have been previously implicated in melanoma tumorigenesis. We then performed two-part gene regulatory network analysis to identify biological pathways implicated in aggressive melanomas. Combined use of these two resources allowed us to identify active genetic pathways in aggressive melanomas.

Results: Examination of 163 genes associated with unfavorable prognosis in malignant melanomas revealed that majority—

specifically 114 genes—has not previously been identified as playing a role in melanomagenesis. Additional 34 genes have only rarely been identified as playing a role in melanoma tumorigenesis, with reports limited to a single or a couple of preclinical studies per gene. Remaining 15 genes have been well-studied, with an average of 26 published reports linking each gene to melanoma tumorigenesis. When we compared understudied genes category (less than three published report per gene; n = 148) to well-studied genes (26 published report per gene on average; n = 15), the difference is statistically significant ($p = 4.9 \times 10^{-10}$, two-tailed test). Finally, our gene pathway analysis showed that genes associated with unfavorable prognosis in malignant melanomas belong to DNA replication and cell cycle pathways.

Conclusions: Combining publically-available raw datasets and bioinformatics platforms provides an attractive alternative for pathology-based research. Our study highlights that most genetic factors governing melanoma tumorigenesis are understudied and that more work is needed to elucidate the genetic basis of melanoma growth.

546 Comparative Methylome Analysis in Cutaneous Malignant Peripheral Nerve Sheath Tumors and Spindle/Desmoplastic Melanomas

George Jour[1], *Victor Prieto*[2], *Carlos Torres-Cabala*[3], *Nicole K Andeen*[4], *Jie Yang*[5], *Erik Sulman*[6], *Phyu Aung*[7]. [1]MD Anderson at Cooper, Philadelphia, PA, [2]UT - MD Anderson Cancer Center, Houston, TX, [3] Houston, TX, [4]Oregon Health & Science University, Portland, OR, [5]MD Anderson Cancer Center, [6]MD Anderson Cancer Center UT Graduate School of Biomedical Science, [7]U. T. - M. D. Anderson Cancer Center, Houston, TX

Background: Superficial / cutaneous malignant peripheral nerve sheath tumor (cMPNST) is a rare, soft tissue neoplasm that shares an immune molecular signature and morphological features with spindle and desmoplastic melanoma (S/DM). Herein we seek to investigate a possible DNA methylome signature based on differentially methylated regions (DMR) for diagnostic and prognostic purposes.

Design: DNA from formalin-fixed, paraffin-embedded (FFPE) tissue was extracted and processed. Methylation status was assessed using Infinium Methylation EPIC array targeting >850,000 methylation site (CpG) islands. Data from raw files were normalized and analyzed in order to detect differentially methylated regions for coding genes and miRNA (using ANOVA test with adjusted FDR's) with subsequent enrichment and pathway analysis.

Results: Thirty patients (S/DM=15, cMPNST=15, male n=22, female n=8) were included. ANOVA test adjusting for cofounders including age, sex and location, identified 12,209 cancer associated differentially methylated regions (cDMRs) in coding genes and miRNAs (figure 1). Hypo-methylated loci regulating key genes relevant to MPNST were also seen in c-MPNST such as *EZH2 (*but not *BRD4). S*ome hyper-methylated loci relevant to melanoma were identified in the SDM including *mir124* and *mir125b. Mir-205* was selectively hypo-methylated in the SDM group. 47 hypo-methylated loci regulating zinc finger ZNF family genes involved in transcriptional regulation were identified (27 and 20 hypo methylated loci in cMPNST and SDM, respectively). Loci regulating *ZNF473* were hypo methylated in both cMPNST and SDM. 50 long non-coding RNA (lncRNA) loci regulating key genes such as *DDITL4* (part of mTOR signaling pathway) were hypermethylated in the SDM group. KEGG Pathway analysis showed the cDMRs to be enriched for *BCAT1/c* (related Valine, Leucine and isoleucine biosynthesis) in cMPNST but not SDM, adj. $p < 0.05$. GO pathways analysis showed hypomethylation was increased in multiple pathways related to cell migration, including focal adhesion, cell adhesion, transendothelial migration and extracellular matrix interactions in c-MPNST but not SDM

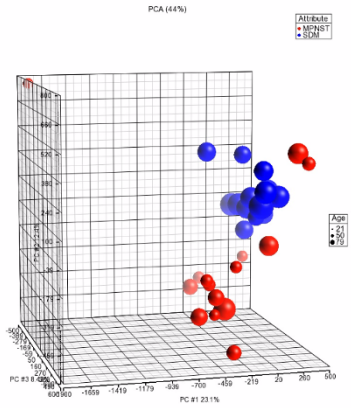

Conclusions: Methylation profile in c-MPNST and SDM differ from MPNST and conventional melanoma . *ZNF473* upregulation is involved in cMPNST and SDM tumorigenesis. *BCAT1/c* is a novel and potentially targetable (BCAT1/c inhibitors) methylome signature differentiating cMPNST from SDM. Integration of methylation data with gene expression data is warranted and is underway.

547 SLAM Family Member 8 Is Involved in the Oncogenic KIT-Mediated Growth of Mastocytosis via SHP-2

Tatsuki Kataoka[1], *Akihiko Sugimoto*[2], *Masahiro Hirata*[3], *Yusuke Takei*[4], *Chiyuki Ueshima*[3], *Sachiko Minamiguchi*[5], *Hironori Haga*[5]. [1]Kyoto University Hospital, Kyoto, [2]Kyoto University Hospital, Sakyo-ku, Kyoto City, Kyoto, [3]Kyoto University Hospital, [4]Kyoto University Hospital, Kyoto, Japan, [5]Kyoto

Background: The signaling lymphocytic activation molecule (SLAM) family members are transmembrane proteins and play positive and negative roles in hematopoietic cells. Their signals are mediated by SLAM-associated protein (SAP) or Ewing's sarcoma-associated transcript 2 (EAT-2) in T, NK, B and macrophage cells. SLAMF8 (CD353) is a member of the SLAM family, and negatively regulates the function of human macrophage, though its ligand has not been identified. There is no report on the expression or function of SLAMF8 in other cell types to our knowledge. Here, we investigated the expression and function of SLAMF8 in human mastocytosis, which is occurred by gain of function mutations in KIT-mediated proliferation of human mast cells.

Design: RT-PCR and immunoblotting were performed to confirm the expression of SLAMF8, SAP, and EAT-2 in human mastocytosis cell lines, HMC1.2 (expressing mutated KIT) and LAD2 (expressing wild type KIT) cells. The SLAMF8-knockdown mastocytosis cells were established using the lentiviral shRNA silencing technique. The ELISA assay and immunoblotting were used to detect the status of signal molecules of mastocytosis cells. The Cell Counting Kit-8 was used to evaluate the growth of mastocytosis cells. Immunohistochemistry was performed to evaluate the expression of SLAMF8 in pathological specimens of mastocytosis. The interaction between SLAMF8 protein and Src homology region 2 domain-containing phosphatase (SHP)-2 protein was assessed using the DuoLink in situ kit.

Results: Human neoplastic mast cell lines HMC1.2 and LAD2 expressed SLAMF8 mRNA and protein, though these cell lines were deficient in the expression of mRNAs for SAP and EAT-2. The SLAMF8-knockdown significantly decreased KIT-mediated growth of HMC1.2 cells, but did not that of LAD2 cells. The SLAMF8-knockdown in HMC1.2 cells significantly attenuated the activation of SHP-2 and did oncogenic KIT-mediated RAS – RAF – ERK signal. The interaction between SLAMF8 protein and SHP-2 protein was observed in the membrane domain of HMC1.2 cells, but not in LAD2 cells. SLAMF8 protein expression and its interaction with SHP-2 were confirmed in all-examined pathological specimens of mastocytosis.

Conclusions: SLAMF8 would be involved in oncogenic KIT-mediated RAS – RAF – ERK signal and the followed growth of human mastocytosis via SHP-2, not SAP or EAT-2. SLAMF8 is a possible therapeutic target of mastocytosis.

548 ALK Gene Fusions in Epithelioid Fibrous Histiocytoma: a Study of 14 Cases, with New Histopathological Findings

Dmitry Kazakov[1], *Liubov Kyrpychova*[2], *Petr Martinek*[3], *Petr Grossmann*[4], *Petr Steiner*[5], *Tomas Vanecek*[4], *Michael Michal*[6], *Michal Michal*[7]. [1]Bioptical Laboratory SVO, Pilsen, Czech Republic, [2]Bioptical Laboratory s.r.o, Pilsen, Czech Republic, [3]Bioptical Laboratory, Pilsen, Czech Republic, [4]Bioptical Laboratory, Pilsen, Czech Republic, [5]Charles University, Pilsen, Czech Republic, [6]Faculty of Medicine in Pilsen, Charles University, Prague and Biomedical Center, Faculty of Medicine in Pilsen, Charles University, Czech Republic, [7]Bioptical Laboratory s.r.o., Plzen

Background: Epithelioid fibrous histiocytoma (EFH) is considered as a variant of benign fibrous histiocytoma in which more than 50% of cells are epithelioid. A subset of EFH shows ALK expression on immunohistochemistry. Two cases of EFH with *ALK* gene fusions have been recorded. Our objective was to study a series of EFH to present histopathological variations of EFH, identify novel *ALK* gene fusions and determine whether there is correlation between histopathological features and particular gene fusion.

Design: Studied were 14 cases of EFH, all ALK immunopositive. The cases were assessed histopathologically as well as for *ALK* and *TFE-3* rearrangements using FISH and *ALK* gene fusions using next generation sequencing.

Results: There were 8 female and 6 male patients, ranging in age from 18 to 79 years. All presented with a solitary lesion on the trunk, lower extremities and face, varying from 5 mm to 20 mm. Microscopically, the lesions were mostly polypoid, with or without an epidermal collaret. Two cases exhibited a non-polypoid architecture with an intradermal proliferation of the neoplastic cells. The cells were usually arranged

in well-demarcated sheets, rarely with a focal nested/whirling pattern, fascicular areas and perivascular cuffs. The predominant cell type were mononucleated medium-sized to large epithelioid cells with ample eosinophilic to amphophilic cytoplasm. Additionally, a variable number of bi-, tri- or multinucleated, spindled, multilobated, cells with eccentric nuclei, cells with nuclear pseudoinclusions, mucinous and grooved cells were admixed. In 5 cases, the predominant epithelioid cell component consisted of rather small cells, whereas spindled cells dominated in 3 cases. Of these, 2 lesions were composed rather of pale eosinophilic to clear cells, occasioning a resemblance to PEComa or leiomyoma. Immunohistochemically, 11 were positive for TFE-3. The break apart test for *ALK* was positive in 11 analyzable cases. *ALK* genes fusions were found in all 11 analyzable cases included *SQSTM1-ALK* (3), *VCL-ALK* (3), *TMP3-ALK* (2), *PRKAR2A-ALK* (1), *MLPH-ALK* (1), and *EML4-ALK* (1). *TFE-3* rearrangements/fusions were not found.

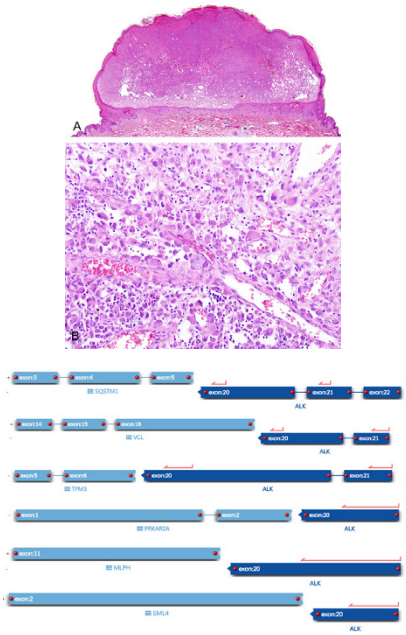

Conclusions: ALK-immunopositive EFH shows *ALK* gene fusions that involve various protein-coding genes, implicated in a variety of biological processes. Rare variants of EFH consists rather of spindled "non-epitheliod" cells. TFE-3 is often expressed in ALK positive EFH. There are no correlations between histopathological features and particular gene fusions.

549 Novel ALK Gene Fusions in Spitzoid Melanocytic Lesions: a Clinicopathological Study of 16 Cases, Including FISH Analysis for Chromosomal Copy Number Changes and TERT Promoter Mutations

Dmitry Kazakov[1], *Liubov Kyrpychova*[2], *Petr Martinek*[3], *Petr Grossmann*[4], *Petr Steiner*[5], *Tomas Vanecek*[4], *Ladislav Hadravsky*[6], *Michal Michal*[7]. [1]Bioptical Laboratory SVO, Pilsen, Czech Republic, [2]Bioptical Laboratory s.r.o, Pilsen, Czech Republic, [3]Bioptical Laboratory, Pilsen, Czech Republic, [4]Bioptical Laboratory, Pilsen, Czech Republic, [5]Charles University Prague, Czech Republic, [6]Charles University, Prague, Czech Republic, [7]Bioptical Laboratory s.r.o., Plzen

Background: Three previous studies identified a subset of spitzoid melanocytic lesions carrying *ALK* fusions, including conventional Spitz nevus, atypical Spitz tumor (AST) and spitzoid melanoma. Few of these nevi and AST were studied by FISH for chromosomal copy number changes and found no features associated with melanoma. Another study investigated 7 lesions for mutations in *TERT* promoter (*TERT-p*), with negative results. We present a series of 16 *ALK*-fused spitzoid neoplasms, describing novel *ALK* fusions, results of FISH for copy number changes and *TERT-p* mutations.

Design: All included spitzoid lesions were ALK positive on immunohistochemistry. FISH for ALK break apart probe as well as two sets of FISH targeting 6p25, 11q13, 6p/CEP6, 6q/CEP6, 9p21 and cep9 were performed. *ALK* gene fusions were studied by next generations sequencing, whereas *TERT-p* mutations by Sanger sequencing.

Results: There were 10 female and 6 male patients aged 5-40 years. All presented with a solitary lesion, mostly on the extremities. Histopathologically, most lesions were polypoid or dome shaped with a plexiform predominantly dermally located proliferation of fusiform to spindled melanocytes usually with mild to moderate pleomorphism. Due to atypical features (mitoses > 2 per mm2, mitoses at base, heavy inflammation, perineural invasion, marked pleomorphism), 11 cases were classified as AST. The remaining 5 cases represented Spitz nevus. The ALK break apart test was positive in 11 cases, negative in 1 and non-analyzable in 4. RREB1 deletion was detected in 1 case; 11 cases were negative and the remaining 4 lesions were non-analyzable. *ALK* gene fusions were detected in all 14 analyzable cases, including 3 novel fusion types (*MLPH-ALK:* 4 cases, *VCL-ALK*: 1 case and *EEF2-ALK:* 1 case) and as well as 2 previously reported ones (*TMP3*-ALK: 6 cases and *DCTN1-ALK:* 2 cases). One lesion carried a *TERT-p* mutation (C228T, i.e c.-124C>T). In all patients, the lesions were surgically removed; re-excision was conducted in 2 cases. Follow-up was available for 13 patients, none of whom showed evidence of disease. Follow-up ranged from 4 to 202 months (mean 47.6 mos). In none of the patients was a sentinel lymph node biopsy performed.

Conclusions: Most ALK-immunopositive spitzoid melanocytic neoplasms appear to represent AST. Most harbor various *ALK* gene fusions. A majority of these lesions lack chromosomal copy number changes associated with melanoma or *TERT*-p mutations. Most cases appear to follow an uneventful clinical course.

550 Utility of PD-1/PDL-1 in Differential Diagnosis of Spindle Cell Melanoma and its Histologic Mimickers

Chae Hwa Kim[1], *Andrew Rosenberg*[2]. [1]University of Miami / Jackson Memorial Hospital, Miami, FL, [2]University of Miami Miller School of Medicine, Miami, FL

Background: The diagnosis of malignant melanoma, especially the spindle cell variant, can be challenging because it resembles morphologically other spindle cell tumors and it often lacks immunohistochemical staining with conventional melanoma markers. To date, there is limited information available about the diagnostic utility of expression of PD-1 and PDL-1 in tumors in the differential diagnosis of spindle cell melanoma. The goal of this study is to determine whether the expression of PD-1 and PDL-1 is a useful diagnostic aid.

Design: We identified a cohort of well characterized spindle cell melanoma and its mimickers (different types of benign and malignant peripheral nerve sheath tumors) and retrieved49 cases (13 spindle cell melanomas, 13 MPNSTs, 11 Schwannomas, and 12 neurofibromas). We examined the histological slides, and performed immunohistochemistry for PD-1 and PDL-1 on the block with the greatest amount of well-preserved viable tumor. The percentage of PDL-1 tumor cell staining was scored and PD-1 staining in the tumor and immune cells was assessed. A statistical analysis evaluating the significance of staining patterns was performed to determine whether or not PD-1 and PDL-1 staining has diagnostic utility.

Results: PDL-1 staining of at least 1% of the tumor cells was seen in 9/13(69.2%) spindle cell melanoma, 6/13 (46.2%) MPNST, 0/11 Schwannoma, and 0/12 neurofibroma. More than 5% of PDL-1 staining was seen in 8/13 (61.5%) spindle cell melanoma and 4/13 (30.8%) MPNST. Tumor cell epression of PD-1 was identified in all the cases of PDL-1 staining. One Schwannoma and one neurofibroma showed PD-1 positivity without PDL-1 staining. PDL-1 staining was heterogeneous in the tumor with moderate intensity and cytoplasmic and membranous patterns. PD-1 expression was observed in tumor infiltrating lymphocytes and peritumoral lymphocytes. The percentage of PDL-1 positive tumor cells is higher in spindle cell melanoma than in MPNST, however the result is not statistically significant. PDL-1 expression in malignant tumors (spindle cell melanoma and MPNST) helps to exclude Schwannoma and neurofibroma with statistical significance ($p<0.05$).

Conclusions: Both spindle cell melanoma and MPNST show expression of PD-1/PDL-1 and staining for these antigens is not helpful in this differential diagnosis. However benign peripheral nerve sheath tumors do not express PDL-1, therefore, a positive result is evidence against these possibilities and this finding can be of diagnostic importance.

551 Immunohistochemistry of p16 in Nevi of Pregnancy and Nevoid Melanomas

Stephen Koh[1], *Brian F Roehmholdt*[2], *David Cassarino*[3]. [1]Kaiser Permanente Med Ctr, Anaheim, CA, [2]Southern California Permanente Medical Group, Fontana, CA, [3]Southern California Permanente Med Grp, Los Angeles, CA

Background: Hormonal changes in pregnancy have been known to alter melanocytic lesions. Histopathologically, some nevi observed within the context of pregnancy have shown increased mitotic figures with corresponding Ki-67. Additionally, cytomorphologic changes have also been noted, referred to as superficial micronodules of pregnancy. Such changes may alarm the pathologist for malignancy, particularly nevoid melanoma. Immunohistochemistry for p16 have been utilized to distinguish benign nevi from melanoma. We propose the use of p16 immunohistochemistry as utility for characterizing melanocytic nevi from pregnant patients to confirm its benignity.

Design: Formalin Fixed Paraffin-Embedded tissue blocks were obtained for nevi from pregnant patients and also for nevoid melanomas. 14 nevomelanocytic lesions were obtained from 12

pregnant patients with gestational ages averaging 24.7 weeks. Biopsies were from various locations and the average size of the lesion was 6.5 mm. 12 nevoid melanomas were obtained from 12 separate patients from various locations for comparison. Immunohistochemistry with p16 were performed on each melanocytic lesion. Percentage of positive nuclear p16 staining of dermal melanocytes were grouped on a scale of <5%, 5-25%, 25-50% and >50%.

Results: For nevi from pregnant patients (n=14), results of p16 nuclear immunohistochemistry were as follows: <5% (1 case, 7%), 5-25% (7 cases, 50%), 25-50% (3 cases, 21.5%), >50% (3 cases, 21.5%). For nevoid melanomas (n=12), results were as follows: <5% (8 cases, 67%), 5-25% (3 cases, 25%), 25-50% (1 case, 8%), >50% (0 case, 0%). Additionally, three nevi from pregnant patients had superficial micronodules of pregnancy with increased dermal mitosis (2-3 mitotic figures/mm^2 within hotspots). Analysis of p16 IHC within the areas of hotspot mitosis did not show any significant difference in p16 staining pattern.

Conclusions: Results from the current study of nevi from pregnant patients show majority of cases (13 of 14 cases, 93%) with positive p16 nuclear staining that was greater than 5%. In contrast, majority of nevoid melanoma cases (8 of 12 cases, 67%) showed virtually complete loss of p16 nuclear staining or less than 5% of p16 nuclear staining. Its application as a potential immunohistochemistry diagnostic marker to confirm benignity of nevi from pregnant patients may become a useful tool in comparison to nevoid melanomas.

552 Utility Of A Comprehensive Cost-Effective Targeted DNA/RNA Panel (170 Genes) On A Next Generation Sequencing (NGS) Platform In Evaluation Of Melanoma For Tumor Specific Information, Microsatellite Instability (MSI) And Calculating The Overall Tumor Mutation Burden (TMB)

Ravindra Kolhe[1], *Ashis MOndal*[2], *Chetan Pundkar*[2], *Vamsi Kota*[3], *Alka Chaubey*[4]. [1]Augusta University, Augusta, GA, [2]Augusta University, [3]Emory University, [4]Greenwood, SC

Disclosures:
Ravindra Kolhe: *Speaker,* Illumina Inc, Affymetric Inc; *Consultant,* BMS Inc, Asuragen Inc

Background: Currently, NGS techniques are being widely used as a tool in ~~a~~ routine oncology workflows. Majority of labs use either DNA based panels or two separate DNA and RNA panel to investigate cancer specimens. Any NGS assay choice in a CLIA setting requires careful consideration of the content of the panel, the inclusion of evidence-based markers, and it's compatibility with low quality and quantity of nucleic acids. The objective of our project was to evaluate the utility of a comprehensive 170 genes enrichment-based targeted panel that simultaneously analyzes DNA and RNA in Melanoma. The panel targets all coding exons in 170 genes, 55 genes for fusions and splice variants, 151 SNVs and indels, and 59 amplifications. Assessment of fusions, splice variants, insertions/deletions and single-nucleotide variants (SNVs), and amplifications in one assay using DNA and RNA creates efficiencies in sample usage, time, and cost.

Design: Under an approved IRB protocol (n= 8) Melanoma cases were identified. All these cases were positive for one of molecular abnormalities routinely tested for Melanoma (variants in, BRAF, NRAS, PDGFRA, KIT etc). H&E slides were examined and the diagnoses were confirmed. Subsequently, sequencing was performed on DNA/RNA isolated from FFPE tissue on a NGS platform (NextSeq, Illumina). The variant and fusion calls were read and interpreted on the software provided by the manufacture (Illu

Results: All the calls with high confidence on the NGS platform matched 100% with the PCR findings on all the 8 cases

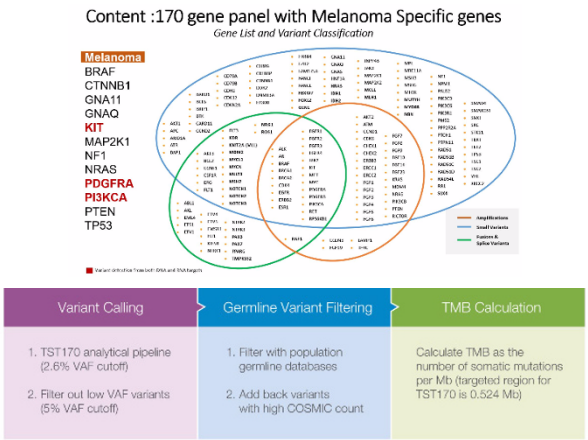

Conclusions: Evidence-based information on variants from these genes (fig 1) adds substantial value to the personalized management of these patients. As we sequence all the MSI associated genes (such as MLH1, MSH2 or MSH6) in the assay, we have previously designed and validated (n=56 cancer cases) a bioinformatics algorithm to evaluate the MSI status in these tumors. Using the same algorithm, we were able to assess the MSI status in our current brain tumor cases. Similarly, an algorithm was previously created to assess the overall TMB (fig 2) using WES data (TCGA, clinical trials), and reevaluated by informatically extracting the targeted regions in 170 genes from the WES data in silico. We used the same algorithm to extract the TMB in our cases. In this study, we present a NGS panel in which tumor-specific information on genes which are considered highly important in Melnaoma can be investigated in a single panel, thus providing sample efficiency & cost reduction.

553 Sebaceous Neoplasms With Rippled, Labyrinthine/Sinusoidal, Petaloid and Carcinoid-Like Patterns: a Study of 56 Cases Validating Their Occurrence as a Morphological Spectrum and Showing no Significant Association with Muir-Torre Syndrome or DNA Mismatch Repair Protein Deficiency

Liubov Kyrpychova[1], *Katharina Flux*[2], *Ozlem Tanas Isikci*[3], *Dominic Spagnolo*[4], *Heinz Kutzner*[5], *Arno Rütten*[5], *Maria Teresa Fernandez-Figueras*[6], *Natalja Denisjuk*[7], *Saul Suster*[8], *Michal Pavlovsky*[9], *Fredrik Petersson*[10], *Michal Michal*[11], *Katrin Kerl*[12], *Dmitry Kazakov*[13]. [1]Bioptical Laboratory s.r.o, Pilsen, Czech Republic, [2]Labor für Dermatohistologie und Oralpathologie, München, Germany, [3]Ankara Education and Research Hospital, Ankara, [4]Path West Laboratory Medicine, Nedlands, WA, AUS, [5]Dermatopathologie Friedrichshafen, Friedrichshafen, Germany, [6]Hospital Universitari General de Catalunya, Barcelona, Spain, [7]Dermatopathology Institute, Zürich, Switzerland, [8]The Medical College of Wisconsin, Milwaukee, WI, [9]Regional Hospital, Most, Czech Republic, [10]National University Hosp, Singapore, [11]Bioptical Laboratory s.r.o., Plzen, [12]University Hospital of Zürich, Zürich, Switzerland, [13]Bioptical Laboratory SVO, Pilsen, Czech Republic

Background: Sebaceoma is a benign sebaceous neoplasm that manifests histologically as a well-circumscribed tumor which composed mostly of immature, small, basophilic sebocytes with a variable admixture of mature sebocytes and sebaceous ducts. Some sebaceomas and rare sebaceous carcinomas have been shown to manifest organoid growth patterns, including rippled, labyrinthine/sinusoidal, carcinoid-like and petaloid. The objectives of this study were to validate this proposition by studying a large number of cases, determine if there are specific associations with clinical features including age, sex and location and determine if they have any association with Muir-Torre syndrome.

Design: The authors have studied 56 sebaceous neoplasms (53 sebaceomas, 3 sebaceous carcinomas) with organoid growth patterns. For each case, particular patterns (rippled, labyrinthine/sinusoidal, carcinoid-like and petaloid), alone or in combination were documented, and the dominant pattern was also recorded. In 22 cases with available tissue blocks, immunohistochemistry with MMR protein was performed.

Results: The neoplasms occurred in 35 males and 18 females (gender unknown in 3), with ages at diagnosis ranging from 22 to 89 years. Of the 56 tumors, 23 manifested a single growth pattern, 23 had a combination of 2 patterns and 10 a combination of 3 patterns, indicating that these patterns are part of a morphological continuum of changes. The carcinoid-like pattern was the most frequent in the "monopatterned" neoplasms (13 cases), whereas the labyrinthine/sinusoidal pattern comprised most of the "polypatterned" lesions, in which various combinations occurred. Immunohistochemically, MMR deficiency was detected in 3 of the 22 cases studied, whilst 5 of the 33 patients with available follow-up had an internal malignancy; this however is not indicative of a significant association of these lesions with Muir-Torre syndrome.

Table 1. Main clinicopathological data

Clinical data	
Gender distribution	
Male	35
Female	18
Unknown	3
Age, yrs	
Range	22-89
Mean	63
Median	67
Size, mm	
Range	3-27
Mean	11
Median	10
Location	
Scalp	36
Nose	6
Cheek	3
Other parts of head/neck area	9
Association with internal malignancy	5 of 33 with follow-up
Histopathological data	
Sebaceoma vs carcinoma	53:3
"Monopatterned" lesions	23 of 56
Carcinoid-like only	13
Labyrinthine/sinusoidal only	6
Rippled only	4
Petaloid only	0
Two pattern combination	23 of 56
Labyrinthine/sinusoidal+carcinoid-like	13
Labyrinthine/sinusoidal+rippled	6
Labyrinthine/sinusoidal+petaloid	2
Carcinoid-like+petaloid	1
Carcinoid-like+rippled	1
Three pattern combination	10 of 56
Labyrinthine/sinusoidal+carcinoid-like+rippled	6
Labyrinthine/sinusoidal+carcinoid-like+petaloid	4
Predominant pattern in 33 "polypattrened" lesions	
Labyrinthine/sinusoidal	18
Carcinoid-like	7
Rippled	6
Petaloid	2
MMR protein deficiency	3 of 22 studied

MMR : mismatch repair

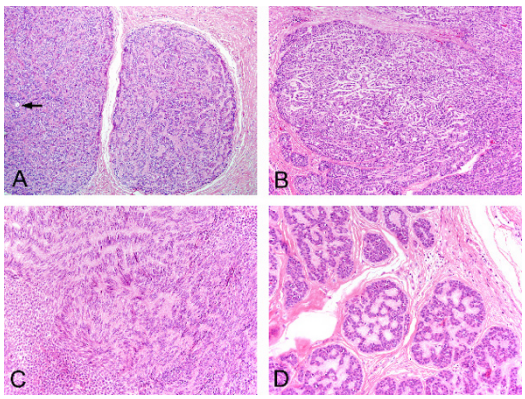

Conclusions: Sebaceous neoplasms with organoid growth patterns are predominantly sebaceomas having a predilection for the scalp. In most cases, more than one of the organoid patterns are present. Mature sebocytes may be inconspicuous in these lesions, requiring distinction from other cutaneous adnexal neoplasms. However, these patterns per se may serve as a clue to sebaceous differentiation. These lesions do not appear to be associated with internal malignancy or MMR deficiency in the majority of cases. However, confirmation of the absence of any significant association with MTS will require genetic studies.

554 A Subset of Adenoid Cystic Carcinoma of The Skin is Associated With Alterations of The MYBL1 Gene Similar to Their Extracutaneous Counterparts

Liubov Kyrpychova[1], *Tomas Vanecek*[2], *Petr Grossmann*[2], *Petr Martinek*[3], *Ladislav Hadravsky*[4], *Irena E Belousova*[5], *Ksenia Shelekhova*[6], *Marian Svajdler*[7], *Michal Michal*[8], *Dmitry Kazakov*[9]. [1]Bioptical Laboratory s.r.o, Pilsen, Czech Republic, [2]Bioptical Laboratory, Pilsen, Czech Republic, [3]Bioptical Laboratory, Pilsen, Czech Republic, [4]Charles University in Prague, Czech Republic, [5]Medical Military Academy, Saint-Petersburg, Russia, [6]Petrov's Research Institute of Oncology, Saint-Petersburg, Russia, [7]Biopticka laborator s.r.o, Plzen, Plzen, [8]Bioptical Laboratory s.r.o., Plzen, [9]Bioptical Laboratory SVO, Pilsen, Czech Republic

Background: Adenoid cystic carcinoma (ACC) of the skin is a rare, low-grade malignant adnexal neoplasm histologically identical to homonymous tumors in other organs. Approximately 60% of the studied cases of cutaneous ACC have been found to harbor *MYB* gene activations, either through *MYB* chromosomal abnormalities or by generation of the *MYB-NFIB* fusion. In addition to the *MYB* gene, alterations in *MYBL1*, the gene closely related to *MYB,* have been reported in salivary gland ACC. Since we are not aware of any studies on cutaneous ACC studying alterations in *MYBL1*, our main goal was to find out whether this gene is involved in cutaneous ACC.

Design: Ten cases of cutaneous ACC with available blocks were randomly selected. In all cases the *MYB-NFIB* fusions were detected by FISH using one commercial probe, ZytoLight® SPEC MYB Dual Color Break Apart Probe, as well as two own designed SureFish probes, NFIB Break Apart probe and MYB-NFIB Fusion. The break of *MYBL1* gene was detected using an own designed SureFish MYBL1 Break Apart probe.

Results: There were 6 females and 4 males, with ages at diagnosis ranging from 51 to 83 years. Locations included the head (n= 4), thigh (n= 2), back (n= 2), and vulva (n=2). All patients presented with a solitary neoplasm, varying is size from 5 to 50 mm in largest dimension (mean 18.6 mm). Histologically, in all but one case, there was a mixture of cribriform, tubular and solid patterns forming variably shaped nodules in the dermis. In the remaining case, solid areas were lacking. In all cases, both true small bilayered ducts and pseudocysts were recognized. Perineural invasion was seen in 4 cases.

MYB-NFIB fusions were found in 4 cases. Remarkably, in 2 of these cases the *MYB* break-apart probe was negative. The break of *MYBL1* was found in in 2 cases. In one of them, the *NFIB* break apart probe was positive, strongly indicating a *MYBL1-NFIB* fusion, whereas in the second case, the fusion partner remained unknown. In two cases, the *MYB* break apart test was positive, whereas no *MYB-NFIB* was detected, strongly suggesting another fusion partner. In one case, all 4 FISH tests were negative and the remaining case was not analyzable.

FOR TABLE DATA, SEE PAGE 215, FIG. 554

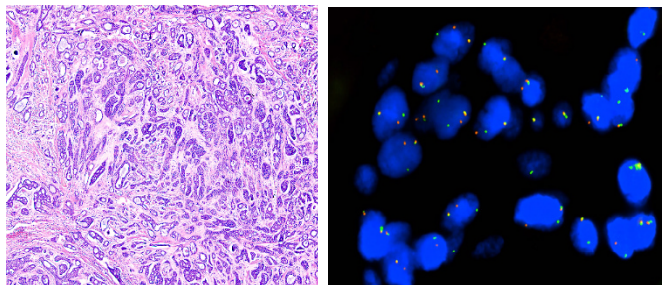

Conclusions: In addition to *MYB* alterations, some cutaneous ACC exhibit involvement of *MYBL1* similar to their extracutaneous counterparts.

555 Insulinoma-associated protein 1 (INSM1) Immunohistochemistry Offers Improved Sensitivity for the Diagnosis of Endocrine Mucin-Producing Sweat Gland Carcinoma: A Single Institution Experience

Mohammed T Lilo[1], *Shaofeng Yan*[2], *Konstantinos Linos*[3], *Robert E LeBlanc*[4]. [1]Dartmouth-Hitchcock Medical Center, Lebanon, NH, [2]Dartmouth-Hitchcock Med.Ctr., Hanover, NH, [3]Dartmouth-Hitchcock Medical Center, Lebanon, NH, [4]Dartmouth-Hitchcock Medical Center

Background: Endocrine Mucin-Producing Sweat Gland Carcinoma (EMPSGC) is a rare low-grade adnexal malignancy with predilection for the eyelids of older adults. It can recur months to years following incomplete excision although there are no reported metastases. EMPSGC is challenging to distinguish from metastatic breast carcinoma given their overlapping immunophenotypes, and it is easily misdiagnosed in partial biopsies as the requisite neuroendocrine expression and mucin production can be subtle or focal. INSM1 is a new marker that has shown promising sensitivity and specificity in the diagnosis of extracutaneous neuroendocrine carcinomas.

Design: A retrospective search of pathology archives (between 1/2003 and 07/2017) yielded 10 cases of EMPGS. Slides and medical records were reviewed. P63, calponin, synaptophysin, chromogranin, GATA3, ER, PR and INSM1 immunostains were performed on all samples.

Results: Five women and 5 men with median age 78 years (range 56-86) had papules on the eyelid (7 cases) and cheek (3 cases). Clinical work-up excluded the possibilities of metastatic breast carcinoma. 6 received wide excision and 4 Mohs surgery. 2 patients who underwent Mohs and wide excision had local recurrences at 17 and 41 months

respectively. 6 had no recurrence over 75 months median duration and 2 were lost to follow-up. 2 lesions had infiltrative architecture and no intact myoepithelial layer (one of them recurred). 2 arose from the linings of hidrocystomas with intact myoepithelial layers (one recurred). The rest showed conventional solid, cystic, and papillary architecture. All had at least focal mucin production. A myoepithelial layer suggesting a probable in situ component was partially intact in 7 cases. 100% of EMPSGC were INSM1 positive (strong nuclear staining in 50%-75% of tumor cells in most cases), 83% stained with synaptophysin, and 67% with chromogranin. All cases were GATA3, ER and PR positive.

Conclusions: INSM1 may have greater sensitivity than synaptophysin and chromogranin for demonstrating neuroendocrine differentiation in EMPSGC. GATA3, ER, and PR are not useful for distinguishing EMPSGC from metastatic breast carcinoma; however, identification of an in situ component supports the diagnosis of EMPSGC. Our cases demonstrated indolent behavior independent of whether the lesions appeared predominantly infiltrative or in situ. Mohs surgery may be a valuable alternative to traditional wide excision in treatment of this disease.

556 Clinicopathologic Features and Calcium Deposition Patterns in Calciphylaxis: Comparison with Peripheral Artery Disease, Chronic Stasis, and Thrombotic Vasculopathy

Emily R McMullen[1], *Lori Lowe*[1], *Douglas Fullen*[1], *May P Chan*[1]. [1]University of Michigan, Ann Arbor, MI

Background: Diagnosis of calciphylaxis is crucial in prompting timely treatment, yet its distinction from other vascular diseases can be challenging. While vascular calcification and thrombosis are histopathologic hallmarks of calciphylaxis, the incidence and patterns of these features in other vascular diseases have not been well characterized. In particular, it remains unclear whether stippled calcium deposits identified on von Kossa (VK) stain only are specific for calciphylaxis, or may be seen in other conditions as well.

Design: Cases of calciphylaxis (n=24), peripheral artery disease (gangrene and uninvolved skin at amputation margin, n=21 each), chronic stasis (n=22), and thrombotic vasculopathy (n=19) were retrospectively reviewed. VK stain was performed and examined in all cases.

Results: Clinical and histopathologic findings are summarized in the Table. Patients with calciphylaxis were much more likely to be on hemodialysis (p<0.0001) and have documented hypercalcemia, hyperphosphatemia, and/or hyperparathyroidism (p<0.0001). Concentric calcification of subcutaneous small vessels appreciable on H&E is relatively specific for calciphylaxis, although sensitivity was limited (50%). VK allowed for detection of stippled calcium deposits otherwise not appreciable on H&E, but the specificity of such deposits was low. In fact, stippled calcium deposits in subcutaneous small vessels were more common in clinically normal skin (amputation margin) of patients with severe peripheral artery disease (86%) than in calciphylaxis (46%). Specificity of stippled calcium in subcutaneous small vessels (identified on VK only) improved when concomitant thrombosis was present. Calcium deposits in medium-sized vessels, eccrine gland basement membranes, and elastic fibers had minimal specificity.

	Calciphylaxis (n=24*)	Gangrene (n=21)	Amputation margin (n=21)	Chronic Stasis (n=22**)	Thrombotic vasculopathy (n=19)
Clinical					
Mean age	60	68		59	55
Sex (male:female)	3:20	13:8		3:18	11:8
Diabetes	11 (48%)	11 (52%)		6 (29%)	4 (21%)
Chronic kidney disease	16 (70%)	6 (29%)		6 (29%)	8 (42%)
Hemodialysis	10 (43%)	0		0	0
Peripheral artery disease	4 (17%)	21 (100%)		2 (10%)	2 (11%)
Elevated calcium, phosphate, or parathyroid hormone	20 (83%)	4 (19%)		3 (14%)	1 (5%)
Histopathology					
Thrombosis in subcutaneous small vessels	22 (92%)	14 (67%)	0	4 (18%)	5 (26%)
Calcium in subcutaneous small vessels:					
- Identified on H&E	12 (50%)	3 (14%)	0	0	0
- Identified on VK	23 (96%)	12 (57%)	18 (86%)	5 (23%)	1 (5%)
- Identified on VK only	11 (46%)	9 (43%)	18 (86%)	5 (23%)	1 (5%)
Calcium and thrombosis in subcutaneous small vessels:					
- Ca identified on H&E	10 (42%)	2 (10%)	0	0	0
- Ca identified on VK	21 (88%)	9 (43%)	0	1 (5%)	0
- Ca identified on VK only	11 (46%)	7 (33%)	0	1 (5%)	0
Calcium in medium vessels:					
- Identified on H&E	17 (71%)	4 (19%)	6 (29%)	1 (5%)	0
- Identified on VK	20 (83%)	8 (38%)	19 (90%)	4 (18%)	3 (16%)
- Identified on VK only	3 (13%)	4 (19%)	13 (62%)	3 (14%)	3 (16%)
Calcium in eccrine gland basement membranes (VK)	13 (54%)	2 (10%)	7 (33%)	1 (5%)	3 (16%)
Calcium in elastic fibers (VK)	14 (58%)	3 (14%)	4 (19%)	10 (45%)	0
Extravascular calcification (H&E)	8 (33%)	6 (29%)	6 (29%)	6 (27%)	0
Neutrophils in fat	14 (58%)	19 (90%)	1 (5%)	4 (18%)	8 (42%)
Fat necrosis	23 (96%)	21 (100%)	7 (33%)	21 (95%)	5 (26%)
Septal fibrosis	18 (75%)	21 (100%)	7 (33%)	21 (95%)	3 (16%)
*24 Biopsies from 23 patients. **22 Biopsies from 21 patients.					

Conclusions: Despite limited sensitivity, concentric calcification of subcutaneous small vessels appreciable on H&E is relatively specific and sufficient to favor a diagnosis of calciphylaxis. VK is useful in enhancing detection of calcium and avoiding false negative diagnosis based on H&E only. When stippled calcium deposits are identified on VK only, concomitant thrombosis of the subcutaneous small vessels is necessary to support a diagnosis of calciphylaxis in the correct clinical setting. As none of the examined histopathologic features are definitively diagnostic of calciphylaxis, correlation with clinical and laboratory findings remains imperative.

557 RNA-FISH/IF multiplex assay for evaluation of message stability and post-translational processing in Epidermolytic Ichthyosis

Haris Mirza[1], *Keith Choate*[2]. [1]Yale School of Medicine, New Haven, CT, [2]Yale University

Background: Epidermolytic ichthyosis is a rare heterogenous group of disorders caused by keratin 1 or 10 mutations. KRT1 and 10 together form heteropolymers. Mutations in either genes result disruption of KRT1-10 polymers and cause skin fragility. Most EI cases result from dominant misense mutations but a minority of EI cases show recessive inheritance. Dominant EI mutations produce misfolding of KRT10 protein. Etiology of recessive EI on the other hand is suspected to be nonsense mediated decay (NMD) of *KRT10* mRNA, however there is limited evidence to support this assertion. Both dominant and recessive EI exhibit loss of epidermal anti-KRT10 staining, making distinction between the two entities challenging on histology and immunohistochemistry.

Design: Here we present a case of recessive EI. Both the patient and unaffected parents were evaluated for *KRT10* mutations using sanger sequencing. Cellular toxicity of the mutant proteins found in recessive and dominant EI cases is evaluated by expression of the proteins in HaCat cells. More importantly a novel RNA-FISH/IF multiplex system for paraffin embedded tissue is developed for in-situ evaluation of NMD in EI.

Results: Recessive EI skin biopsy showed degeneration of the suprabasal keratinocytes, thickening of the granular layer and coarse keratinohylin granules. Sequencing showed homozygous *KRT10* mutation, c.950insC introducing a premature termination codon (PTC) in exon 4. Heterozygous parents were phenotyopically normal. Mutant protein expression in HaCat cells, after

bypassing NMD, caused KRT10 aggregation and cell death. Using RNA-FISH/IF multiplex assay we compared the *KRT10* mRNA and protein expression of our recessive case with dominant EI cases. Significant reduction in anti-KRT10 was observed in recessive EI epidermis while heterozygous parents showed KRT10 levels comparable to normal skin. *KRT10* mRNA in cytoplasm was significantly reduced in recessive EI cells compared to normal epidermis. Interestingly, nuclear *KRT10* mRNA in recessive EI remained unaffected suggesting active transcription of *KRT10* and post trancriptional decay in cytoplasm. Conversely dominant EI mutant skin showed abundant cytoplasmic *KRT10* mRNA but reduced KRT10 protein suggesting aberrant post-translational polymerization.

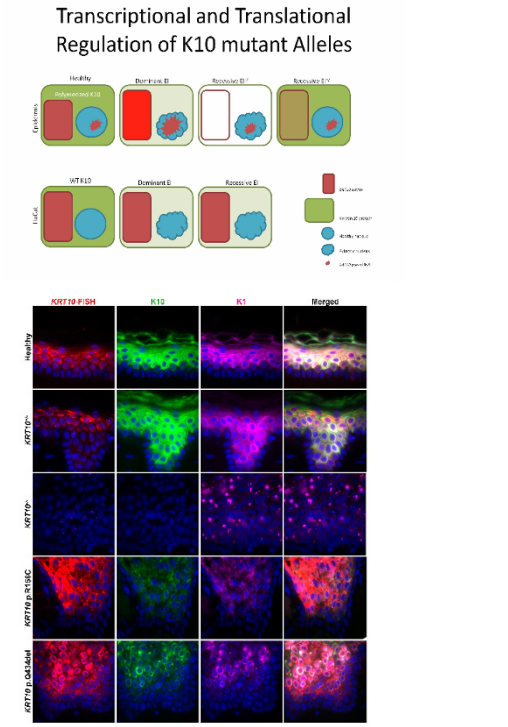

Conclusions: The reduced cytoplasmic *KRT10* mRNA in the presence of abundant nuclear *KRT10* confirms the role of NMD in keratin PTC mutations. The study demostrates usefullness of multiplex RNA-FISH/IF to evaluate NMD in human diseases.

558 PREVIOUSLY PUBLISHED

559 Primary anorectal melanoma: Distinct histopathologic parameters of the primary tumor correlate with disease specific survival (DSS) depending upon the stage at presentation

Priyadharsini Nagarajan[1], *Jin Piao*[2], *Jing Ning*[3], *RASHMI T SAMDANI*[4], *Laura E Noordenbos*[3], *Jonathan Curry*[5], *Carlos Torres-Cabala*[5], *Phyu Aung*[6], *Doina Ivan*[7], *Wei-Lien Billy Wang*[8], *Richard E Royal*[9], *Asif Rashid*[10], *Alexander Lazar*[7], *Merrick I Ross*[3], *Michael A Davies*[3], *Victor Prieto*[11], *Jeffrey E Gershenwald*[8], *Michael Tetzlaff*[10]. [1]The University of Texas MD Anderson Cancer Center, Houston, TX, [2]University of Southern California, Los Angeles, CA, [3]MD Anderson Cancer Center, [4]MDACC, Houston, Texas, [5]Houston, TX, [6]U. T. - M. D. Anderson Cancer Center, Houston, TX, [7]M. D. Anderson Cancer Center, Houston, TX, [8]UT MD Anderson Cancer Ctr, Houston, TX, [9]MD Anderson Cancer Center, Houston, Texas, [10]UT-MD Anderson Cancer Center, Houston, TX, [11]UT - MD Anderson Cancer Center, Houston, TX

Background: Primary anorectal melanoma (AM) is an uncommon melanoma subtype. Although often staged according to the AJCC staging system for cutaneous melanoma (CM) there is limited evidence base to support this practice in AM. Therefore, we analyzed a retrospective cohort of AM patients (pts) to determine if additional or other primary tumor features correlate with DSS.

Design: We identified pts with AM diagnosed and treated at our center and collected clinical (age at diagnosis, sex, ethnicity, anatomic site) and primary tumor pathologic features (tumor thickness, level of rectal wall invasion, vertical growth phase, mitotic rate, ulceration, regression, lymphovascular invasion, perineural invasion, satellitosis, cytology and final resection margin status); and stage at presentation: (L) disease localized to anorectum with (LpN-) or without (LcN-) pathologic lymph node sampling; (R) regional metastases that were clinically occult (RpN+) or clinically evident (RcN+); and (D) distant metastases (Fig 1). Kaplan Meier methods estimated DSS (Fig 1). Univariate and multivariate Cox proportional hazards regression models determined associations with DSS.

Results: 160 AM pts were identified. Median survival was 1.75 years from diagnosis; 1, 5 and 10 year DSS rates were 77%, 22% and 15%; and 121 pts (76%) died due to disease. Within the full cohort, multiple clinical and pathologic features independently associated with DSS, including stage at presentation (Fig 2). However, when considering distinct subgroups of patients according to stage at presentation, a subset of distinct parameters independently associated with DSS (Fig 2).

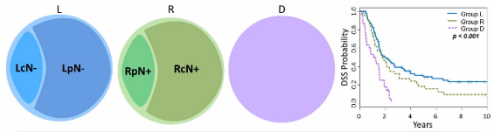

Whole cohort n=160	
L: Disease localized to primary site n=67 (42%)	**LcN-:** Localized disease; regional lymph nodes not sampled n=27 (17%)
	LpN-: Localized disease; regional lymph nodes negative by pathologic evaluation n=40 (25%)
R: Disease involving regional lymph node(s) n=55 (34%)	**RpN+:** Clinical occult regional disease, i.e. imaging negative, but pathologically confirmed micrometastasis n=18 (11%)
	RcN+ Clinically evident regional lymph node metastasis, i.e., imaging positive macrometastasis n=37 (23%)
D: Distant metastasis n=38 (24%)	

Clinical and pathologic features associated with DSS in AM

*	Whole cohort	Group L	Group LcN-	Group LpN-	Group R	Group RpN+	Group RcN+	Group D
Univariate Analysis for Association with DSS (p-value)								
Age ≥62y	-	-	0.013	-	-	-	-	-
TT	<0.001	0.001	0.016	0.025	0.004	0.033	-	-
LEV	-	-	-	-	-	-	-	0.03
ULC	-	-	-	-	-	-	0.045	-
-REG	0.010	-	-	-	0.039	-	-	0.052
LVI	<0.001	0.020	-	0.006	0.006	0.018	-	-
PNI	0.037	-	-	-	0.010	0.030	-	-
+MAR	<0.001	-	-	-	0.035	0.045	-	-
STAGE	< 0.001	-	-	-	-	-	-	-
Group R	0.053	-	-	-	-	-	-	-
Group D	< 0.001	-	-	-	-	-	-	-
Multivariate Analysis for Association with DSS (p-value)								
Age ≥62y	-	-	0.026	-	-	-	-	-
TT	0.04	0.001	-	-	0.001	0.010	-	-
LEV	-	-	-	-	-	-	-	0.03
ULC	-	-	-	-	-	-	0.045	-
-REG	0.005	-	-	-	0.004	-	-	-
LVI	<0.001	-	-	0.006	0.015	0.008	-	-
+MAR	<0.001	-	-	-	-	-	-	-
STAGE	<0.001	-	-	-	-	-	-	-
Group D	< 0.001	-	-	-	-	-	-	-

TT, tumor thickness; LEV, level of colonic wall invasion; ULC, ulceration; -REG, absence of regression; LVI, lymphovascular invasion; PNI, perineural invasion; +MAR, final resection margin positive for invasive melanoma; STAGE, stage at presentation

Conclusions: AM is a highly aggressive melanoma subtype with frequent metastasis and death. Similar to CM, increasing tumor thickness associated with reduced DSS in our cohort of AM pts with localized disease or regional metastases. In contrast, primary tumor ulceration was not robustly prognostic of DSS in our cohort of AM pts. Our findings underscore the importance of integrating clinical stage at presentation when determining associations between primary tumor parameters and DSS. Also, our findings strongly support the rationale for additional studies designed to further refine staging and prognostic assessment in AM pts.

560 Loss of Mismatch Repair Protein Expression Predicts Better Survival In Melanoma

Saleh Najjar[1], *David Cubero Rego*[2], *Byoung Uk Park*[3], *Christine Sheehan*[1], *Jeffrey S Ross*[4], *John Carlson*[1]. [1]Albany Medical College, Albany, NY, [2]Albany Medical Center, Albany, NY, [3]Universidad Francisco Marroquin, Guatemala City, Guatemala, [4]Foundation Medicine, Cambridge, MA

Disclosures:
Jeffrey Ross: *Employee*, Foundation Medicine, Inc.

Background: Mismatch repair (MMR) proteins including MLH1, MSH2, MSH6, and PMS2 are integral components of the DNA mismatch repair system. Loss of MMR expression is a hallmark of microsatellite instability (MSI). MSI has been reported in 2-30% of primary melanomas and 20-77% of metastatic melanomas. In this study, we aim to evaluate MMR protein expression in malignant melanocytic proliferations and its correlation with survival and other histopathologic parameters.

Design: Formalin-fixed, paraffin-embedded sections from 100 malignant melanocytic proliferations were retrieved from our institution archive. The cohort consisted of 54 primary melanoma, 24 metastatic melanoma, 17 melanoma in situ, 4 mucosal melanoma, and 1 ocular melanoma. The sections were immunostained by automated methods with mouse monoclonal antibodies to MSH2, MLH1, MSH6, and rabbit monoclonal PMS2. MMR protein expression was determined by the percentage of tumor cells with nuclear positivity (PTNP). In addition, the nuclear intensity was scored as absent (0), weak (1), moderate (2),

or intense (3). Expression was correlated with histologic variables and survival.

Results: A total of 100 samples were collected from 91 patients (ages 22-90 years, median 64 years, M:F= 1.17:1). The mean MLH1 PTNP was 75.3% ± 17.8, MSH2 67.8% ± 21.8, MSH6 48.2% ± 29.9 and PMS2 65.3% ± 23.9. Loss of 70% or more of any MMR protein expression with weak or absent nuclear intensity score (PTNP< 31% and nuclear intensity score 0 or 1) was associated with 58% reduction in the risk of death (Hazard ratio= 0.42, p = 0.036, Conf. Interval 0.1879-0.9456) and with lower AJCC T category (Tis, T1 or T2) (Pearson chi2 =6.83, p=0.009). Loss of 70% expression or more of any MRR protein regardless of nuclear intensity score (PTNP< 31%) was associated with lower AJCC T category (-0.31, p=0.026) and Clark level (-0.33, p=0.015). Increased MSH6 PTNP correlated with higher AJCC T category (0.41, p=0.0031) and Clark level (0.35, p=0.0096). Increased MSH2 PTNP correlated with higher AJCC T category (0.34, p=0.015). PMS2 PTNP correlated with mitotic index (0.37, p=0.01) and ulceration (0.35, p=0.03). Increased MLH1 PTNP correlated with higher AJCC T category (0.31, p=0.025), and ulceration (0.36, p=0.026).

Conclusions: We found that loss of MMR protein expression is associated with better survival and lower AJCC T category. Our findings support growing evidence that MSI has a prognostic and predictive value in melanoma.

561 BRAF (V600E) Mutation and P16 Expression in Malignant Melanoma in Nigerians: A 10 Year Retrospective Study

Omobolade Obadofin[1], *KABIR BADMOS*[2], *Nick Orsi*[3], *Matthew Bipin*[4], *Olorunda Rotimi*[5], *Adekunbiola A Banjo*[6]. [1]Federal Medical Center Ebute- Metta, Lagos, Nigeria, Surulere, [2]College of Medicine of University of Lagos, Mushin, Lagos, [3]St James's University Hospital, Leeds, United Kingdom, [4]St James's University Hospital, Leeds, United Kingdom, [5]Leeds, [6]Lagos University Teaching Hospital, Nigeria, Lagos

Background: Malignant melanoma (MM) is the most lethal of all skin cancers, accounting for about 79% of skin cancer related deaths. In blacks, it is associated with greater morbidity and mortality compared to Caucasians. Studies have shown that MM with BRAF V600E mutation and those with loss of p16 protein expression are associated with aggressive behavior and worse prognosis. BRAF kinase inhibitors have also been approved for treatment of BRAF V600E mutant cases while p16 expression is being proposed as a prognostic marker for MM. No previous study however has been carried out in Nigeria and West African (WA) to determine these facts.

Design: The aim of the study was to determine the BRAF V600E mutation and loss of p16 expression in MM cases in Lagos, Nigeria within the last 10 years and to correlate these with prognostic markers.

Formalin-fixed paraffin-embedded (FFPE) tissue blocks and corresponding archival routine H&E stained slides of all confirmed cases of MM from January 2005 to December 2014 in Anatomic and Molecular Pathology Department of Lagos University Teaching Hospital (LUTH) were retrieved. Cutaneous MM cases were classified into histologic variants. Clark's stage, Breslow thickness and ulceration statuses were determined. Fresh sections from the FFPE tissue blocks were taken for Immunohistochemical (IHC) studies to determine mutant BRAF V600E and p16 protein expression using the VE1 and anti-CDKN2A/p16INK4a monoclonal antibodies respectively.

Results: During the study period 52 MM cases were histologically diagnosed in LUTH which represented 1.0% of total solid malignancies; 43 of these occurred in the skin accounting for 19.7% of all skin cancers and making MM the 3rd commonest skin cancer after SCC and Kaposi sarcoma. IHC was carried out on 45 cases with viable tissue blocks: 37 cutaneous MM, 3 musosal MM, 2 ocular MM and 3 lymph node metastases. 11% of the cases had BRAF V600E for mutation while 69% had loss of p16 expression.

Conclusions: MM cases in a Nigerian/WA setting are the wild type (BRAF *wt*) and as such BRAF kinase inhibitors may only be effective in treating very few of our patients. However, the CDKN2A gene pathway is mutated in majority of our cases. Hence, loss of p16 protein expression and delayed presentation may be responsible for the huge and aggressive MM seen in our environment.

562 Histopathological and Immunophenotypic Features of Cutaneous Involvement by Angioimmunoblastic T-cell Lymphoma

Naoki Oishi[1], *Julio Sartori-Valinotti*[2], *Mark A Cappel*[3], *Andrew Feldman*[4]. [1]Mayo Clinic, Rochester, MN, [2]Rochester, MN, [3]Mayo Clinic, [4]Mayo Clinic, Rochester, MN

Background: Angioimmunoblastic T-cell lymphoma (AITL) is a peripheral T-cell lymphoma characterized by generalized lymphadenopathy, B symptoms, follicular helper T-cell (T_{FH}) immunophenotype, and frequent *RHOA* and *IDH2* mutations. Approximately 50% of AITL patients have cutaneous manifestations, including maculopapular rash and erythematous eruption, often mimicking inflammatory dermatoses. Moreover, unlike the well characterized pathological features of nodal AITL, the pathological features of cutaneous AITL have not been fully established. Therefore, it is sometimes challenging to differentiate AITL from inflammatory conditions in cutaneous biopsies.

Design: We evaluated the clinical, histological, and immunophenotypic features of 30 cutaneous biopsy samples from 17 AITL patients. Immunohistochemistry for CD2 (n=8), CD3 (n=26), CD4 (n=22), CD5 (n=13), CD7 (n=20), CD8 (n=18), TCR βF1 (n=15), TCR γδ (n=14), CD10 (n=18), BCL6 (n=17), PD1/CD279 (n=23), and CXCL13 (n=12) was performed. Epstein-Barr virus (EBV) was detected using in situ hybridization (ISH) for EBER (n=15).

Results: Samples were obtained from the trunk (n=10), upper extremity (n=9), or lower extremity (n=11). Perivascular infiltration of small- to medium-sized lymphocytes with or without periadnexal distribution was seen in 23/30 (77%) samples; the density of the infiltrating lymphocytes varied considerably. Infiltrates with nodular, interface, and diffuse distributions were identified in 5 (17%), 1 (3%), and 1 (3%) samples, respectively. Granulomas were identified in 3/30 (10%) samples. Infiltrating lymphocytes were generally positive for pan-T cell markers including CD2, CD3, and CD5, while aberrant diminished or absent expression of CD7 was found in 8/30 (27%) samples. The CD4/CD8 ratio was >1 in 13/18 (72%) samples. PD1 was most the frequently expressed T_{FH} marker (22/23 [96%] samples), while CD10, BCL6, and CXCL13 were positive in 10/18 (56%), 15/17 (88%), and 9/12 (75%) samples, respectively. EBV-positive B-cells were detected in 3/15 (20%) samples with varying density.

Conclusions: Despite their histopathological resemblance to inflammatory conditions, cutaneous lesions of AITL are consistently positive for T_{FH} markers, especially PD1, as seen in nodal AITLs. The presence of EBV-positive B cells may support the diagnosis of AITL, although its prevalence is less than in nodal AITL. Therefore, an immunohistochemical panel of T_{FH} markers and EBER ISH are important tools for the accurate diagnosis of cutaneous involvement by AITL.

563 Mantle Cell Lymphoma in the Skin: Clinicopathologic Analysis in a Series of Nine Cases

Gauri Panse[1], *Antonio Subtil*[2]. [1]Yale School of Medicine, New Haven, CT, [2]Yale University, New Haven, CT

Background: Mantle cell lymphoma (MCL) is an aggressive B-cell neoplasm with cutaneous involvement in a very small subset of cases. Rarely, cutaneous involvement may be the first manifestation of the disease and varied morphologies could lead to a potential misdiagnosis of other lymphomas. Herein, we present nine cases of secondary cutaneous involvement by systemic MCL and review the clinicopathologic features.

Design: MCLs with cutaneous involvement from our institution were retrospectively reviewed with diagnosis confirmed by expert review.

Results: Twelve specimens from nine patients met the criteria. Patients ranged from 60-87 years (median, 70 years), including 6 males and 3 females. Sites of involvement included head & neck (n=3), trunk (n=5) and extremities (n=4). Of the nine cases, 3 showed classic morphology, 2 were blastoid, 3 pleomorphic and 1 showed marginal zone lymphoma (MZL)-like areas juxtaposed to classic MCL. Four cases presented with cutaneous lesions as the first tissue manifestation of the disease. A second malignancy was identified in 3/9 cases (2 melanoma and 1 papillary thyroid carcinoma). One case showed MCL associated with metastatic melanoma in the same biopsy specimen. By immunohistochemistry, the cells were CD20+ (9/9), CD5+ (8/9), CD23- (9/9), CD10- (7/7), CD43+ (5/6), CyclinD1+ (9/9) and Ki-67 ranged from 60-95%. Peripheral blood flow cytometry was available in 7 cases and was consistent with MCL. FISH was performed on two cases and demonstrated the characteristic t(11,14) translocation. Immunofluorescence studies were done on one case (clinically resembling vasculitis) and showed IgM positivity within the tumor cells. Follow up, available on six cases (mean 32.5 months, range 4-77), showed that 6/6 had Stage IV disease; one patient was alive with disease (4 months follow-up) and the remaining 5 died of disease.

Conclusions: Six out of nine cases in our series demonstrated blastoid, pleomorphic or MZL-like morphologies that could potentially mimic other primary cutaneous lymphomas or leukemia cutis. Rare cases of MCL may show surface IgM expression on immunofluorescence or may occur in association with other malignancies such as metastatic melanoma. Immunohistochemistry for cyclin D1 and FISH for t(11,14) is helpful for diagnosis. Imaging studies may be necessary to detect systemic involvement in MCL with cutaneous presentation as the first manifestation of the disease as seen in 4/9 cases in our series.

564 Melanomas with NF1 Mutations: Histopathologic, Clinical and Molecular Correlation

Gauri Panse[1], *Ying-Chun Lo*[2], *Antonietta Antonietta*[3], *Ruth Halaban*[3], *Marcus Bosenberg*[4], *Anjela Galan*[3]. [1]Yale School of Medicine, New Haven, CT, [2]Yale School of Medicine, North Haven, CT, [3]Yale University School of Medicine, [4]Guilford, CT

Background: *NF1* mutations have been identified in a subset of *BRAF* and *NRAS* wild-type melanomas on chronically sun damaged skin. Herein, we describe the clinicopathologic and molecular findings in melanomas with truncating / loss of function *NF1* mutations.

Design: A retrospective review of whole-exome sequencing results was performed to identify melanomas with *NF1* mutations. Twenty-three cases with nonsense *NF1* mutations that usually result in truncated, non-functional proteins were identified and evaluated for histopathologic features and molecular alterations using 45 melanomas without *NF1* mutations as controls. Chi-square or Fisher exact test were used to calculate p-values as appropriate using GraphPad Prism software.

Results: The cohort of *NF1* mutated melanomas included primary / locally recurrent (n=11) and metastatic tumors (n=12), from 14 males and 9 females, aged 47-98 years (median, 78 years). Primary sites included head & neck (n=8), extremities (n=7), trunk (n=5), unknown (n=2) and ovary (melanoma arising in mature cystic teratoma, n=1). Primary tumors were available for evaluation in 21 cases, of which 18 (86%) showed histopathologic evidence of chronic sun damage. Morphologically, the tumors were predominantly epithelioid (n=13), spindle cell (n=8), desmoplastic (n=1) and pleomorphic / sarcomatoid (n=1). Five of the 23 cases had two or more inactivating *NF1* mutations. Of the patients with NF1 mutations, 2 (8.7%) displayed $BRAF^{V600E/K}$, 2 (8.7%) had $NRAS^{Q61L/Q70X}$ and 1 (4.3%) showed KIT^{D816V} mutation. Non-V600 *BRAF* mutations were identified in 4 *NF1* mutated melanomas & included F468S (case 1); D594N (case 2); S114F, D594N and G758E (case 3) and P74S and P75L (case 4). The non-NF1 mutated melanomas displayed $BRAF^{V600E/K}$, $NRAS^{Q61H/K/L/V}$, $RAC1^{P29S}$ and KIT^{L160V} mutations in 18 (40%), 10 (22.2%), 2 (4.4%) and 1 (2.2%) cases. Univariate analysis revealed that non-V600 *BRAF* and $RAC1^{P29S}$ mutations were more common in the cohort of *NF1* mutated melanomas than the control group (p=0.04), while $BRAF^{V600E}$ mutations were less frequent in the *NF1* subtype (p=0.01).

Conclusions: Melanomas with truncating *NF1* mutations exhibit a wide range of morphologies and evidence of chronic sun damage in majority of the cases. Melanomas with inactivating *NF1* mutations are less likely to harbor $BRAF^{V600E/K}$ mutations, while non-V600 *BRAF* and $RAC1^{P29S}$ mutations occur at a higher frequency in these tumors when compared to melanomas without *NF1* mutations.

565 Akt/mTOR and β-catenin/Cyclin D1 in Dermatofibrosarcoma Protuberans with a Special Reference to Fibrosarcomatous Variant

Sun Young Park[1], *Euno Choi*[2], *Sun-ju Byeon*[3], *Mee Soo Chang*[4]. [1]Seoul National University Boramae Hospital, Seoul National University College of Medicine, Seoul, Korea, [2]Seoul National University Boramae Hospital, Seoul, [3]Seoul Nat'l Univ/Medicine, Seoul, [4]Seoul National University Boramae Hospital, Seoul National University College of Medicine

Background: Dermatofibrosarcoma protuberance (DFSP) is a rare, locally aggressive cutaneous tumor with intermediate malignancy. In DFSP, there is little known about oncoprotein alteration except for COL1A1-PDGFB fusion, furthermore, some debates about clinical outcomes of fibrosarcomatous variant are still existing.

Design: This retrospective study enrolled 24 patients undergone wide local excision for DFSP from 2004 to 2010. We performed immunohistochemistry for pSTAT3, ERK, pAkt, mTOR, β-catenin and cyclinD1 oncoproteins involved in signal transduction such as JAK/STAT3, MEK/ERK, Akt/mTOR and Wnt/β-catenin/cyclin D1 pathways. As a control for immunohistochemical evaluation, 92 cases of dermatofibroma tissues were used.

Results: The mean age of DFSP patients was 35 years ~~in mean~~ (range: 19 ~ 64). The ratio of male:female was 3:5. Local recurrence of tumor was occurred in 38% (9/24) of DFSP (recurrence interval: 6.5 months in mean). The tumor size (the largest diameter) was 29 mm in mean. The mitotic figures was 5/ 10 HPF in mean (range: 1 ~25/ 10HPF). Immunohistochemically, mTOR positive and β-catenin cytoplasmic expressions were observed more often in DFSP (mTOR, 33 % of DFSP vs. 9% of dematofibroma; β-catenin, 33% of DFSP vs. none of dermatofibroma; $P < 0.05$, respectively). Interestingly, β-catenin cytoplasmic expression in DFSP was correlated with tumor local recurrence ($P < 0.05$). None of DFSP cases showed pSTAT3 positive, and ERK positive was observed in only a DFSP case. In terms of the histologic variant, there were 8 cases of fibrosarcomatous DFSP and 16 conventional DFSP. Fibrosarcomatous DFSP showed frequent mitotic figures than conventional DFSP (mean/10 HPF: 10 mitoses vs. 3; $P < 0.05$). Two cases of fibrosarcomatous DFSP invaded muscle and bone tissue, which revealed frequent mitotic figures than subcutaneous extension cases (mean/10 HPF: 3 mitoses vs. 10; $P < 0.05$). Local recurrence occurred more commonly in fibrosarcomatous DFSP than in conventional DFSP (63% of fibrosarcomatous vs. 31% of conventional; $P < 0.05$). One case of fibrosarcomatous DFSP showed metastasis to pleura at 2 years after excision. CyclinD1 was expressed more predominantly in fibrosarcomatous DFSP than in conventional DFSP ($P < 0.05$).

Conclusions: The β-catenin could be used as a predictive marker for local recurrence of DFSP. The mTOR and β-catenin may be involved in tumorigenesis of DFSP. CyclinD1 may be associated with aggressive behaviors of fibrosarcomatous DFSP.

566 A Comparative Study Of Filaggrin Immunohistochemical Staining In Basal Cell Carcinoma And Squamous Cell Carcinoma

Nikoo Parvinnejad[1], *Ami Wang*[2], *Yuka Asai*[3]. [1]Queen's University, Kingston, ON, [2]Kingston General Hospital, Kingston, ON, [3]Kingston General Hospital

Background: Basal cell carcinoma (BCC) and squamous cell carcinoma (SCC) are the two most common types of skin cancer. The morphologic features of BCC and SCC are usually distinct, although it is not uncommon to encounter difficult cases with overlapping features. The correct diagnosis is not only important for prognosis, but also crucial for treatment; this has a significant impact for special sites such as the vulva, where SCC with greater than 1 mm tumour thickness is treated with additional groin lymph node dissection. Filaggrin is an integral skin barrier protein in the epidermis, which is normally concentrated at the junction of stratum granulosum and stratum corneum.Given the localization of this protein in the upper layers of the normal epidermis, we present a pilot study assessing the utility of filaggrin as an immunohistochemical marker in distinguishing BCC and SCC. Furthermore, mutations in filaggrin have been shown to cause thinner skin and increased UV penetration to the basal layer. Therefore, we also investigated the role of filaggrin in the pathogenesis of BCC and SCC by comparing filaggrin expression in tumour tissue and adjacent normal epidermis.

Design: Tissue microarrays (TMA) were constructed using formalin fixed paraffin embedded tissue of 141 cases of SCC and 66 cases of BCC, each case containing duplicate tumour cores and adjacent normal skin. TMA were stained with anti-filaggrin antibody (FLG01, Abcam) and the staining intensity is stratified manually into negative, weak, moderate and strong . To compare filaggrin expression in tumour and adjacent normal epidermis, digitally scanned sections were analyzed for optical density scores.

Results: Filaggrin is expressed in 65.2% of SCC with various intensity, and 0% of BCC (Table-1). Also, after excluding cases with missing tissue, the remaining pairs showed loss of filaggrin in 96.1% of SCC and 100% of BCC (Table-2).

Table1- Filaggrin immunohistochemical staining in BCC and SCC.

Staining intensity	SCC (n=141)	BCC (n=66)
Negative	49 (34.7%)	66 (100%)
Weak	57 (40.4%)	N/A
Moderate	32 (22.6%)	N/A
Strong	3 (2.1%)	N/A

Table2- Relative filaggrin expression of tumour versus adjacent normal epidermis based on optical density scores.

Relative filaggrin expression	SCC (n=129)	BCC (n=49)
decreased expression	124 (96.1%)	49 (100%)
Increased expression	5 (3.8%)	0 (0%)

Conclusions: Our preliminary data suggest filaggrin is a potential immunohistochemical marker for differentiating BCC from SCC. Secondly, the loss of normal filaggrin expression in most of the tumours suggests that filaggrin loss may be a risk factor for skin cancer development. In the future, we plan to expand the sample size for validation of preliminary results and analysis of filaggrin expression in relationship to various clinicopathological parameters.

567 PD-L1 Expression in Tumour Infiltrating Lymphocytes, Not in Tumour Cells, Is a Poor Prognostic Factor for Primary Acral Melanoma Patients

Min Ren[1], *Bo Dai*[1], *Yunyi Kong*[1], *Jiaojie Lv*[2], *Xu Cai*[3]. [1]Fudan University Shanghai Cancer Center, Shanghai, [2]Fudan University Shanghai Cancer Center, [3]Fudan University Shanghai Cancer Center, Shanghai

Background: Melanoma is a highly malignant tumor with a marked propensity for early metastatic spread. Recently, anti programmed cell death-1 (PD-1)/programmed death-ligand 1 (PD-L1) immunotherapy has shown notable therapeutic benefit in metastatic melanoma, while the clinical relevance of PD-L1 expression remains unclear in melanoma, especially in acral melanoma which is the most common subtype in Asians. Our study aimed to comprehensively evaluate the clinical relevance of PD-L1 expression in acral melanoma.

Design: We quantified PD-L1 expression in tumour cells and tumour infiltrating lymphocytes (TILs) by immunohistochemistry, and analyzed their associations with clinicopathologic features and survival in 78 primary acral melanoma patients from China. The

extent of TILs infiltration was the percentage of total tumor stromal area occupied by mononuclear inflammatory cells on H&E staining, and we defined the presence of TILs when the extent of TILs reached at least 5%. PD-L1 expression in tumor cells was classified into low and high groups according to the mean H-score. And PD-L1 positivity in TILs was defined as H-score of 5 or more.

Results: We found that expression of PD-L1 in tumour cells and TILs (Fig. 1) were all present in a tumour-stroma interface pattern, consistent with the predominant pattern of TILs infiltration (Fig. 2). Furthermore, PD-L1 expression in tumour cells and TILs showed a closely parallel relationship (Spearman'rho=0.381, P=0.001). However, PD-L1 expression neither in tumor cells nor in TILs was significantly correlated with other clinicopathological features (Table 1). In univariate analysis, the disease-specific survival (DSS) was significantly worse in TILs PD-L1pos group than in TILs PD-L1neg group (median DSS: 40.7 months vs. 78.0 months; P=0.008. Table 2). In contrast, there was no significant difference in DSS between tumor cell PD-L1high and tumor cell PD-L1low groups (median DSS: 64.4 months vs. 69.2 months; P=0.378. Table 2). In multivariate analysis, PD-L1 expression in TILs was an independent factor for poor prognosis (P=0.032. Table 3), while PD-L1 expression in tumour cells was not significantly correlated with survival (P=0.354. Table 3).

Table 1 Correlation of PD-L1 expression in tumor cells and TILs with clinicopathologic features.

Clinicopathologic features	NO. (%)	H-score of PD-L1 expression in tumor cells		P value	H-score of PD-L1 expression in TILs		P value
		low	high		<5	≥5	
Sex							
Male	48(61.5)	30	18		39	9	
Female	30(38.5)	19	11	0.941	25	5	0.816
Age							
<55	19(24.4)	13	6		18	1	
≥55	59(75.6)	36	23	0.599	46	13	0.167
Site of lesion							
Hand	5(6.4)	1	4		3	2	
Foot	73(93.6)	48	25	0.061	61	12	0.217
Duration of the lesion before diagnosis, years							
<2.5	48(61.5)	34	14		38	10	
≥2.5	30(38.5)	15	15	0.064	26	4	0.217
Breslow thickness, mm							
≤2.0	13(16.6)	8	5		12	1	
>2.0	65(83.4)	41	24	0.917	52	13	0.917
Clark level							
II-IV	53(68.0)	31	22		45	8	
V	25(32.0)	18	7	0.249	19	6	0.339
Ulceration							
No	43(55.1)	24	19		35	8	
Yes	35(44.9)	25	10	0.168	29	6	0.867
Mitotic rates, mm−2							
≤15	74(94.9)	45	29		61	13	
>15	4(5.1)	4	0	0.291	3	1	0.555
Vascular invasion							
Absent	76(97.4)	47	29		63	13	
Present	2(2.6)	2	0	0.527	1	1	0.329
Regional lymph node metastasis at diagnosis							
Yes	27(34.6)	21	6		22	5	
No	51(65.4)	28	23	0.053	42	9	0.924
Pathologic stage							
I-III	11(14.1)	7	4		10	1	
V	67(2.6)	42	25	1.000	54	13	0.510
Extent of TILs infiltration (%)							
<5	17(21.8)	15	2		17	0	
≥5	61(78.2)	34	27	0.021	47	14	0.032

Table 2 Univariate analysis of clinicopathologic features correlated with DSS in the cohort.

Clinicopathologic features	HR (95%CI)	P value
Sex		
Male		
Female	1.056(0.569-1.958)	0.862
Age		
<55		
≥55	1.468(0.748-2.882)	0.257
Site of lesion		
Hand		
Foot	1.444(0.444-4.690)	0.535
Duration of the lesion before diagnosis, years		
<2.5		
≥2.5	2.570(1.265-5.222)	0.006
Breslow thickness, mm		
≤2.0		
>2.0	0.161(0.039-0.670)	0.004
Clark level		
II-IV		
V	0.366(0.199-0.673)	0.001
Ulceration		
Yes		
No	0.325(0.170-0.610)	<0.001
Mitotic rates, mm−2		
≤15		
>15	0.375(0.132-1.069)	0.054
Vascular invasion		
Absent		
Present	0.121(0.028-0.529)	0.001
Regional lymph node metastasis at diagnosis		
Yes		
No	0.336(0.183-0.616)	<0.001
Pathologic stage		
I		
II-IV	0.088(0.012-0.642)	0.002
H-score of PD-L1 expression in TILs		
<5		
≥5	0.405(0.201-0.814)	0.008
H-score of PD-L1 expression in tumor cells		
Low		
High	1.341(0.693-2.595)	0.378
Extent of TILs infiltration (%)		
<5		
≥5	1.064(0.522-2.168)	0.864

Table 3 Multivariate analysis of characteristics correlated with DSS in the cohort.

Characteristics	HR (95%CI)	P value
Sex (Male vs Female)	0.905(0.449-1.852)	0.838
Age (<55 vs ≥55)	1.319(0.636-2.733)	0.232
Site of lesion (Hand vs Foot)	2.262(0.670-7.630)	0.365
Duration of the lesion before diagnosis (<2.5 vs ≥2.5)	1.996(0.953-4.179)	0.112
Breslow thickness (≤2.0 vs >2.0)	0.616(0.056-6.718)	0.087
Clark level (II III IV vs V)	0.973(0.424-2.236)	0.411
Ulceration (Yes vs No)	0.405(0.208-0.790)	0.008
Mitotic rates (≤15 vs >15)	0.725(0.232-2.266)	0.718
Vascular invasion (Absent vs Present)	0.509(0.092-2.815)	0.326
Regional lymph node metastasis at diagnosis (Yes vs No)	0.455 (0.237-0.873)	0.018
Pathologic stage (I vs II III IV)	0.150(0.020-1.153)	0.059
H-score of PD-L1 expression in TILs (<5 vs ≥5)	0.455 (0.222-0.934)	0.032
H-score of PD-L1 expression in tumor cells (Low vs High)	1.565(0.675-3.628)	0.354
Extent of TILs infiltration (<5 vs ≥5)	0.884(0.378-2.069)	0.908

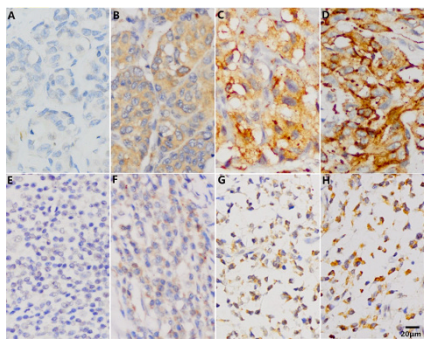

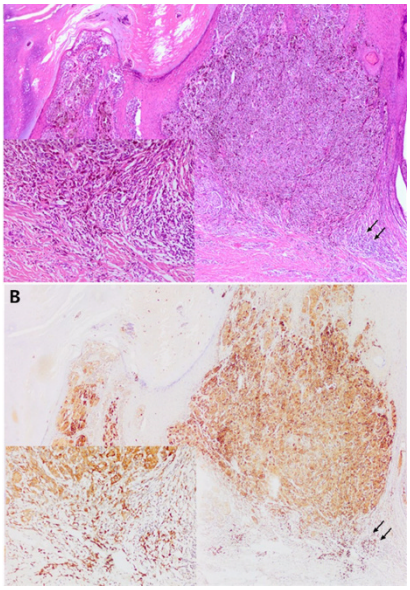

Conclusions: This is the first study which comprehensively evaluated PD-L1 expression both in tumor cells and TILs in acral melanoma. Our data indicated that PD-L1 expression in TILs, not in tumor cells, was an independent predictor of poor prognosis in primary acral melanoma patients.

568 Histologic Patterns of Cutaneous Metastases of Breast Carcinoma: A Clinicopathological Study of 158 Cases

Shira Ronen[1], *Wei-Shen Chen*[2], *Sri Krishna Chaitanya Arudra*[3], *Celestine Marie Trinidad*[4], *Saul Suster*[5], *Doina Ivan*[6], *Victor Prieto*[7]. [1]Medical College of Wisconsin, Milwaukee, WI, [2]University of Texas MD Anderson Cancer Center, [3]University of Texas MD Anderson Cancer Center, Houston, Texas, [4]University of Texas MD Anderson Cancer Center, Houston, TX, [5]The Medical College of Wisconsin, Milwaukee, WI, [6]M. D. Anderson Cancer Center, Houston, TX, [7]UT - MD Anderson Cancer Center, Houston, TX

Background: Cutaneous metastases have a great impact on detection, management, and prognosis of the primary tumor. We have studied 158 cases of cutaneous metastasis of invasive breast carcinoma in 157 females and 1 male to determine the histologic features and distribution of the metastases.

Design: Cases of metastatic breast carcinoma to the skin diagnosed between 2010-2017 were retrieved from our files. 178 cases in 174 patients were found, of which 23 were consultation cases and the remainder originated at our medical centers. Demographic information, tumor site, morphology, depth of invasion, perineural invasion (PNI), perivascular invasion (PVI), adnexal involvement, and clinical findings were collected. Estrogen (ER), Progesterone (PR) and HER2/neu status of both the primary breast and skin metastasis were also gathered.

Results: The primary lesion in 138 patients was invasive ductal carcinoma (IDC) and in 14 patients invasive lobular carcinoma (ILC). Correlation of the primary tumor with the metastasis showed that metastases occurred predominantly in the ipsilateral side (127 cases). The most common distribution was chest wall (117 cases), back & abdomen (8 cases each), scalp (6 cases), shoulder & axilla (5 cases each), neck (4 cases), arm (3 cases), cheek & forehead (1 case each). The metastases from IDC showed 3 main patterns: an interstitial pattern of growth - 92 cases, nodular pattern - 29 cases, and an inflammatory carcinoma-like pattern (exclusively intravascular) - 11 cases. The metastases from ILC showed mostly an interstitial pattern of growth and in 1 case an intravascular pattern. Pagetoid spread was seen in 16 cases and subcutaneous involvement was noted in 49 cases. LVI and PNI were present in 60 and 35 of the cases, respectively. Correlation of PR, ER and HER2/neu status was done in 75 cases and showed 28 cases with different results.

Conclusions: Metastatic breast carcinoma shows predilection for the ipsilateral chest wall but can involve other locations, including abdomen, axilla, and neck which are consistent with the lymphatic draining sites of the mammary gland. In rare cases, aberrant pathways may result in metastasis to other locations (scalp, forehead, cheek). The original histology at the metastatic site is usually preserved. Metastatic carcinoma with interstitial growth pattern can be confused for metastatic carcinoma from other sites and interstitial dermatitis. Immunohistochemical stains plus careful clinical history helped to establish the correct diagnosis.

569 Emperipolesis May Be Seen in Cutaneous Xanthogranulomas: A Multi-Institutional Observation

Kristen Ruby[1], *April C Deng*[2], *Jingwei Zhang*[3], *Robert E LeBlanc*[4], *Shaofeng Yan*[5]. [1]Dartmouth-Hitchcock Medical Center, Lebanon, NH, [2]University of Massachusetts School of Medicine, [3]Carolinas Dermatology Group, [4]Dartmouth-Hitchcock Medical Center, [5]Dartmouth-Hitchcock Med.Ctr., Hanover, NH

Background: Cutaneous Rosai-Dorfman Disease (RDD) may be clinically and histologically difficult to distinguish from other non-Langerhans cell histiocytoses, particularly xanthogranuloma (XG). Pathologists use S100 immunopositivity, abundant plasma cells, and the presence of emperipolesis to differentiate RDD histologically. However, S100 expression has been reported in XG and in practice we have observed emperipolesis in cases otherwise clinicopathologically consistent with XG. The purpose of this study was to evaluate and document occasional emperipolesis observed in XG and further characterize subtle histologic findings of XG.

Design: A pathology database search of our institution (between 1/2011 and 12/2016) yielded 35 cases with XG as diagnosis or among a differential diagnosis. Slides and medical records were reviewed, and the histologic features were evaluated. S100, CD68 and CD1a immunohistochemistry were used to further evaluate all lesions exhibiting emperipolesis.

Results: Emperipolesis was identified in 5 of 35 cases. Additionally, 5 histologically similar cases were contributed by colleagues at peer institutions, resulting in 10 total: 7 were clinically and histologically consistent with XG, and 3 raised a histologic differential diagnosis of XG versus RDD while their clinical presentations favored XG. Patient ages ranged from 19 months to 59 years, all had solitary subcentimeter papules, and none had lymphadenopathy or systemic involvement. All biopsies showed emperipolesis of lymphocytes and/or eosinophils in large histiocytes (a prominent feature in 5 cases including those with a differential diagnosis) along with foamy mononuclear forms and Touton giant cells. Notably, none of these cases showed abundant plasma cells, as is common in RDD. Nine cases showed variable S100 expression: focal/weak expression (4 cases), focal/strong (1 case), diffuse/moderate (2 case), and diffuse/strong (2 case). Histiocytes in all cases were CD68 positive and CD1a negative.

Conclusions: Emperipolesis and S100 immunopositivity in a skin biopsy may not reliably distinguish XG from RDD. To avoid this diagnostic pitfall, clinical correlations are essential as well as the histologic findings of Touton giant cells, foamy mononuclear cells, and absence of abundant plasma cells.

570 Pathology Of Skin Lesion Associated With Pediatric Solid Organ Transplantation

Claudia M Salgado[1], *Miguel Reyes-Múgica*[2], *Rita Alaggio*[3]. [1]Children's Hospital of Pittsburgh, Pittsburgh, PA, [2]Children's Hospital of Pittsburgh of UPMC, Pittsburgh, PA, [3]Pittsburgh, PA

Background: Despite abundant information on skin malignancies associated with solid organ transplantation (SOT) in adults, limited information exists regarding malignant and nonmalignant skin changes in children. Our aim was to describe skin biopsy changes in pediatric patients with SOT and correlate these changes with clinical and prognostic findings.

Design: Retrospective cohort study of STO recipients under 20 years of age followed at Children's Hospital of Pittsburgh who had an allograft biopsy (heart, lung, kidney, intestine, liver and multivisceral) from July 2015 to July 2017, with at least 3 months of follow-up. The subgroup with skin biopsies was selected and the final diagnoses (dx) and clinical histories reviewed. Statistical analysis was performed using SPSS 22.

Results: There were 433 SOT recipients (164 liver, 135 heart, 78 bowel, 44 kidney, 7 lung and 5 multivisceral), with mean age of 10.8 ± 5.4 years, 237 (54.7%) males and follow-up after transplant (tx) from 3 months to 18 years (mean 5.7 years ± 4.2). 49 skin biopsies were performed in 45 patients (10.3%). Interface and perivascular dermatitis was identified at histology in 22/49 (44.8%) biopsies. After clinicopathological correlation, graft versus host disease (GVHD) was diagnosed in 12 patients; viral infection in 4 (3/4 adenovirus); drug reaction in 2; and 2 cases were non-specific. GVHD was found in 9/78 (11.5%) of bowel and 3/164 (1.8%) of liver tx recipients (p=0.0087). GVHD manifested within 100 days after tx in 9/12 cases (75%); two patients died. Other findings included: skin infections (14 biopsies/12 patients); benign skin tumors (4); scar post-surgical procedure (4); subcutaneous Burkitt lymphoma (2); and anetoderma (1). The etiology of infectious processes was identified in 7/14 (50%) cases: 5/14 (35.7%) were HPV-related, one mycobacterial and one fungal. Intriguingly, 2 liver transplant cases showed neutrophilic dermatitis and/or vasculitis and kidney biopsies with IgA nephropathy confirming Henoch-Schonlein purpura.

Conclusions: Ten percent of pediatric SOT recipients underwent to skin biopsies. GVHD more frequenty follows bowel tx but also

occurs after liver tx. Clinicopathological correlation is indispensable in patients with interface/perivascular dermatitis to identify its etiology. In liver tx recipients a peculiar association with neutrophilic dermatitis and/or vasculitis and IgA nephropathy was found. This should be considered in the diagnostic work up of liver tx patients with leucocytoclasic vasculits.

571 Degranulation and shrinkage of dark cells in eccrine glands and elevated serum carcinoembryonic antigen in patients with acquired idiopathic generalized anhidrosis

Kenji Sano[1], *Takeshi Uehara*[2]. [1]Iida Municipal Hospital, Iida, Nagano, [2]Shinshu University School of Medicine, Matsumoto

Background: Acquired idiopathic generalized anhidrosis (AIGA) is characterized by anhidrosis/hypohidrosis without other autonomic and neurological dysfunctions. Pathologically, AIGA is considered to usually present no significant morphological alterations in eccrine glands, the secretory portion which consists of clear cells, dark cells, and myoepithelial cells. AIGA patients recently have been reported to show high serum concentrations of carcinoembryonic antigen (CEA).

Design: We performed comparative analysis of eccrine glands between sweat-preserved and non-sweating skin in four AIGA patients. Serum CEA concentrations in 22 cases with AIGA were measured with healthy volunteers. Furthermore, we semiquantitatively investigated dermcidin, FoxA1 and CEA expression in eccrine glands of 12 cases with AIGA and 5 cases with non-AIGA. For one patient, electron microscopic examination was added.

Results: Marked degranulation and shrinkage of dark cells consistently occurred in AIGA. Furthermore, high serum CEA concentrations were found in 14 of 22 AIGA patients (over 60%), but serum CEA levels were not correlated with CEA expression in eccrine glands. Dermcidin expression in dark cells apparently decreased in AIGA patients, severely in those with high serum CEA and moderately in those with low serum CEA, while well-preserved expression was found in non-AIGA subjects. EM examination also showed dark cell shrinkage.

Conclusions: Our study suggests morphological damage and molecular dysregulation of dark cells, leading to impairment of their functions in AIGA patients. Severely damaged dark cells correspond to high serum CEA. Accordingly, these pathological changes in eccrine dark cells may be involved in anhidrosis/hypohidrosis of AIGA.

572 Comparison of SNParray and Melanoma FISH assays in Atypical Pigmented Lesions with Heterozygous loss of CDKN2A

Kabeer Shah[1], *William R Sukov*[1], *Lori Erickson*[1], *Thomas Flotte*[1].[1]Mayo Clinic, Rochester, MN

Background: Atypical melanocytic lesions infrequently require additional ancillary testing for enhanced classification via identification of copy number variations (CNV). However, Spitzoid melanocytic lesions comprise a majority of ambiguous lesions tested with ancillary molecular methodologies, such as fluorescence in-situ hybridization (FISH). CDKN2A (9p21.3), a known tumor suppressor in melanoma, is one loci evaluated within the expanded eight probe FISH assay [6p25 (RREB1), 6q23 (MYB), 11q13 (CCND1), 8q24 (MYC) and 9p21.3 (CDKN2A), centromeres 6, 8 and 9] utilized at our institution. Homozygous loss of CDKN2A is a known molecular alteration in melanoma, however isolated heterozygous loss by FISH is not well characterized and seen in 7.7% of our cohort with chromosomal abnormalities. In this study we evaluate heterozygous loss of CDKN2A, an equivocal FISH finding, with comparative methodologies p16 immunohistochemistry (IHC) and SNParray.

Design: Ambiguous melanocytic lesions with isolated heterozygous loss of CDKN2A (monosomy 9) by FISH were identified (N=14). Available tissue was recalled, DNA extracted from formalin fixed paraffin embedded tissue (N=8) for SNParray (Affymetrix, Oncoscan V3), and clinical follow-up obtained. p16 IHC was performed on available cases (N=9). Control tissue from histologically and FISH negative nevi (2) and melanomas (2) were used to verify results.

Results: Fourteen cases (4M;10F; mean age 27 years, range 2-54 years) showed isolated heterozygous loss of CDKN2A by FISH, with no evidence of recurrence after complete excision. Cases had a predominant spitzoid morphology (N=10), dermal mitoses, and an increased Ki-67 index. Of the tested cases (N=8), five cases (cases 1, 4, 6, 7, 8) showed additional chromosomal gains and losses when interrogated by SNParray (see table 1). A single case (case 2) revealed a normal karyotype by SNParray.

Case 4 showed a cryptic 9p21.1 lesion with additional CNVs, unrecognized by FISH. Additionally, IHC showed protein expression loss of CDKN2A via p16 loss. Case 7, identified gain of 11p, a benign finding, unrecognized by FISH. Cases 1, 6, & 8, showed additional CNVs inferring greater suspicion for mutagenesis. No cases had clinical recurrence.

Case #	Age	Sex	Histologic Category	FISH	SNParray	p16 IHC
1	36	F	Nevoid	Mono-somy 9	Monosomy 9,10,X	Intact
2	54	M	Spitzoid	Mono-somy 9	Normal	X
3	2	M	Spitzoid	Mono-somy 9	Monosomy 9	Intact
4	19	F	Spitzoid	Mono-somy 9	Bi-allelic del(9p21.1), Monosomy (1p31,1p13.3,3 p12,3p,5q,9,12p11,21p11.1, 12q,12q14.1)	Loss
5	39	F	DPN	Mono-somy 9	Monosomy 9	Intact
6	55	F	Spitzoid	Mono-somy 9	Monosomy 9, Mono X	Intact
7	24	F	Blue Nevus	Mono-somy 9	Monosomy 9, gain 11p	Intact
8	32	F	Dysplastic	Mono-somy 9	Monosomy 1p, 2p, 9, 10	Intact
9	40	F	Spitzoid	Mono-somy 9	No Tissue	Intact
10	3	F	Spitzoid	Mono-somy 9	No Tissue	X
11	28	F	Spitzoid	Mono-somy 9	No Tissue	X
12	38	M	Spitzoid	Mono-somy 9	No Tissue	Intact
13	5	F	Spitzoid	Mono-somy 9	No Tissue	X
14	4	M	Spitzoid	Mono-somy 9	No Tissue	X

Conclusions: Cases with heterozygous loss of CDKN2A by FISH share a Spitzoid morphology and indolent clinical behavior with 4-year mean follow-up. SNParray can reveal cryptic or additional CNV's not detected by FISH. Conversely, FISH can be diagnostically superior in low disease burden specimen.

573 Genetic Overlap between Primary Dermal Melanoma and Cutaneous Melanoma Metastases

Sheila Shaigany[1], *Klaus Busam*[2], *Basil Horst*[3]. [1]New York University Langone Medical Center, New York, NY, [2]Memorial Sloan-Kettering CC, [3]Vancouver General, University of British Columbia, Vancouver, BC

Background: Primary dermal melanoma (PDM) is a rare malignancy which histologically mimics melanoma metastasis, but carries a significantly more favorable prognosis. Diagnosis of PDM cannot be established on histologic grounds alone, but requires absence of evidence of melanoma elsewhere by clinical history and whole-body imaging studies. Despite unique characteristics in biologic behavior of these often deep dermal melanomas, limited data on molecular characterization is available from isolated case reports, in some of which diagnosis of primary dermal melanoma remains doubtful due to adverse outcome. Considering the favorable prognosis associated with PDM and stark contrast in biologic behavior when compared to nodular and metastatic melanoma, we studied a larger case series of PDM to determine mutational frequency in genes with high prevalence of mutations in metastatic melanomas, as well as in non-metastatic dermal melanocytic proliferations such as blue nevi.

Design: Studies were approved by respective Institutional Review Boards. Nine cases fulfilling strict histologic criteria of primary dermal melanoma were identified in patients with absent history of melanoma elsewhere, negative sentinel node biopsies and/or PET scans, as well as uneventful clinical history upon follow-up. DNA was extracted from FFPE-tissue, and eight cases passed quality control measures and were subjected to targeted exon sequencing.

Results: BRAF/NRAS hotspot mutations were detected in four of eight tumors. Two cases showed probable low-activating BRAF or NRAS mutations in combination with additional aberrations in other MAPK-pathway effectors, suggesting that a majority of primary dermal melanomas relies on MEK-ERK signaling. No oncogenic mutations were identified in two cases. Furthermore, none of the analyzed tumors showed activating mutations in Gα subunits, including GNAQ and GNA11.

Conclusions: Although primary dermal melanoma is genetically heterogeneous, our findings suggest the predominance of MAPK pathway aberrations, in agreement with the mutational profile of cutaneous melanomas in general. Due to absence of genetic overlap with other distinct primary dermal melanocytic proliferations, in particular blue nevi, mutational profiling of GNAQ/GNA11 will unlikely aid in the difficult differential diagnosis of PDM versus melanoma metastasis. Furthermore, our findings suggest potential benefit of BRAF/MEK inhibition for disease control in rare instances of PDM metastases.

574 MCPyV mRNA in situ Hybridization: Validation Against CM2B4 Immunohistochemistry

Wonwoo Shon[1], *Andrew Siref*[2], *Robert Monroe*[3], *Richard Essner*[4], *David Frishberg*[5], *Bonnie Balzer*[2]. [1]Cedars-Sinai Medical Center, [2]Cedars-Sinai Medical Center, Los Angeles, CA, [3]Advanced Cell Diagnostics, [4]Cedars-Sinai Medical Center, [5]Cedars-Sinai Med Ctr, West Hollywood, CA

Disclosures:
Robert Monroe: *Employee,* Advanced Cell Diagnostics

Background: Merkel cell carcinoma (MCC) is a rare aggressive primary neuroendocrine tumor of the skin. Prior studies have shown strong link to infection with Merkel cell polyomavirus (MCPyV). Detection of MCPyV in tumor cells plays an important diagnostic role and may be valuable in predicting clinical behavior. The key diagnostic assays for MCPyV detection are qPCR and CM2B4 immunohistochemistry. While the qPCR method is more sensitive and considered as the gold standard for MCPyV detection, it is labor intensive and does not allow correlation with morphologic aspects of the tissue sample with the virus status. Therefore, CM2B4 immunohistochemistry is commonly employed as a surrogate marker of MCPyV infection. In this study, we evaluated the RNAscope chromogenic in situ hybridization (CISH) for MCPyV detection and compared the results with CM2B4 immunohistochemistry.

Design: MCPyV mRNA CISH (RNAscope probe V-MCPyV-LT-ST-Ag, Advanced Cell Diagnostics) was manually performed on TMA slides containing 38 cases of MCC and compared with CM2B4 immunohistochemistry. Subsequently, the fully automated method was formulated using the Leica Bond III autostainer.

Results: MCPyV mRNA CISH detected 100% (18/18) of the CM2B4-positive MCCs. In addition, MCPyV mRNA expression was also present in 2/20 CM2B4-negative cases. The concordance between the manual and automated MCPyV mRNA CISH was 100%.

Conclusions: Our study is the first to compare the in situ detection results of MCPyV mRNA and MCPyV LTAg protein expression. These findings suggest that RNAscope CISH is a more sensitive and reliable method than CM2B4 immunohistochemistry in MCPyV detection. Moreover, this novel CISH assay can be easily integrated into surgical pathology practice using a fully-automated method.

575 Symmetric Drug-Related Intertriginous and Flexural Exanthema (SDRIFE): A Clinicopathologic Study

Emily H Smith[1], *Andrew Schuler*[2], *May P Chan*[3]. [1]University of Missouri, [2]University of Michigan, [3]University of Michigan, Ann Arbor, MI

Background: Symmetric drug-related intertriginous and flexural exanthema (SDRIFE) is a cutaneous drug reaction characterized by erythema of the gluteal/perianal area and/or V-shaped erythema of the inguinal/perineal area with symmetric involvement of at least one other intertriginous/flexural site in the absence of systemic signs or symptoms. Most published cases were induced by antibiotics. The histopathologic features have only been described in scattered case reports.

Design: Our pathology database was searched for SDRIFE and "baboon syndrome" biopsied from intertriginous sites. Seventeen cases meeting clinical criteria for SDRIFE were selected for further medical record and histopathologic review.

Results: A complete list of clinical and histopathologic features is shown in the Table. Clinical morphology was most commonly described as erythematous plaques (88%) or papules (65%). Many cases were scaly (41%) and edematous (41%). Up to 35% of cases were attributed to antibiotics, with non-steroidal anti-inflammatory drugs being the second most common culprit (12%). The rest were attributed to various other types of medications. The eruptions typically occurred within weeks of exposure to the inciting medications (median: 14 days; range: 2 days to 4 months). The top five clinical differential diagnoses included SDRIFE (35%), morbilliform drug reaction (35%), eczematous dermatitis (24%), drug eruption not-otherwise-specified (24%), and acute generalized exanthematous pustulosis (AGEP) (18%). Notably, 7 (41%) patients had a history of hematologic malignancies or solid tumors.

Histopathologically, most cases resembled an eczematous dermatitis with frequent findings of a superficial perivascular lymphocytic infiltrate (100%), parakeratosis (88%), dermal eosinophils (88%), and spongiosis (76%). Other common features included extravasated erythrocytes (65%), papillary dermal edema (59%), and acanthosis (53%). Sparse dermal neutrophils (41%) and interstitial histiocytes (29%) suggested an urticarial or interstitial granulomatous dermatitis-like component in a subset of cases. Overlapping features with AGEP, namely subcorneal or intraepidermal pustules, were identified in 24% of cases.

Clinical Morphologies		Histopathologic Features	
Erythema	15 (88%)	Superficial perivascular lymphocytic infiltrate	17 (100%)
Plaques	15 (88%)	Parakeratosis	15 (88%)
Papules	11 (65%)	Dermal eosinophils	15 (88%)
Scaly	7 (41%)	Spongiosis	13 (76%)
Edematous	7 (41%)	Extravasated erythrocytes	11 (65%)
Dusky	4 (24%)	Papillary dermal edema	10 (59%)
Patches	2 (12%)	Acanthosis	9 (53%)
Vesicles/bullae	2 (12%)	Sparse dermal neutrophils	7 (41%)
Urticarial	2 (12%)	Langerhans cell microabscesses	5 (29%)
Pustules	1 (6%)	Interstitial histiocytic infiltrate	5 (29%)
Macules	1 (6%)	Subcorneal/intraepidermal pustules	4 (24%)
Annular	1 (6%)	Basal vacuolar change	3 (18%)
Pruritic	1 (6%)	Spongiotic vesicles	1 (6%)
Violaceous	1 (6%)	Psoriasiform hyperplasia	1 (6%)
Lichenified	1 (6%)	Dyskeratosis	1 (6%)
Hyperpigmented	1 (6%)	Subepidermal split	1 (6%)
Blanchable	1 (6%)	Deep perivascular lymphocytic infiltrate	1 (6%)

Conclusions: To our knowledge, this is the largest clinicopathologic study of SDRIFE. Besides antibiotics, a wide variety of other medications may cause SDRIFE. Recognition of the range of clinical and histopathologic features in SDRIFE will help confirm a drug etiology and guide appropriate management.

576 Neurofilament is Superior to Cytokeratin 20 in Supporting Cutaneous Origin for Neuroendocrine Carcinoma

Lauren Stanoszek[1], *May P Chan*[2], *Nallasivam Palanisamy*[3], *Shannon Carskadon*[4], *Javed Siddiqui*[5], *Rajiv Patel*[6], *Lori Lowe*[5], *Douglas Fullen*[2], *Paul Harms*[2]. [1]University of Michigan, Ann Arbor, MI, [2]University of Michigan, Ann Arbor, MI, [3]Henry Ford Health System, Detroit, MI, [4]Henry Ford Health System, [5]University of Michigan, [6]Univ. of Michigan, Ann Arbor, MI

Background: Merkel cell carcinoma (MCC) is a rare and aggressive primary cutaneous neuroendocrine carcinoma. Because MCC cannot be reliably distinguished morphologically from small cell carcinomas from other sites, immunohistochemistry is required to confirm cutaneous origin. Expression of cytokeratin-20 (CK20), especially in a paranuclear, dot-like pattern, is commonly used to confirm the diagnosis of MCC, but is negative in 5-10% of cases. Diagnostic challenges also arise in the setting of metastatic neuroendocrine carcinoma of unknown primary.

Design: Neurofilament and CK20 expression was evaluated in 53 MCC specimens from 37 unique patients, including 8 previously characterized CK20-negative MCC tumors. Twelve cases had results from previously performed Merkel cell polyomavirus (MCPyV) immunohistochemistry. Neurofilament and CK20 expression was also assessed in 60 non-cutaneous neuroendocrine carcinomas (NEC) with primary sites including lung (27), bladder (18), cervix (3), gastrointestinal tract (3), sinonasal tract (2), or other sites (7). CK20 and neurofilament immunohistochemistry was scored as either negative or positive (with or without paranuclear dot staining).

Results: Neurofilament expression was observed in 40/53 (75.5%) MCC cases, including 6/8 (75.0%) CK20-negative MCC cases. Neurofilament was expressed in 9/9 (100%) MCPyV-positive tumors and 2/3 (66.7%) MCPyV-negative tumors. Neurofilament expression was observed in 2 non-cutaneous NEC cases (one sinonasal and one lung); the specificity of neurofilament for MCC versus non-cutaneous NEC was 96.7%. CK20 expression was observed in 25/60 (41.7%) NEC cases. Specificity of CK20 immunostaining for MCC versus non-cutaneous NEC was 58.3%; specificity was only slightly improved (65.0%) by considering only cases with paranuclear dot-like CK20 staining to be positive. Because CK20 expression was a controlled variable in our MCC cohort, sensitivity of CK20 staining for MCC was not calculated.

Conclusions: Neurofilament expression has superior specificity to CK20 expression in distinguishing MCC from non-cutaneous NEC. Neurofilament is a useful diagnostic marker in the majority of CK20-negative MCC cases and may be expressed in MCPyV-negative MCC tumors. Limitations of neurofilament immunohistochemistry include predicted lower sensitivity than CK20 and subtle staining in some tumors. However, our findings indicate neurofilament is a useful addition to diagnostic panels for excluding non-cutaneous NEC.

577 Melanocytic Tumors with Peripheral Nerve Sheath (Schwannian) Phenotype: Analysis of Small Series with Molecular Data

Lauren Stanoszek[1], *Paul Harms*[2], *Rajiv Patel*[3], *Douglas Fullen*[2], *Min Wang*[4], *Peter Pavlidakey*[5], *Alison B Durham*[4], *Lori Lowe*[4], *Alexandra Hristov*[3], *Aleodor Andea*[2]. [1]University of Michigan, Ann Arbor, MI, [2]University of Michigan, Ann Arbor, MI, [3]Univ. of Michigan, Ann Arbor, MI, [4]University of Michigan, [5]University of Alabama at Birmingham Medical Center

Background: Melanocytic tumors with unusual features present particular challenges to diagnosis. Here, we report 5 cases of melanocytic tumors with prominent peripheral nerve sheath phenotype and variable degrees of cellular atypia.

Design: Five patients were identified with skin shave biopsies performed between 2011 and 2017. All cases underwent histologic examination and immunohistochemical analysis including p16, HMB-45, and/or Ki-67/MART-1. Three of 5 cases underwent SNP array testing and sequencing analysis for GNAQ and GNA11 mutations and common BRAF mutations.

Results: Patients demonstrated a wide age range from 6 to 67 years, and 4/5 patients were male. The lesions were located on the head/neck (2), back (2) and lower extremity (1). Histology showed a combined melanocytic proliferation which included a conventional nevus with varying atypia and a deeper spindle cell component with primitive nuclei, fascicular-like growth and occasional Verocay body-like structures without maturation with dermal descent. Two cases demonstrated rare mitotic figures and cytologic atypia. Necrosis was not noted. HMB-45 stain showed gradual decrease in dermal expression expected for a nevus in 2 cases, while 3 cases demonstrated patchy dermal staining. Diffuse expression of p16 and ki-67 low-labeling index was seen. No GNAQ, GNA11 or common BRAF mutations were identified in 3 analyzed cases. Two cases showed no chromosomal numerical abnormalities (CNAs); one case showed numerous CNAs involving chromosomes 3, 8, 11 and 15. A diagnosis of atypical combined nevus was rendered in 4 cases with a component resembling a cellular blue nevus mentioned in 3. The lesion with multiple CNAs was diagnosed as borderline. A sentinel lymph node biopsy performed in this case was negative.

Conclusions: We report a 5-case series of melanocytic tumors with a schwannian morphology resembling peripheral nerve sheath tumors. While some morphologic findings resemble cellular blue nevi, other features including pattern of HMB-45 staining, lack of GNAQ and/or GNA11 mutations and combined junctional and dermal morphology are not typical of this nevus variant. Such lesions may represent a distinct category of nevi or borderline melanocytic tumors. Awareness of this phenotype is important to ensure accurate classification and prevent misdiagnosis.

578 CD10 Is Expressed in Endothelial Cells of Glomuvenous Malformation with Higher Sensitivity than Conventional Solid Glomus Tumor

Toyohiro Tada[1], *Takashi Tsuchida*[2], *Satoshi Baba*[3], *Makoto Ito*[4], *Hisashi Tateyama*[5]. [1]Toyokawa City Hospital, Toyokawa, Aichi-ken, [2]Hamamatsu University Hospital, [3]Hamamatsu University School of Medicine Hospital, [4]Kariya Toyota General Hospital, [5]Kasugai City Hospital

Background: Glomus-cell associated benign lesions (GCABL) have been classified broadly into conventional solid glomus tumor (CSGT) and glomangioma. Recently, glomangioma tends to be considered as a kind of venous malformation and referred to as glomuvenous malformation (GVM). However, except for typical cases, histological differentiation between CSGT and GVM is often arbitrary, and immunohistochemical characteristics of vascular endothelial cells (ECs) of these lesions are not known. The aim of this study is to examine pathological significance of CD10 expression in ECs of GVM, and investigate its pathological attribute on the classification in benign vascular tumor/malformation.

Design: Forty-five cases of GCABL of skin and subcutis were divided histologically into GVM and CSGT, and stained immunohitochemically with antibodies to CD10, CD31, CD34, podoplanin, and GLUT1. As control studies, cavernous hemangiomas (venous malformation) (5 cases), arteriovenous malformation (5 cases), lobular capillary hemangiomas (10 cases), cherry hemangiomas (5 cases), and normal skin/subcutis (10 cases) with various sized vascular vessels were examined as well.

Results: GCABLs were composed of 10 cases of GVM and 35 cases of CSGT. Immunohistochemical expression of CD10 in ECs of each case is summarized in Table 1. Of note is that CD10 in GVM showed high positivity (50%) in contrast to CSGT (9%). In GVM, 5/10 (50%) were highly positive, 3/10 (30%) mildly positive, and 2/10 (20%) negative. In CSGT, 3/35(9%) were highly positive, 12/35 (34%) mildly positive, and 20/35 (57%) negative. CD34 expression in ECs was varied. Podoplanin, and GLUT1 were negative in all the cases. ECs of all cases of cavernous hemangiomas (venous malformation) and arteriovenous malformation showed CD10 positivity. However, CD10 was completely negative in ECs of lobular capillary hemangiomas, cherry hemangiomas, and normal skin/subcutis.

Lesions	n	CD10 Expression in Endothelial Cells (Immunohitochemistry)		
		Negative. No. (%)	Mildly Positive Area:10-50%. No. (%)	Highly Positive Area: more than 50%. No. (%)
GVM	10	2/10 (20%)	3/10 (30%)	5/10 (50%)
CSGT	35	20/35 (57%)	12/35 (34%)	3/35 (9%)
Cavernous Hemangioma (Venous Malformation)	5	0 /5 (0%)	0/5 (0%)	5/5 (100%)
Arteriovenous Malformation	5	0/5 (0%)	0/5 (0%)	5/5 (100%)
Lobular Capillary Hemangioma	10	10/10 (100%)	0/10 (0%)	0/10 (0%)
Cherry Hemangioma	5	5/5 (100%)	0/5 (0%)	0/5 (0%)
Normal Skin/Subcutis	10	10/10 (100%)	0/10 (0%)	0/10 (0%)

Conclusions: CD10 could be a useful marker for vascular malformation as demonstrated in vascular ECs of cavernous hemangiomas (venous malformation) and arteriovenous malformation. Highly frequent positivity for CD10 in vascular ECs of GVM (glomangioma) might indicate that GVM to be vascular malformation in nature, and the term "GVM" is thought to be appropriate. However, the etiological significance of endothelial CD10 expression in the vascular malformation including GVM, and the biological nature (neoplasm or not) of glomus-cell like cells surrounding vascular vessels remain to be studied in future.

579 The Role of CD70 in Benign and Malignant Cutaneous Skin Lesions

Christopher Trindade[1], *Markku Miettinen*[2], *Shakuntala Mauzo*[3], *Dragan Maric*[4], *Martha Quezado*[5], *Abhik Ray-Chaudhury*[6], *Stephen M Hewitt*[6], *Astin Powers*[2], *Abiye T Kassa*[7], *Chyi-Chia Richard Lee*[8], *Sara Peters*[9]. [1]Bethesda, MD, [2]National Cancer Institute, [3]Houston, TX, [4]NINDS, [5]NIH, Bethesda, MD, [6]National Cancer Institute, Bethesda, MD, [7]National Cancer Institute, Bethesda, MD, [8]NCI/NIH, Bethesda, MD, [9]Wexner Medical Center at The Ohio State University, Columbus, OH

Background: Immune therapy has been a mainstay of treatment for melanoma with IL-2, INF-gamma, and BCG therapy used for high stage disease and immune checkpoint inhibitors for adjuvant therapy. However, immunotherapy has not been well studied in non-melanoma skin lesions. A major pathway involved in immunotherapy is the CD70-CD27 pathway. Recently it has been shown that CD70 is also expressed both on malignant hematological and solid tumor cells. CD70 expression is associated with poor prognosis and is seen in metastatic disease. In thymic tumors, it differentiates between benign versus malignant. It is thought CD70 itself does not have any downstream impact on tumor cells but rather its expression and interaction with CD27 plays a role in pathogenesis by causing proliferation of nTregs and iTregs that in turn can suppress any adaptive anti-tumor response. Furthermore, expression of CD70 promotes exhaustion of effector T-cell responses through the CTLA-4 pathway and PD-1/PDL-1 pathways. Currently CD70 has not been well studied in both benign and malignant skin lesions. In this study, we explore CD70 expression in variety of skin lesions and explore possible mechanisms of action in CD70+ lesions.

Design: Over 300 deidentified patient lesions contained in tissue microarrays and sections from Biomax, National Cancer Institute, University of Virginia, and Ohio State University were stained with CD70 immunonohistochemical stain (monoclonal, clone TNFSF7) and scored from no expression to increasing intensity using a rating of 0-3. Benign and malignant skin lesions included melanoma, nevi, basal cell carcinoma, squamous cell carcinoma, merkel cell carcinoma, dermatofibromas, and dermatofibrosarcoma protuberans (DFSP). Sections that stained positive for CD70 were further studied looking specifically at T-reg and effector T-cell responses using multiparameter fluorescent microscopy.

Results: CD70 staining was seen on membranes, cytoplasm, or both. Also most cases had focal expression. Squamous cell and non-pigment melanoma lesions had the most expression with at least 50 percent of squamous and 20 percent of melanoma cases expressing CD70. CD70 expression was seen in 10-15 percent of cases for basal and merkel cell carcinoma and DFSP. There was no expression seen in dermatofibromas and congenital nevi.

Conclusions: CD70 expression was seen mainly in squamous cell carcinoma and melanoma and was associated with malignant

cutaneous lesions. Its expression may serve as a target for future therapies.

580 Recurrent/Persistent Nevus: A Clinical and Histologic Evaluation of Features Associated With Recurrence and Persistence of Melanocytic Nevi

Celestine Marie Trinidad[1], *Monty Hawkins*[2], *Victor Prieto*[3], *Carlos Torres-Cabala*[4], *Priyadharsini Nagarajan*[5], *Michael Tetzlaff*[6], *Jonathan Curry*[4], *Doina Ivan*[7], *Phyu Aung*[8]. [1]University of Texas MD Anderson Cancer Center, Houston, TX, [2]University of Texas MD Anderson Cancer Center, [3]UT - MD Anderson Cancer Center, Houston, TX, [4]Houston, TX, [5]The University of Texas MD Anderson Cancer Center, Houston, TX, [6]UT-MD Anderson Cancer Center, Houston, TX, [7]M. D. Anderson Cancer Center, Houston, TX, [8]U. T. - M. D. Anderson Cancer Center, Houston, TX

Background: Recurrence or persistence of hyperpigmentation at the previous biopsy site may occur after (partial) removal of a melanocytic nevus. Clinically, and even histologically, these may be difficult to distinguish from melanoma. This study aimed to investigate the clinical and histopathologic features of melanocytic nevi and their association with the development of recurrent/persistent nevi (RPN).

Design: A total of 93 patients (M:F=~1:1) with 100 RPN were identified from the period of 7/2005 to 6/2017. The original specimens were available for review for 57 cases (13 conventional nevi (RPCN) and 44 dysplastic nevi (RPDN)). Clinical and histologic features of the original nevi were reviewed. Also recorded were the possible history of a prior or subsequent melanoma and presence of sentinel lymph node (SLN) metastasis. A group of 87 non-recurrent/persistent dysplastic nevi (non-RPDN) was used as a control group. Chi-squared and Fisher Exact tests were employed for statistical analysis.

Results: RPN occurred predominantly in Caucasians (77%), most commonly in the trunk (33%). Compared with RPCN, RPDN was more significantly associated with prior positive margins (p=0.03), lack of congenital features (p=0.01) and trunk/abdomen location (p=0.03). Time to recurrence of less than 12 months was significantly associated with presence of more than 50% cohesive nesting of the melanocytes (p=0.03), overall both in the epidermis and dermis. Compared with non-RPDN, RPDN was significantly more associated with a younger age at diagnosis (mean 48.7, range 10-88, p<0.0001; HR=0.93 (0.91, 0.96), higher degree of cytologic and architectural atypia (p<0.0001), trunk/abdomen location (p<0.0001), a prior or subsequent melanoma on a separate location (p=0.008, HR=4.71 (1.51, 14.7)), and positive SLN (p=0.001).

Conclusions: RPDN, compared to RPCN, are more associated with positive margin status in the prior lesion and trunk/abdomen location. A greater degree of cohesion of melanocytic nests in dysplastic nevi is also associated with a shorter recurrent interval. Compared to non-RPDN, RPDN significantly showed higher degrees of cytologic and/or architectural atypia, younger age at diagnosis, and trunk and abdomen location. Interestingly, RPN showed a significant correlation with the location of a prior or subsequent melanoma and positive SLN metastasis. Our data suggests close clinical follow-up of nevi with positive margins, trunk/abdomen location, and high degree of atypia for the possibility of future recurrence.

581 Expression of Neuroendocrine Markers In Sebaceous Carcinoma: A Potential Diagnostic Pitfall

Celestine Marie Trinidad[1], *Michael Tetzlaff*[2], *Doina Ivan*[3], *Priyadharsini Nagarajan*[4], *Carlos Torres-Cabala*[5], *Jonathan Curry*[5], *Bita Esmaeli*[6], *Victor Prieto*[7], *Phyu Aung*[8]. [1]University of Texas MD Anderson Cancer Center, Houston, TX, [2]UT-MD Anderson Cancer Center, Houston, TX, [3]M. D. Anderson Cancer Center, Houston, TX, [4]The University of Texas MD Anderson Cancer Center, Houston, TX, [5]Houston, TX, [6]University of Texas MD Anderson Cancer Center, [7]UT - MD Anderson Cancer Center, Houston, TX, [8]U. T. - M. D. Anderson Cancer Center, Houston, TX

Background: Sebaceous carcinoma accounts for 0.2-4.6% of cutaneous neoplasms and are characterized morphologically by cells with variably basophilic cytoplasm and intracytoplasmic vacuoles, which typically indent (scallop) the nucleus. However, these vacuoles may not be readily evident in poorly differentiated tumors, making distinction from other cutaneous neoplasms challenging. Occasionally, immunohistochemical studies are required to confirm the diagnosis, but in this context, aberrant expression of neuroendocrine markers may be a diagnostic pitfall and interpreted incorrectly as Merkel cell carcinoma.

Design: Immunohistochemical studies for synaptophysin and chromogranin were performed on ten (10) cases of previously diagnosed sebaceous carcinomas and five (5) cases of sebaceous adenomas, from a total of fourteen (14) patients, including 10 men and 4 women with a median age of 61 years (range 45-84 years). Nine (9) of the cases were from the head and neck (including 6 periocular).

Results: Two of the 10 cases (20%) of sebaceous carcinoma exhibited positivity for neuroendocrine markers, while none of the sebaceous adenomas showed neuroendocrine differentiation. One case showed strong, diffuse positivity (95%) for both synaptophysin and chromogranin, leading to the diagnosis of Merkel cell carcinoma (primary cutaneous neuroendocrine carcinoma). However, on review, adipophilin staining highlighted the presence of diffuse intracytoplasmic vacuoles, which together with the periocular location supported the diagnosis of sebaceous carcinoma. Another case also showed focal positivity (20%) for chromogranin, but was negative for synaptophysin. Both cases were from female patients, located in the periorbital area, and were not associated with Muir-Torre syndrome. One patient with positivity for neuroendocrine markers exhibited multiple local recurrences, while the other was free of disease for 7 years after wide local excision.

Conclusions: Sebaceous carcinomas may show strong and diffuse expression of neuroendocrine markers, which has not been reported previously. This represents an important diagnostic pitfall, as poorly differentiated tumors may appear similar to neuroendocrine tumors, including Merkel cell carcinoma. Recognition of this immunophenotypic pattern in sebaceous carcinomas is vital to make the accurate diagnosis of sebaceous carcinoma, which is typically less aggressive than Merkel cell carcinoma.

582 Evaluation of TLE1 in Cutaneous Tumors: Frequent Expression in Sebaceous Neoplasms, Basal Cell Carcinoma and Squamous Cell Carcinoma

Yiqin Xiong[1], *Karen Dresser*[2], *Kristine M Cornejo*[3]. [1]University of Massachusetts, Worcester, MA, [2]UMass Memorial Healthcare, Worcester, MA, [3]University of Massachusetts Medical School, Worcester, MA

Background: Transducin-like enhancer of split 1 (TLE1) is a gene involved in cell differentiation and Wnt/β-catenin signaling. TLE1 immunohistochemistry is widely used as a biomarker for synovial sarcoma. Recently, we identified TLE1 expression in a subset of melanomas. TLE1 immunohistochemistry has not been well studied in cutaneous tumors. The aim was to investigate TLE1 expression in sebaceous neoplasms, basal cell carcinoma (BCC) and squamous cell carcinoma (SCC).

Design: Cases of sebaceous adenoma (n=28), sebaceoma (n=12), sebaceous carcinoma (n=19), BCC (n= 20) and SCC (n=20) diagnosed at a tertiary medical center from 2007-2017 were randomly selected. After review, 5 cases (sebaceous adenoma n=2; sebaceoma n=2; SCC n=1) had insufficient tissue remaining and were excluded from the study. TLE1 immunohistochemistry was performed on the remaining 94 cases and positivity was defined as dark brown nuclear staining and graded as 3+ (strong staining of >50% of cells identified at 4x), 2+ (moderate staining of 10-50% of cells at 4x or >50% of cells staining above background at 10x) and 1+ (weak staining of <50% of cells above background at 10x). No visible staining was scored as 0. Staining for TLE1 was considered positive for 2-3+ and negative for 0-1+.

Results: Nuclear TLE1 expression was identified in 25 of 26 (96%) sebaceous adenomas, 8 of 10 (80%) sebaceomas and 17 of 19 (90%) sebaceous carcinomas (Table 1, Figure 1). TLE1 positivity was typically diffuse and strong in the mature sebocytes, in comparison to the basaloid cells which often displayed weaker or patchy staining. TLE1 positivity was also identified in 19 of 20 (95%) BCC and 12 of 19 (63%) SCC cases. All of the neoplasms considered to be negative showed weak (1+) staining and none were completely absent of staining.

Table 1. Summary of TLE1 Expression in Cutaneous Tumors (n=94).

Tumor Type	TLE1 POS (2-3+)	TLE1 NEG (0 or 1+)
Sebaceous Neoplasms (n=55)	50 (91%)	5 (9%)
• Sebaceous adenoma (n=26)	25 (96%)	1 (4%)
• Sebaceoma (n=10)	8 (80%)	2 (20%)
• Sebaceous Carcinoma (n=19)	17 (90%)	2 (10%)
BCC (n=20)	19 (95%)	1 (5%)
SCC (n=19)	12 (63%)	7 (37%)

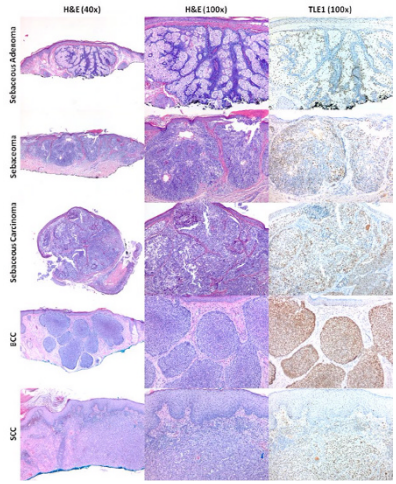

Conclusions: TLE1 immunohistochemistry frequently highlights sebaceous neoplasms, BCC and SCC with a fairly high sensitivity (63-96%). Therefore, TLE1 is not a specific biomarker for synovial sarcoma and should be evaluated with caution, particularly in cases in which the differential diagnosis may include other cutaneous tumors.

583 DExH-box Helicase 34 is a Poor Prognostic Biomarker and Modulated by MicroRNA-939 in Melanoma

Lijun Xue[1], *Xiyong Liu*[2], *Yun Yen*[3], *Justin Kerstetter*[4]. [1]Loma Linda, CA, [2]California Cancer Institute, Sino-America Cancer Foundation, [3]Taipei Medical University, [4]Loma Linda University Medical Center

Background: DHX34 gene encodes DExH-box Helicase 34, which is a putative RNA helicase that belongs to DEAD box proteins with conserved motif Asp-Glu-Ala-Asp (DEAD). It can activate nonsense-mediated decay of aberrant mRNAs. Members of the DEAD box family of RNA helicases play critical roles in cellular metabolism and in many cases have been implicated in cellular proliferation and/or neoplastic transformation. However, the clinical significance of DHX34 still remains unknown.

Design: Here, we conducted a survival analysis for DHX34 in two published gene array data set (GSE65904 and E-MTAB4725) with total 418 cases of melanoma tissue samples. We also performed gene set enrichment analysis (GSEA) to clarify how the expression of DHX34 would enrich gene signatures in melanoma. We further analyzed the eligible microRNAs of DHX34 by using TargetScan Human v7.1. A correlation test was used to see how DHX34 mRNA expression correlates with miR-939 in melanoma tissue samples. A survival analysis for miR-939 in the two gene array data set mentioned above was analyzed as well.

Results: The survival analysis for DHX34 in the two gene array data set revealed that high DHX34 mRNA expression levels were significantly related to poor overall survival (Log-rank p=0.007) and progression-free survival (Log-rank p=0.009) of Melanoma. As with increase of mRNA expression levels, the survivability of patient got poorer with a dose-dependent manner. The GSEA showed that expression of DHX34 could significantly enrich gene signatures including undifferentiation, and cancer invasiveness and metastasis. TargetScan Human v7.1. analysis revealed that miR-939-3p might be potentially binding the DHX34 transcript at position from 49-56 (Context score -0.54, 99%). A correlation test showed that DHX34 mRNA expression was significantly and inversely correlated with miR-939 level in melanoma tissue samples. Further analysis validated that miR-939 was significantly associated with better overall and progression-free survival of melanoma.

Table 1. Uni- and multivariate analysis for DHX34 and miR939 survival in melanoma data set

Data set		Overall survival		Progression-free survival	
		HR (95%CI)	Adjusted HR (95%CI)*	HR (95%CI)	Adjusted HR (95%CI)*
DHX34	Q_1	Reference	Reference	Reference	Reference
	Q_2	1.13 (0.61-2.12)	1.43 (0.73-2.85)	1.34 (0.69-2.69)	1.61 (0.79-3.38)
	Q_3	1.44 (0.80-2.66)	2.00 (1.04-3.98) †	1.47 (0.76-2.94)	1.53 (0.72-3.33)
	Q_4	2.40 (1.36-4.37) ‡	2.98 (1.58-5.88) ‡	2.76 (1.45-5.47) ‡	3.48 (1.71-7.45) ‡
miR939	Q_1	Reference	Reference	Reference	Reference
	Q_2	0.88 (0.51-1.48)	0.88 (0.49-1.57)	1.20 (0.67-2.17)	1.16 (0.60-2.27)
	Q_3	0.69 (0.40-1.17)	0.59 (0.32-1.08)	0.69 (0.38-1.26)	0.65 (0.33-1.30)
	Q_4	0.50 (0.29-0.87) †	0.44 (0.23-0.83) †	0.46 (0.24-0.87) †	0.49 (0.23-1.01)

Note: we re-stratified four grades (Q1, Q2, Q3, and Q4) based on the percentile of DHX34 or miR-939 expression. Uni- and multivariate analysis were conducted to evaluate HR of DHX34/miR-939 (vs. Q1).

* For multivariate analysis, HR was adjusted by age, organism, sex, tumor stage in the melanoma GSE65904 data set.

† Statistical significance, $P<0.05$; ‡ Statistical significance, $P<0.01$

Conclusions: High DHX34 mRNA expression level is significantly related to poor survival that might be modulated by miR-939 in melanoma cells. This result indicates that DHX34 has a potential to serve as a prognostic biomarker.

584 The Prognostic Impact of Tumor Thickness by Using Different Measurement methods in Cutaneous Squamous Cell Carcinomas

Pelin Yildiz[1], *Chad Hruska*[2], *Doina Ivan*[3], *Phyu Aung*[4], *Jonathan Curry*[5], *Priyadharsini Nagarajan*[6], *Carlos Torres-Cabala*[5], *Michael Tetzlaff*[7], *Victor Prieto*[8]. [1]Bezmialem Vakıf Universitesi, Istanbul, Fatih, [2]MD Anderson Cancer Center, Houston, Texas, [3]M. D. Anderson Cancer Center, Houston, TX, [4]U. T. - M. D. Anderson Cancer Center, Houston, TX, [5]Houston, TX, [6]The University of Texas MD Anderson Cancer Center, Houston, TX, [7]UT-MD Anderson Cancer Center, Houston, TX, [8]UT - MD Anderson Cancer Center, Houston, TX

Background: Cutaneous squamous cell carcinoma (cSCC) is the second most cause of non-melanoma skin cancers. Although it has relatively low mortality rate, it may recur and metastasize. Tumor thickness is one important parameter associated with aggressive behavior. However, such measurement may be performed in different ways depending on the anatomic location and subspeciality. Furthermore, the soon-to-be implemented AJCC 8th edition has changed the recommended method of measurement from a modified Breslow thickness to measuring from the granular layer of adjacent, normal-appearing skin to the deepest tumor cell

Design: The study includes 79 patients from our institute between January 2010-December 2012. Thickness was evaluated using four currently available methods and results where correlated with clinical follow-up. Measurement was performed using the digital ruler of an image analysis software.

Results: Overall, there was no association between any measurement technique (used as continuous variables) and recurrence free survival. However, when measurements were grouped using different cutoff values, there appeared to be significant differences. According to multivariable model, traditional Breslow thickness method (analogous to that one used in cutaneous melanoma) was the only factor independently associated with recurrence free survival. A 6-mm cutoff resulted in significant difference and was associated to disease free survival; however, in this series, the strongest correlation appeared when the cut-off was 8.7 mm (p<0.001).

Conclusions: In our series of cutaneous squamous cell carcinoma, it seems that measurement of thickness using the Breslow method provides appropriate correlation with disease-free survival and thus may be used in Pathology reports.

585 High Rate of FISH False Negative Results in the Detection of Homozygous Loss of CDKN2A in Difficult Melanocytic Tumors

Nicholas A Zoumberos[1], *Kenneth Yu*[2], *Min Wang*[2], *Paul Harms*, *May P Chan*, *Rajiv Patel*[3], *Lori Lowe*[2], *Douglas Fullen*, *Aleodor Andea*. [1]University of Michigan, Ann Arbor, MI, [2]University of Michigan, [3]Univ. of Michigan, Ann Arbor, MI

Background: Although histologic interpretation remains the gold standard for the diagnosis of melanoma, molecular methods based on the detection of copy number changes by single nucleotide polymorphism (SNP) microarrays or fluorescence in-situ hybridization (FISH) are increasingly being used in the diagnosis of histologically ambiguous lesions. One of the most significant markers of melanoma is homozygous deletion of the *CDKN2A* gene, which encodes p16. Detection of this abnormality by FISH is considered to correlate with increased risk for adverse outcome and is often used to favor a diagnosis of melanoma.

Design: From our SNP array database of 263 melanocytic tumors we identified 32 cases with homozygous loss of *CDKN2A.* FISH with a commercially available 9p21 probe for *CDKN2A* was performed in 14 cases with available material and compared with the SNP array results. For the remaining 18 cases, the results of FISH testing were predicted based on the location of the 9p21 probe relative to the area of homozygous deletion.

Results: The typical pattern on SNP array consisted of deletion of a large portion of 9p or entire chromosome 9 on one allele combined with a smaller deletion of the other allele overlapping the *CDKN2A* gene. The average size of the area of homozygous deletion was 2.6 MB (range 0.02-13.75 MB). FISH detected homozygous deletions of 9p21 in only 8/14 cases (57%). The average size of deletion in cases with false negative FISH was smaller than in cases with positive FISH: 0.22 MB (range 0.02-0.6 MB) versus 4.26 MB (range 0.25-13.75 MB) respectively. Failure to detect the homozygous *CDKN2A* deletion was associated with lack of complete overlap between the FISH probe (designed with a larger overhang towards the p-terminus) and an area of homozygous deletion that was small or extended only towards the centromere (see Figure below for the 6 cases with false negative FISH results). For the 18 cases without FISH, the location of the probe relative to area of deletion predicted detection of homozygous loss in 14 cases (61%).

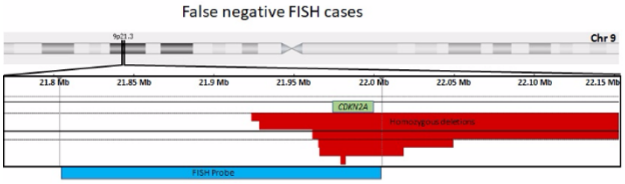

Conclusions: We report a relatively high rate of false negative FISH results (41%) for detection of homozygous loss of *CDKN2A* gene compared to SNP array, especially when the deleted area is small (<0.6 MB) or asymmetrically located. This represents a significant diagnostic pitfall when using FISH in the diagnosis of difficult melanocytic tumors.

FIG. 528

Case Number	1	2	3	4
Presenting history				
Age	76	57	52	51
Sex	M	F	M	F
Ethnicity	C	H	C	C
Anatomic location	Right cheek	Left postauricular	Right posterior ear	Chin / submental
Gross appearance	Brown papule	Irregularly pigmented dark brown nodule	Tan pink papule	Irregularly pigmented lesion
Duration	2 years	At least 3 months	NA	4 years
Size	9 mm	17 mm	9 mm	> 6 mm
Evolution	Change of color	Progressive growth	NA	Rapid growth and change of color
Other skin lesions	None	Multiple pink / tan papules in left postauricular area	None	None
Family history of malignancy	None	None	None	None
Personal history of malignancy	Prostatectomy for adenocarcinoma 10 years ago	Melanoma in situ of right mid arm	None	None
Histopathology				
Type	Predominantly dermal nodular melanoma	Predominantly dermal nodular melanoma	Predominantly dermal nodular melanoma	Predominantly dermal nodular melanoma
Breslow thickness (mm)	2.95	2.57	3.25	2.60
Clark level	IV	IV	IV	IV
Mitotic rate/mm^2	2	3	6	2
Associated nevus	Intradermal type	Intradermal type	Intradermal type	Intradermal type
In situ component	focal	none	none	none
Management and follow-up				
Margin status post wide local excision	Negative	Negative	Negative	Positive
Lymph node status	0/3 SLN	0/1 SLN	0/2 SLN	2/23 RLN
Follow-up	Alive and disease free 28 months	Alive and disease free 8 months	Alive and disease free 12 months	Alive multiple recurrences and regional nodal / in-transit metastasis

FIG. 554

Case N	Sex/age	Location/Size	Predominent patter/Perineural invasion	MYB ba	NFIB ba	MYB-NFIB	MYBL1	Treatment	Follow-up
1	F/58	Scalp	Cribriform/No	Neg	+	+	Neg	N/A	Lost to follow-up
2	M/65	Thigh	Tubular/No	Neg	+	Neg	+	Excision	Pending
3	F/83	Scalp	Tubular/Yes	Neg	Neg	Neg	Neg	Excision	NED at 39 months
4	M/51	Back	Cribriform/No	+	Neg	Neg	Neg	Excision	Pending
5	M/74	Thigh	Solid/No	N/A	N/A	NA	Neg	Excision	Pending
6	F/78	Head	Cribroform/Yes	Neg	+	+	Neg	N/A	DUC at 82 months
7	M/62	Face	Cribriform/No	Neg	Neg	Neg	+	Excision	NED at 9 months
8	F/69	Vulva	Tubular/Yes	+	+	+	Neg	Vulvectomy with lymph-adenectomy	NED at 4 months
9	F/65	Vulva	Cribroform/Yes	+	+	+	Neg	Vulvectomy with lymph-adenectomy	Pulmonary mts in 1 year
10	F/80	Sacral	Solid/No	+	Neg	Neg	Neg	Excision	Pending